Tracking Uptake, Assembly and Egress of ACAM529 Herpes Simplex Virus Type 2 in Complementary Vero Cells for Enhanced Virus Recovery

by

Valentin Malenkov

A thesis
presented to the University of Waterloo
in fulfillment of the
thesis requirement for the degree of
Master of Applied Science
in
Chemical Engineering

Waterloo, Ontario, Canada, 2015

Author's Declaration

This thesis consists of material all of which I authored or co-authored: see Statement of Contributions included in the thesis. This is a true copy of the thesis, including any required final revisions, as accepted by my examiners.

I understand that my thesis may be made electronically available to the public.

Statement of Contributions

Chapter 3 of this thesis was adapted from an unpublished review paper entitled "Downstream Processing of Viral Particles and Virus-like Particles from Cell Culture" authored by myself, Stanislav Sokolenko, Steve George, and Megan Logan. As this is not a published work, no formal reference is possible. I would however like to acknowledge the contribution of these individuals to this thesis.

I was first author on the original document and am solely responsible for the alterations and additions made in order to integrate it into this thesis.

Abstract

Herpes simplex virus (HSV) type 2 is the cause of one of the most wide-spread human infections in the world, affecting millions of people and circumventing all past attempts to cure or prevent infection. One of the biopharmaceutical companies involved in HSV-2 vaccine development, Sanofi Pasteur, has developed a candidate vaccine based on a live, replication-deficient HSV-2 virus. The "ACAM529" strain is subject to two gene deletions and requires a complementary African Green Monkey Kidney (Vero) cell line (AV529-19) to replicate. A bottleneck exists in the production process which is hypothesized to be the result of virus particles being directed towards both cell-cell and cell-substrate (adherent surface) junctions. The overarching goal of this work was to determine if some mature virus particles localize and egress at substrate surface junctions, becoming inaccessible to traditional extraction methods.

To test the hypothesis, an alternate titration method was first developed using induced fluorescence end-point dilution assay with a spectrofluorometer. The second stage of the research involved the use of immunofluorescent staining to locate viral proteins within infected cells in order to inform future process optimization. Mature virus particles were of particular interest and the co-localization of two essential proteins was used to determine their location. A pseudo co-culturing protocol was then developed using cell culture inserts. This system was used in an attempt to determine the extent to which viral budding occurred towards the substrate.

The fluorescence which the HSV2012-121 Vero cells displayed on infection with ACAM529 did not allow for effective differentiation between infected and uninfected cells. Treatment of the cells with Sodium Butyrate (2mM NaBu added at the time of seeding) resulted in a 16.93-fold difference between infected and uninfected cells' fluorescence. Immunofluorescent staining of two virus proteins to determine their co-localization was not successful. Evidence pointed to bleeding of the signals between the 488 and 405nm channels, as well as to a lack of capsid staining in the presence of a tegument of envelope layer. Nevertheless, individual glycoprotein stains were found to be effective and provided good insights into the virus' behaviour. Lastly, the AV529-19 Vero cells were shown to adhere effectively to insert membranes and form confluent monolayers. Staining and counting of the resulting plaques was used to establish a required initial infection titer between 8.3×10^4 and 1.2×10^6 PFU/mL for future cell insert experiments.

Acknowledgements

Table of Contents

List of Figures

List of Abbreviations

AcMNPV	*Autographa californica* multicapsid nuleopolyhedrovirus
a-gD, a-gB, etc	anti-glycoprotein B, anti-glycoproteinB, etc (antibody)
ATPS	Aqueous two-phase systems
BSA	Bovine Serum Albumin
cDNA	Complementary DNA
CV	Coefficient of variability
Da	Daltons (unit of measure)
DISC	Disabled infectious single cycle
DMEM	Dulbecco's Modified Eagle Medium
DMSO	Dimethyl sulfoxide
DNA	Deoxyribonucleic Acid
DPBS	Dulbecco's Phosphate Buffered Saline
DS	Dextran Sulfate
DSP	Down-stream processing
EPDA	End-point Dilution Assay
eGFP	Enhanced Green fluorescence protein
F-Actin	Filamentous Actin
FITC	Fluorescein isothiocyanate
gE, gB, gC, etc	Glycoproteins E, B, C, etc
hpi	hours post-infection
HSV	Herpes simplex virus
HVEM	Herpesvirus entry mediator

ICP	Infected Cell Protein
IS	Immunofluorescent staining
LAT	Latenc-associated transcript
LLD	lower limit of detection
MC	Micro-carriers
MOI	Multiplicity of infection
MQ Water	Ultra-pure deionized water
NaBu	Sodium Butyrate
PBS-T	Phosphate Buffered Saline with 0.1% Tween 20
PET	Polyethylene terephthalate
PFU	Plaque-forming unit
qPCR	Quantitative PCR
RNA	Ribonucleic Acid
RT-PCR	Real-time polymerase chain reaction
STI	Sexually transmitted infection
TCID50	Tissue culture infective dose
TGN	Tran-Golgi Network
VLP	Virus-like particles

Chapter 1 – Introduction

Herpes simplex virus (HSV) type 2 is the cause of one of the most wide-spread human infections in the world, affecting millions of people and circumventing all past attempts to cure or prevent infection. While its most common symptoms are mild compared to many other viral infections, especially those transmitted through intimate contact, it is known to cause severe lesions, blindness, and even death in vulnerable individuals. The serious harm that HSV can cause to immunocompromised populations coupled with the virus' ability to establish life-long recurrent infections are, in large part, the driving force behind HSV research. Developing a vaccine for HSV has been the subject of extensive efforts with intellectual, humanitarian, and financial incentives to continuing on this path in spite of past failures.

One of the biopharmaceutical companies involved in HSV-2 vaccine development, Sanofi Pasteur, has developed a candidate vaccine based on a live, replication-deficient HSV-2 virus. The "ACAM529" strain is subject to two gene deletions and requires a complementary African Green Monkey Kidney (Vero) cell line (AV529-19) to replicate. Although a process exists for the amplification and recovery of the virus, its labile nature causes significant losses in yield. It has been reported that HSV-2 virus particles do not exit their host cells indiscriminately, but are instead directed towards both cell-cell and cell-substrate (the surface to which the cells adhere) junctions [1]. The hypothesis of my work was that these cells could be contributing to the production bottleneck which occurs at viral harvesting.

A mojor goal of this work was to determine if some mature virus particles localize and egress at substrate surface junctions, becoming inaccessible to traditional extraction methods. To test this hypothesis, three objectives were set. First, a rapid and reliable quantification method was sought. To enhance current practices a novel cell line was developed based on AV529-19 which contained a reporter green fluorescent protein gene under a virally inducible promoter. This cell line is referred to as HSV2012-121. The second objective of this work was to determine the intracellular location of the virus through the co-localization of multiple viral proteins present in fully matured virus particles. The final objective of this work was to develop a culturing method that would allow the preferential viral egress to be studied.

A summary of current down-stream processing (DSP) technology for purification of virus particles is allotted an entire chapter of this thesis (Chapter 3) due to the importance of this topic to virus production processes. While the focus of the research did not relate to the DSP of the virus, the requirements and limitations of viral purification for vaccines influenced the methods used.

Viral titration is required for any production process, and determining viral titer is often a tedious and time-consuming process. Plaque assays are currently the most reliable and accurate method for enumeration of the ACAM529 virus but are time consuming and highly dependent on operator experience. Chapter 5 describes the use of the HSV2012-121 fluorescing Vero cell line to establish an alternative enumeration assay.

Chapter 6 aimed to determine the intracellular localization of mature virus particles in infected cells. The replication of HSV involves a complex cascade of viral gene expression and the creation of a host of gene products. Of these, several essential proteins were selected and tagged using direct and indirect immunofluorescent staining. Antibodies against glycoproteins involved in cell entry, fusion, and cell-to-cell transmission (a-gB, a-gE, a-gC, and a-gD) as well as major structural proteins (a-ICP5, a-ICP27, and a polyclonal antibody against late structural proteins of HSV-2) were investigated as the proteins targeted by them are all essential for infectious mature virus particles.

In Chapter 7, a culturing and infection technique was developed to determine the fraction of progeny virus particles which exits the cell towards the surface on which the cells are growing. Cell culture inserts allowed two separate Vero cell monolayers to interact without direct contact. First, the efficacy of the cell culture insert as a substrate for the genetically modified Vero cells was established. The pseudo co-culturing protocol was then used to study the extent to which the virus particles bud downwards into their substrate rather than in any other direction (including cell-to-cell transmission).

Chapter 2 – Literature Review

2.1 Introduction to the herpes simplex virus

2.1.1 Epidemiology and Pathogenicity

The Herpesviridae family of viruses is one of the most successful animal pathogens on Earth if success of such entities is measured by their prevalence in the host organisms' population. If measured by their ability to adapt to different hosts or longevity of infection herpes viruses are still near the very top in terms of viral success. Almost every animal species investigated for members of the Herpesviridae family has shown to have at least one such virus adapted to it [2]. In most cases this infection last for the host's entire life and spreads easily to other members of its population. Humans can be infected with several different Herpesvirus members but the most common are infections of herpes simplex viruses (HSV-1 and HSV-2 for types 1 and 2 respectively). HSV-2 is the research focus of this work but its many similarities to HSV-1 and the very much linked nature of the research of these two viruses necessitates the inclusion of HSV-1 in this literature review.

Some studies have shown that as many as 85% of adults have come into contact with HSV-1 and 22-25% with HSV-2 and are therefore sero-positive (meaning tests for anti-HSV antibodies return positive results indicating exposure and possible infection) [3, 4]. In the case of HSV-2, the rate of sero-prevalence has increased by 32% in the 1990's alone [4] and more at-risk populations (such as sexually transmitted infection (STI) clinic attendees) have been found to be 30-50% sero-positive [4]. One research paper estimates Worldwide infection numbers for HSV-2 at 536 million, with 23.6 million newly infected individuals just in 2003 [5]. The percentages are so high that when standard STI blood panels are conducted, HSV is usually not included. Unless overt symptoms appear, it's almost impossible to differentiate between someone simply exposed to the virus and an asymptomatic non-shedding infection.

HSV-1 is the virus most commonly responsible for "cold-sores", the small recurring blisters or lesions usually found around the mouth and nose. HSV-2 mostly presents on the genitals and is most commonly contracted through sexual contact. It also presents as blisters or sores that burst within days of an outbreak and take days or weeks to heal [6, 7]. It is possible for

HSV-1 to infect the genitals and for HSV-2 to cause an orofacial infection and these cases are becoming more common, potentially pointing to changing sexual practices world-wide [8, 9].

These blisters are the direct result of cell death mediated by the virus, as well as the body's inflammatory response to the infection [7]. A fever may also accompany the outbreak, especially during primary infection. For both viruses, the lesions are painful and irritating while also representing major sites of viral "shedding" (release of infectious virus particles), which can transmit the infection [6]. Once primary infection has occurred HSV particles (both type 1 and 2) are then transported through nerve axons and establish a latent infection in dorsal root ganglia (vagal, trigeminal, or sacral, depending on the site of initial infection) [7]. The exact mechanism by which the virus enters a non-replicative latent infection state has not yet been determined [7]. Once there, the virus will re-activate throughout the hosts' life. This occurs most often in response to stress, fever, tissue damage and any other event leading to a weakened host immune system [2, 3, 7].

Both viruses can shed and be transmitted even when the infected individual is asymptomatic. All that is required is contact between a shedding site of the infected individual and the mucosal layer or abrasion in the skin of another [7]. This is of vital importance since only about 10-25% of individuals infected with HSV-2 ever show symptoms and many transmissions occur without any previous history of "Genital Herpes" [10]. Symptomatic individuals are more likely to be shedding at any given point in time (20.1% of days tested, with 43% of those days being symptomatic) than asymptomatic individuals (10.2% of days tested) [10]. Given that a large number of individuals infected with HSV-2 do not know they have it and that most are still infectious, it is no surprise that it continues to be the most common STI in humans.

2.1.2 HSV-2 Lifecycle (Cycle of Infection)

2.1.2.1 HSV-2 Morphology
The HSV-2 particle is fairly complex in its morphology and is composed of four major components: the core, the capsid, the tegument, and outer envelope (Figure 1). The entire particle is roughly 180-200nm in size and is generally spherical in shape [2]. At the very core of any virus' structure is the viral nucleic acid. The ultimate goal of any virus is to deliver this nucleic acid to the nucleus of a host cell and it is therefore very well protected. In the case of the HSV-2

4

virus, the genetic information is stored as linear double-stranded DNA with a genome length of approximately 1.55×10^5 bp [11]. This genome codes for 74-84 distinct proteins, at least three of which are coded for twice. The core is toroidal in shape (resembling a donut) with the DNA wrapped around a proteinaceous core [12, 2].
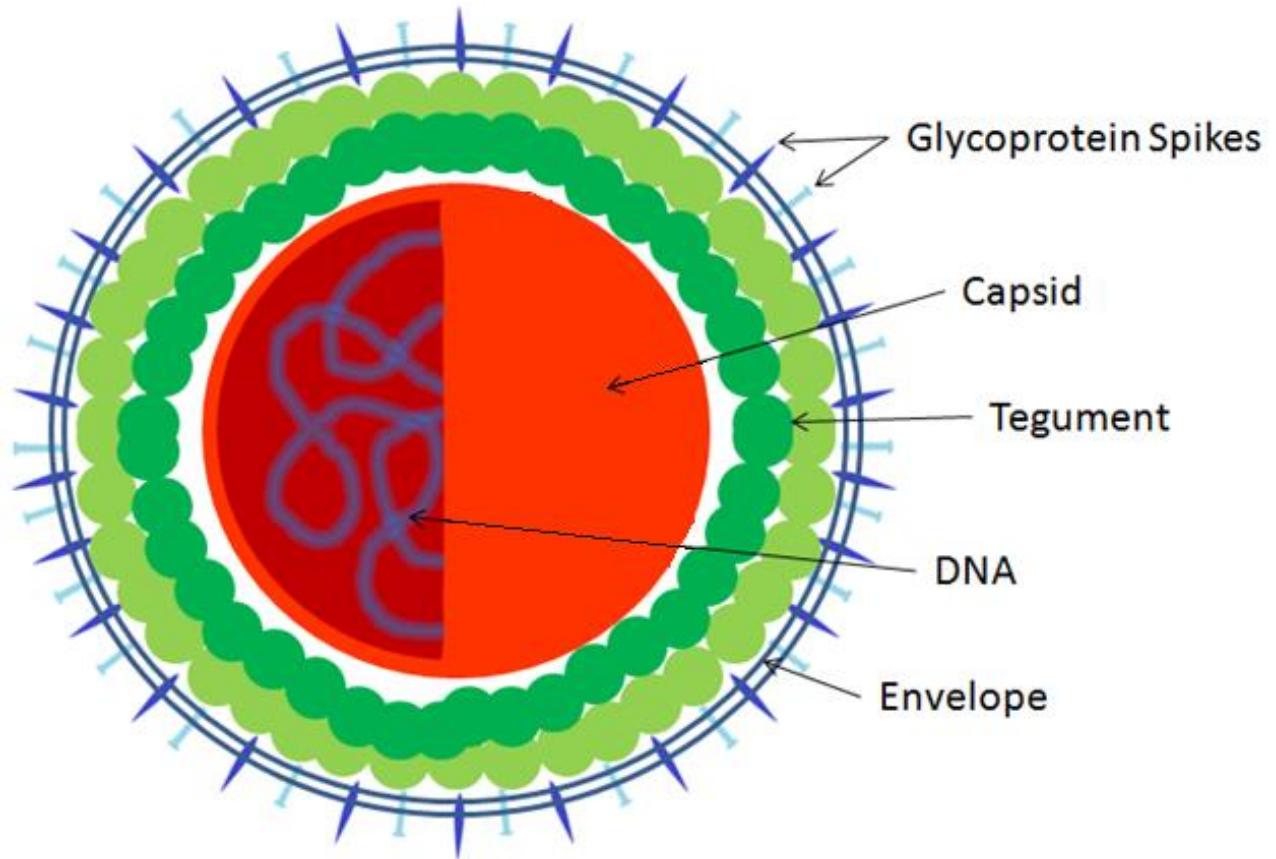
Figure 1: HSV-2 virus particle structure (diameter = ~200nm)

The DNA-containing core of the virus is surrounded by a protein capsid. This capsid is icosahedral in shape and consists of 162 hexagonal capsomeres (geometric shape with 20 sides composed of 162 hexagonal subunits) [12, 2, 13]. It makes up for over half of the virus particle's size at about 95-105nm. Over top of the capsid there is a tegument layer composed primarily of lipids and some proteins. These lipids are acquired from the cellular membranes of the virus' original host cell. The proteins in the tegument enter the host cell at the same time as the capsid. They are required early in the infection process and can be detected within the cell cytoplasm immediately after viral attachment [14, 2]. The tegument layer is bounded by an outer envelope

that is acquired from the virus' original cell. This envelope is stubbed with viral glycoproteins that aid in new host cell location, viral attachment, and fusion.

The morphology described above for HSV-2 is shared by all Herpesviruses [12]. The variation occurs in the specific proteins and DNA sequences of the viruses. HSV-1 and 2 share many of the same glycoproteins and most of their genetic information to the point where a study on the exact size of the HSV-2 genome led to the re-evaluation of what we know about HSV-1's [11]. Luckily, there are differences in protein structure between the HSV-1 and HSV-2 which allow for exact clinical diagnosis of the herpes simplex type[15].

2.1.2.2 Primary Infection

2.1.2.2.1 Fusion and Entry

A herpes simplex virus infection is transmitted through direct intimate contact between an infected and shedding individual's mucus layer and that of an uninfected individual. Co-infection of HSV-1 and 2 is not uncommon and some studies have found that it may actually aid in preventing clinical presentation of symptoms from HSV-2 [16]. Since direct contact of mucus layers is required for infection, the likelihood of transmission through casual contact is minimal. There have, however, been cases of medical professionals acquiring HSV infections through lesions on their hands while working with HSV sero-positive patients [17]. The spread of HSV-2 is not guaranteed on intimate contact with a shedding individual, with a median number of 40 sexual acts required for infection to pass on in serodiscordant partners i.e. where one partner is infected and one is not [18].
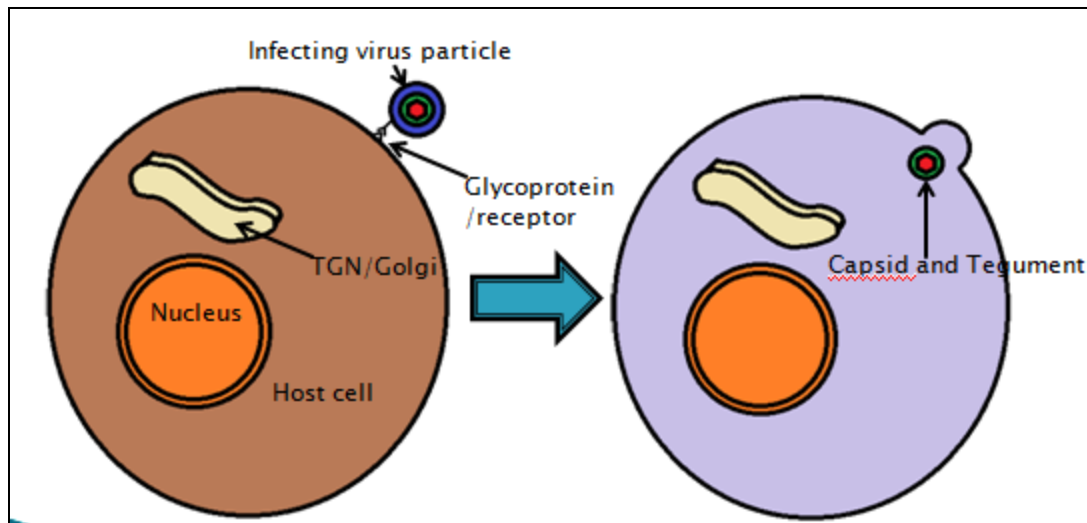
Figure 2: Schematic of fusion and entry of HSV-2 into host cell (not to scale)

In order to infect a host cell, the HSV-2 particle must first latch on to or adhere to the cell's outer membrane (Figure 2). Fusion of the particle occurs through the actions of glycoproteins on its outer membrane rather than with fusion peptides as is observed in other viruses (like influenza or HIV) [19]. Glycoproteins B, D, H, and L (gB, gD, gH, and gL, respectively) are all involved in this mechanism. gD has been shown to enable entry of the virus whether it is expressed on the viral membrane or added in soluble form, indicating its role as a trigger for fusion to a viable cell rather than participating in the fusion itself [20]. This is most likely through induced conformational changes, which allow the other three glycoproteins to fuse to nearby receptors. Glycoprotein C has also been found to serve in this role in some cases making it a fifth, nonessential, glycoprotein involved in fusion [17].

The receptors implicated in HSV fusion are nectin-1, Herpesvirus entry mediator (or HVEM), and 3-O sulphated heparin sulphate [17, 20, 21]. All of these are found on the surface of human cells but are significantly different in structure and purpose. Nectin-1 is a cellular adhesion molecule that is involved in the formation of epithelial cell junctions. It also plays a role in epithelial cell migration and polarization [22]. HVEM is a tumor necrosis factor receptor implicated in certain types of lymphoma in addition to mediating HSV entry [23]. Heparin Sulfate is an important proteoglycan which influences cell growth and other physiological changes [24].

Initial contact with a HSV-implicated surface receptor is not necessary for binding of the virus particle however. The particle is quite likely to come into contact with structural elements of the cell's outer membrane (filopodia cell extensions - dense clusters of actin filaments - for example). In these cases the HSV-2 particle has been shown to engage a mechanism that moves them along the cell's outer surface referred to as "surfing" [25]. Not only that, but the virus particle is also able to increase the number of filopodia on the cell's outer surface by activating key hydrolase enzymes (GTPases). HSV-2 gB also plays a role in surfing [26].

Glycoproteins H and L form a heterodimer on the virus particle's envelope and interacts with gB on fusion to a cell membrane [17, 21]. gD signals the availability of a compatible receptor and initiates conformational changes in the gB and gH/gL "fusion apparatus" which ultimately result in fusion of the virus' outer membrane to the host cell's [21]. The exact manner in which this occurs is not well understood [27]. The combination of these glycoproteins occurs only at the onset of fusion and they don't exist as a complex on the virus' membrane. Once the two membranes have been brought into contact by the fusion glycoproteins, their lipids mix and a "hemifusion intermediate" is formed[28]. The mixing eventually allows a pore to form through which the contents of HSV-2's outer membrane enter the cytoplasm of the host cell, completing the fusion and initiating the viral infection.

The fusion process described above is the most common method for HSV entry into a host cell. However, the virus also has the ability to enter certain cell types through endocytosis [27]. In this case the fusion occurs at a vesicular membrane and involves all of the same glycoproteins. This method is favoured by the virus when infecting CHO, HeLa, RPE, and certain epithelial cells while regular fusion occurs for Vero and Hep2 cells [29, 27]. gD is suspected in playing a role in selecting which entry method is used. It has been shown to down-regulate the nectin-1 receptors on the surface of cells which are entered via endocytosis [30].

2.1.2.2.2 Viral Gene Expression and Viral Replication

The Herpesvirus begins the process of altering the host cell's mechanisms for its eventual reproduction as soon as it becomes initially attached. Interaction between key glycoproteins (gD then gB) causes a phosphorylation of protein kinase B (Akt) and release of Ca^+ ions in the vicinity of the plasma membrane [31]. This in turn starts a signaling chain reaction which affects not only entry of the viral capsid, but also its transport to the nucleus of the cell. The viral

proteins and capsid are transported throughout the cell by first re-purposing cellular messaging mechanisms, most notably the Ras, Raf, MEK, and ERK pathways [32]. HSV-2's ribonucleotide reductase protein ICP10 has been found to mediate, at least in part, the activation of these pathways and prevention of cell death from apoptosis [33, 32]. Other viral proteins entering from the tegument layer induce the shutoff of host cell protein production and participate in the transport of the capsid along microtubules towards the nucleus [17, 34].
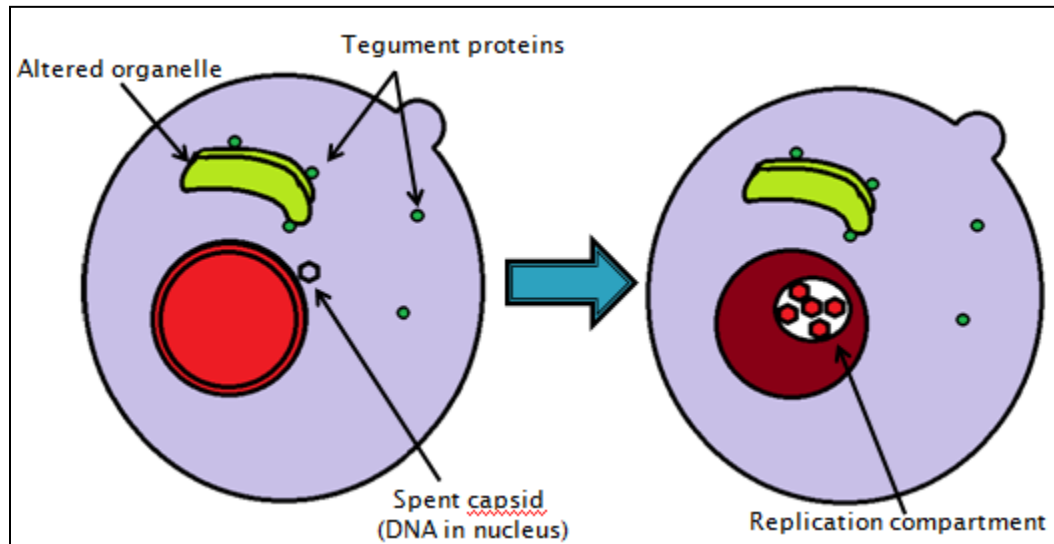
Figure 3: DNA replication and capsid assembly of HSV-2 in host cell

By the time the capsid has reached a nuclear pore and entered the nucleus (Figure 3), the host cell's structure is already in the midst of its alteration. Organelles such as the Golgi apparatus and trans-Golgi network as well as structural elements like the microtubules of the cytoskeleton are all altered to fit the needs of the virus [35, 36, 37]. While this is a common feature of Herpesviruses, the exact purpose of many of the alterations is unknown [37]. The capsids themselves have been found to accumulate around the nuclear membrane indicating that their dissolution is not necessary for the genetic material to enter the nucleus [38, 39]. Once the DNA has entered the nucleus, a series of events occurs which leads to the efficient replication of the viral DNA [2]. By this stage in the infection, the viral DNA's shape has changed from linear to circular [40] and there is strong evidence that the DNA repair mechanisms of the host cell are then recruited to repair any damage suffered by the viral DNA [41, 42].

The HSV-2 DNA localizes at particular nuclear structures, aka "Nuclear Dot 10", within the nucleus while the viral protein ICP0 breaks these structures down [2, 43, 44]. The point at which this localization occurs in the infection is still not well understood and there is some evidence that the Nuclear Dot 10 sites localize to viral DNA and not the other way around [45]. Viral proteins involved in replication are assembled around these same areas, forming small occlusions. The actual replication of the virus occurs within these occlusions (now called "replicative compartments"), resulting in their expansion and collusion (combining together to form fewer large occlusions) [46, 44]. Eventually the occlusions grow to fill the whole nucleus, marginalizing the host DNA in both space and functionality and increasing the host cell nucleus' size [47].

Expression of the viral genes begins once the genetic information has entered the nucleus and follows a very structured chronological order. It is referred to as a "cascade" of expression in much of the literature [48, 49, 50]. This cascade is broken into five different stages or groups of proteins expressed in a similar fashion: α/immediate-early genes, β_1/early-early genes, $\beta2$/late-early genes, γ_1/leaky-late genes, and γ_2/true late genes [11, 2]. These gene expression categories reflect the order in which the gene expression peaks within the host cell. Many viral proteins can be found within the cell as early as 3 hours post infection (hpi) while only reaching peak concentration at around 6 or 12hpi and being classified as a γ gene [51]. In total, the genome of HSV-2 codes for at least 84 proteins, and 16-17 microRNA's.

α genes are coded in such a way as to not require prior gene expression for their own activation and code for products regulating gene expression. The gene expression that follows relies on the α genes to initiate, with each β gene having its own set of requirements. β genes code for products with a wide array of functions, most of which deal with the synthesis and folding of viral DNA. γ genes are in general expressed later than β genes and their products require both α and β genes, and only begin expressing after the start of viral DNA synthesis. They code for products directly involved in packaging viral DNA for entry into capsids, glycoproteins, and other components involved in the final assembly and egress of the HSV-2 progeny particles [2].

Capsid proteins are not produced in the nucleus but rather translocated in from their synthesis sites in the cell cytosol [49]. The capsid is then assembled within the nucleus around a

scaffold composed of $U_L26.5$ gene product which is then replaced by packaged viral DNA. Assembled progeny virus particles consisting of a capsid and replicated viral DNA begin to accumulate within the infected cell as early as 6hpi. The accumulation continues at an exponential rate until 12hpi and then becomes linear until well into the infection (as late as 36hpi) at which point the host cell is likely already dead [2]. The other components of the final virus particle are attained on the way out of the host cell, as discussed below.

2.1.2.3 Nuclear Egress and Envelopment
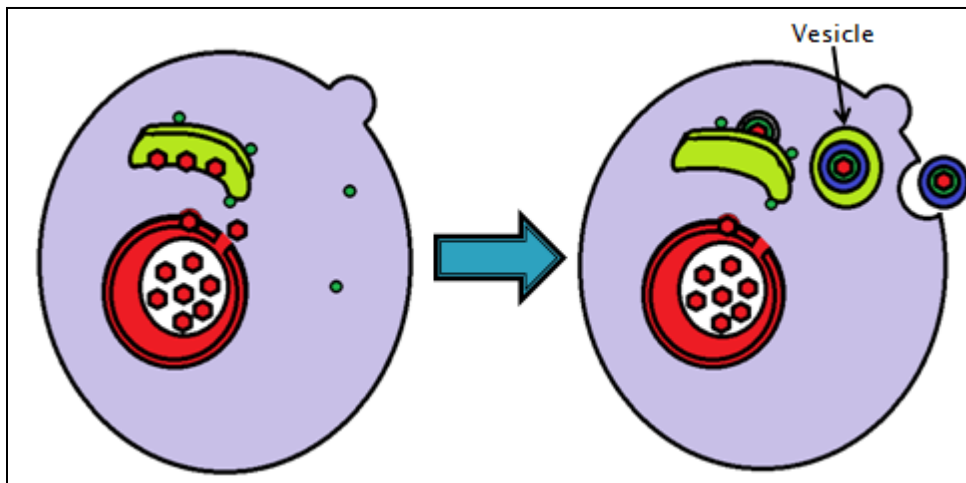
Figure 4: HSV-2 nuclear egress, envelopment, and egress from host cell

Once assembled, newly formed and immature virus particles (immature since they lack a tegument layer or viral envelope) in the nucleus face the challenge of getting through the nuclear membrane (Figure 4). Most transport in and out of the nucleus occurs by translocation through nuclear pores [52, 53] as the two layers of membrane and chromatin/lamin structures at the inner nuclear membrane make it a strong barrier. Unfortunately, viral capsids are too large to be transported through a nuclear pore once assembled and the HSV-2 particles' egress requires more specialized mechanisms [54]. The exact mechanisms of egress has been the subject of no small amount of scientific debate and the currently best-supported model is one of membrane envelopment at the inner nuclear membrane, subsequent de-envelopment at the outer nuclear membrane, and a final envelopment prior to exit from the cell [49, 55]. Much of this process is consistent throughout the *Herpesviridae* family with mostly the same proteins coded for and involved [49, 56].

The first stage of the particles' movement through the nuclear membrane is the formation of a complex between the products of the viral genes U_L31 and U_L34. This complex is integral to the phosphorylation of the nuclear lamin for the creation of budding sites on the inner nuclear membrane [57, 58] and is referred to as the Nuclear Egress Complex (NEC). The exact mechanisms performed by the complex are not well understood but it has been proven that both U_L31 and U_L34 gene products are necessary for the first (or primary) envelopment step of the HSV egress process [55]. The structure of the host chromatin is also disrupted at the sites of budding [59] in order to provide easier access to the inner membrane. From there, the NEC has been found to recruit viral glycoproteins gM, gB, gH, gL, and gD to the inner membrane of the nucleus [60] but the exact mechanisms by which they assist egress has not been determined. What has been observed is a drastic change in the shape of the nuclear membrane as it "becomes extended and tends to fold in on itself – a phenomenon known as membrane reduplication" [2].

With the completion of primary egress, the enveloped virus particle reaches the perinuclear space between inner and outer nuclear membranes. The process by which the virus particle escapes into the cell cytoplasm is one of de-envelopment. The membrane it has acquired from the inner nuclear membrane fuses with the outer nuclear space with the aid of glycoproteins B and the gH/gL complex [61]. The exact mechanism of this fusion is not known, but given the similarity of glycoproteins involved to viral entry to the cell it may be that the processes are similar. The receptors involved on the inside of the outer nuclear membrane must be defined to further understand this process [2]. In addition, there is also a distinct possibility that another nuclear egress pathway exists since HSV-2 particles with gB, gH, and gL deletion mutations can still be readily found in the cytoplasm [62, 63, 64]. It has been hypothesized that egress through nuclear pores (which become enlarged during the infection) allows unenveloped viral capsids to exit the nucleus [65]. While this would explain the presence of naked capsids in the cytoplasm, it would also require active transport on the part of the nuclear pores of which there is no evidence. No studies have shown the presence of nuclear RNA and proteins in the cytoplasm that would indicate passive transport through nuclear pores (spilling out of all material in other words) and several studies have shown nuclear integrity is maintained in spite of shuttling of viral proteins between the cytoplasm and the nucleus [66, 67].

Once virus particles have budded into the cytoplasm they must acquire their tegument and envelope in order to reach maturity and be infectious. Tegumentation of the capsids begins either at the capsid itself, at the future location of envelopment, or both [68]. There is evidence of both occurring within infected cells, and so a simultaneous two-site process with the required components gathering and assembling at both sites may be required [49]. The inner-most part of the tegument of HSV has been found to contain the protein product of the U_L36 gene, and be anchored directly to the capsid [69]. If this is the case, then the U_L36 must interact with all other tegument components as the process of envelopment moves forward [49]. The importance of a given glycoprotein to the tegumentation process varies, with the absence of gE and gM resulting in no reduction in infectious viral titer [70] while $^-$gD and $^-$gE mutants show defects and loss of titer [71].

The exact location of envelopment is difficult to gauge given the rearrangement of host cell organelles and structures during HSV-2 infection [2, 14]. Sites of envelopment have been identified by the presence of various markers which indicate the origin of a given membrane [14]. The acquisition of an envelope seems to occur close to the Golgi apparatus and there is strong evidence that the vesicles involved in the budding belong to the Golgi as well [72, 73]. At the time of budding these vesicles are found in Trans-Golgi Network-like organelles, as identified by morphological indicators, multiple TGN markers [74, 75], and the composition of the envelope of budded virus particles [76].

While the nature of the membranes involved and information on the relative importance of certain glycoproteins have shed light on the secondary envelopment process, the plethora of viral components involved, and redundancy in many of these proteins, have made it difficult to fully characterize this process [49, 14, 68, 75, 77]. The research is further complicated by the existence of both untegumented capsids and enveloped capsid-less teguments (known as L particles) and envelopes in HSV-2 infected cells [68].

2.1.2.3.1 Virus Budding and Cell-to-Cell Transmission

With the successful completion of secondary envelopment, mature virus particles (capsid, tegument, and envelope fully formed) are enclosed within a Golgi-derived excretory vesicle and ready to be transported to the cell's plasma membrane [1, 49]. From there, the virus particles must find their way out of the host cell for the infection to propagate. Virus particles can bud out

of the cell completely, becoming "extracellular free particles" [78] that can then attach to a new host cell. However, this is not the preferred method for HSV [79]. As mentioned earlier, HSV primary infections occur in mucosal layers that are made up of highly polarized epithelial cells [1]. There is strong evidence that in this kind of system, HSV prefers to spread directly through cell-to-cell junctions [78, 1, 35]. This results in lesions forming rather than a more diffuse infection patterns.

This mechanism of spread is attributed mainly to a heterodimeric glycoprotein composed of gE and gI [35, 80]. gE has been found to accumulate first at the TGN in early infection [72, 81, 80], and then at cell-to-cell junctions towards late infection [81]. At the TGN, both gE and gI interact with sorting machinery [79], thereby facilitating the directed shuttling of virus particles to either cell junctions or basolateral surfaces (those surfaces facing the surface to which the cells are attached) by the TGN vesicles [82]. The pattern of localization displayed by gE/gI coinciding with that of the TGN vesicles was confirmed through simultaneous tracking of gE/gI with cell TGN protein TGN46 [72, 79]. Viral mutants lacking either gE or gI have been found to lose their ability to infect in a cell-to-cell manner, while retaining their ability to infect cells through attachment to the outer membrane [81]. In these cells, the budding location of the virus becomes random, just as it seems to do when infecting non-polarized cells and in low-confluence cell cultures (where no cell junctions could form) [82].

The role of the gE/gI complex once the virus particles have reached cell-to-cell junctions is not well understood, but there is evidence that it may bind with junction-associated proteins, thereby acting as a receptor-binding protein (like gD is for extracellular attachment) [81, 72]. Other glycoproteins associated with direct cell-to-cell spread of HSV include gB [83], gD[63], and gH/gL [62], a cast very similar to that which is required for extracellular entry. This overlap suggests that the two methods for entry of the virus into an uninfected cell are not dissimilar in mechanism. Whichever method a particular virus particle utilizes, once it has infected a new host cell the primary lifecycle is complete and the infection moves forward.

2.1.2.4 Latent Infection

As mentioned much earlier, while initial infection and most symptoms present on mucosal layers, HSV-2 is neurotropic and capable of establishing a latent infection in host nerve ganglia [84]. The connection between recurring mucosal infections was not attributed to latency in the

nerves until 1929, when it was proposed by Ernest W. Goodpasture [85]. HSV was not isolated from nerve tissue until over 40 years later and only recently have we come to understand this process well enough to start harnessing it for gene therapy vectors. While the work conducted in this thesis is strictly with epithelial cells and non-latent HSV-2, a discussion of the lifecycle of this virus is not complete without at least a cursory summary of the latent stage.

Once the first replication cycle has been complete, some virus particles attach to axon terminals of sensory neurons beginning the process of latent infection [84, 9]. The ganglion to which these nerves are connected depends on the location of the primary infection. In the case of genital HSV-2 infection, latency is established in the dorsal root ganglion (near the bottom of the spinal cord) [9]. The tegument and viral capsid are transported together in retrograde fashion along the axons to the neuronal soma and infect the nerve cell as it would any other. During this process, the majority of the tegument proteins are lost, and the exact proteins which remain have yet to be determined. In fact, the deletion of no single gene coding for a viral protein has been found to completely stop latent infection in animal models [86, 87]. Whatever tegument proteins remain join the viral capsid and they are transported rapidly along microtubules by host molecular transport machinery [88].

Once HSV-2 capsids reach the nerves' nuclei, they have been found to express their full spectrum of genes for the first 24-72 hours (in animal models), after which they become repressed [89, 90]. The presence of active virus particles in infected ganglia remains constant for the first 7 days before dropping off, which has been found to coincide with the increase in immune response elements such as $CD8^+$ T cells [91, 92]. The exact process by which the virus becomes latent is not well understood, but it seems that the lack of expression of α genes plays a role in interrupting regular viral replication. Whether this is because the host nuclei lack ability to transcribe α genes [93, 94], the expression is repressed by the virus' own encoded latency controls [95], or (knowing what we know about HSV-2) a complex inter-related combination of factors, the virus becomes embedded in the nerve ganglia permanently and latent infection is established.

In its latent state, the virus exists as "non-integrated, nucleosome-associated episome in the host cell nucleus" [96]. This means the viral genetic information is preserved as a closed-circle DNA molecule separate from the host chromosomes and which can replicate separately

from the host DNA. No genes are expressed from the viral genome barring the latency-associated transcript (LAT), the expression of which has been found to be regulated by post-transcriptional modification rather than DNA methylation [84, 96]. The LATs most common form is 2.0kbp long and has been found to be an exceptionally stable intron [97]. A further spliced and stable 1.5kbp species has also been found in neuronal cells [98]. While its exact functions have not been determined, studies have shown its involvement in both establishing latent infection and reactivation [99, 100].

Reactivation of the virus can occur due to local stimulus, such as direct damage to latently infected cells, but is usually associated more with systemic stimulus. In most cases the stimulus is a stressor of one kind or another, with emotional stress and hormonal imbalance being among the most common. Once triggered, reactivation occurs in a small number of the infected nerve cells and the virus is very quickly transported back down to the peripheral tissues. Studies have shown that the envelope/tegument components of the virus are transported separately from the capsid components along the axons [101, 102]. In most cases, the secondary infection will occur very close to the location of first exposure and the nature of the reactivation will vary based on various factors (state of the host immune system for example). Reactivation is often asymptomatic but the host remains infectious as virus particles "shed" from microscopic lesions [2].

2.1.3 Vaccine Development to Date

The search for an effective HSV-2 vaccine has been underway for many decades now without any definitive breakthroughs being accomplished [18]. The difficulty of vaccinating against HSV-2 is two-fold. Firstly, as mentioned previously, many transmissions occur without prior knowledge of any infection by either partner in a given sexual relationship. Whether the initial infection is in truth unknown to either party is difficult to ascertain given the prevalence of asymptomatic, but infectious, carriers and the stigma associated with the infection. The virus' lifelong prognosis means that there is always a huge pool of hosts who can pass it on through carelessness or ignorance.

The second major difficulty comes from the virus' innate ability to circumvent the host's immune system. While both the innate and adaptive portions of the immune system effectively combat the infection in immune-competent individuals, they are unable to prevent latent

infection by the virus or re-activation from this latent state. Built-in mechanisms exist which induce cell death in the event of viral infection. Both HSV-1 and 2 have been shown to mediate the cell apoptosis which delays cell death until the virus has had time to replicate [103]. Once initial infection has occurred, HSV-2 spreads almost exclusively by cell-to-cell transmission, reducing the likelihood of the particles becoming inactivated by neutralizing antibodies [17, 78, 104].

There is growing evidence that shedding of the virus occurs simultaneously at various regions of the genital tract and that shedding is almost 100 times more likely at a given site if shedding is occurring nearby [105]. Either the virus reactivates simultaneously from various locations in the nerve ganglion, the virus is able to spread cell-to-cell even when subverted to a subclinical level of infection, or both are occuring. In any case it is clear that HSV-2's various adaptations have left it more than capable of outwitting the immune system and persisting in spite of the presence of specialized antibodies and T cells.

The search for an effective prophylactic or therapeutic vaccine against HSV-2 has not been given up despite the complexity of the problem. A symptomatic patient with HSV-2 clears the infection more rapidly during secondary outbreaks, and maternal-fetus transmission rates are reduced when HSV-2 specific antibodies are present [4]. Additionally, while co-infection of HSV-1 and 2 are not unheard of, the likelihood of acquiring a second HSV infection of the same type is much lower once one has already been established [7]. All of this points to the relative efficacy of our bodies' adaptive immune response. Anti-viral drugs like acyclovir also exist that suppress viral activity and reduce the symptoms of an outbreak [10, 4].

The first vaccine candidates tested for HSV-2 were subunit vaccines. These are the simplest and safest vaccines to manufacture since they aim to elicit an immune response without ever exposing the patient to an HSV-2 particle. Instead, structural/capsid glycoproteins are used separately or in combinations with an adjuvant to produce the adaptive immune response required. Several combinations of HSV-2 glycoproteins have been tested, and two have made it to phase III clinical drug trials. A combination of glycoproteins B2 and D2 (gB2 and gD2 respectively) with the adjuvant MF59, a proprietary immune response stimulant, was found to increase specific neutralizing antibody and lymphoproliferative activity but did not have a significant effect on the rate of HSV-2 infection of seronegative test subjects in serodiscordant

relationships[18, 4, 106]. A more recent vaccine candidate developed by GlaxoSmithKline is composed of truncated recombinant gD2 and an adjuvant mixture of aluminum hydroxide and 3-deacylated monophosphoryl lipid A [18, 106]. This candidate showed a very promising 70% and 40% reduction in secondary and primary infections respectively, but only in sero-negative women. Unfortunately, these findings could not be repeated in a follow-up study [107].

While subunit vaccines have been the only ones to date to reach phase III of clinical trials, several other vaccine types have been developed and tested. Peptide based vaccines containing T-cell epitopes effective in protecting against HSV-2 have been tested in phase I trials. The vaccine HerpV, which consists of a human heat shock protein (Hsc70), an array of peptides, and a seronin adjuvant, has recently (2011) shown promising response from CD4$^+$ and CD8$^+$ T cells. This is not only the first HSV-2 vaccine candidate to elicit this kind of response, but also the first demonstrated successful use of a human heat shock protein (proteins released by human cells under high stress) in a human vaccine [108, 18]. Unfortunately this is the only peptide-based vaccine that has shown any kind of efficacy against HSV-2.

Live virus vaccines have the advantage of eliciting a broad spectrum immune response from the body. There are however safety concerns with using any live pathogen as a vaccine. It is always a balancing act between making the vaccine safe and having it be effective [109, 18]. Attenuation can be achieved in different ways, but the most common method, in recently developed vaccine candidates, is deletion of key genes responsible for viral self-replication [18, 110]. Several candidates have been tested and some are currently involved in clinical trials after successfully demonstrating induction of partial immunity to infection or reduction of re-current symptoms. Early efforts included HSV-1 virus with a deletion to the gene encoding for ICP27 (an important gene expression regulatory protein [2, 18]). This gene was replaced with another segment encoding for various HSV-2 glycoproteins (gD, gG, gI, and part of gE) making it both an attenuated and a subunit vaccine. This effort was abandoned after demonstrating weak immunogenicity [48]. Both HSV-1 and HSV-2 with deletions to the gene encoding gH (which complexes with gL and is a major factor to infectivity of the virus to host cell membranes [111, 2, 21]) have been shown to reduce lesions from re-current infections in both guinea pig model clinical trials and phase I clinical trials (in the case of the HSV-2 version, called DISC or

disabled infectious single cycle)[112, 18]. The HSV-2 version of the DISC vaccine has not proceeded to further trials in spite of effective induction of immune response [113].

DNA immunization is another method which has been attempted for HSV protection. This form of immunization is intrinsically safer than many other methods (especially live virus vaccines) due to the presence of only viral DNA. As well, vaccines in this form are inexpensive to produce in high doses with very high purity [114]. Delivery of the DNA can be infection free if an aqueous solution of attenuated viral vector is used, easing vaccination. Unfortunately, the doses required for a detectable immune response are very high compared to other vaccines and even then, the T-lymphocyte response was less than anticipated; only 25% of trial participants showed a response [18].

Live virus vaccines are most applicable to this body of work and one very promising example still in the pharmaceutical pipeline is ACAM529. This double-deletion virus strain is completely unable to replicate unless it is infecting its complementing cell line (AV529-19) thanks to the absence of the U_L5 and U_L29 genes [110]. Both of these genes encode proteins related to gene replication and so while the virus is able to infect host cells, cause cell death, and elicit a full immune response, it is unable to replicate further. This vaccine has already succeeded in granting protection against HSV-2 infection in animal models in pre-clinical research [115].

2.2 Production of Virus Particles

Production of virus particles on any scale entails several unique challenges due to the nature of the product. The particles cannot self-replicate and so must be produced in a host cell line just like any cell product. Unlike cell proteins and other metabolites which may be produced through bio-manufacturing, virus particles possess a life-cycle of their own which changes the dynamics of the production process. Viral infection titer must be regulated to achieve optimal yield while also controlling for cell lysis and extracellular virus stability. In addition, most viruses produced are required to be both replication deficient and at a high level of purity given that they are often used as vaccines. There are a variety of ways to achieve replication deficiency in the virus particles and whatever the method used, the production process must account for it. High purity requirements introduce additional costs in down-stream processing which may outweigh the benefits of some production methods. Finally, each virus possesses unique properties which can

cause issues in production, such as HSV's tendency to infect cell-to-cell instead of budding into the supernatant where it is easier to isolate.

2.2.1 Cell Culture for HSV Replication

Cells grown for the express purpose of HSV-2 replication are selected based on several factors. HSV-2 is a mammalian pathogen and cannot be replicated in simpler eukaryotic or prokaryotic cells. Simpler cells lack the required mechanisms to facilitate viral protein production and gene replication. Of the mammalian cell lines available for research and industrial applications African Green Monkey Kidney (Vero) cells [116, 117], Chinese Hamster Ovary (CHO) cells [29], Human Corneal Fibroblasts [118, 119], and HeLa cells (immortal human cancer cells) [29] are the most popular. Other cell lines include Madin Darby Canine Kidney (MDCK) cells, Baby Hamster Kidney (BHK) 21 cells, and Chick Embryo Fibroblasts [120]. In 1998 the World Health Organization recommended the use of Vero cells for the production of vaccines [121], and the majority of work with HSV-2 has been conducted with this cell type. While much of the information discussed below will be applicable to all mammalian cell cultures used in virus production, the focus is on Vero cell culture and HSV-2 replication.

Most cells derived from vertebrates are primarily anchorage-dependent cells [122]. This means that they replicate only while adhering to an appropriate surface and replicate to form a confluent monolayer (a layer one cell thick). When adhered to a surface, the cells' morphology changes and they become much larger along the axes parallel to the surface than they are along the perpendicular axis [123]. Some cells continue growing after having completely filled the space available with their monolayer which necessitates the cells growing on top of each other rather than the artificial substrate [124]. This stratification is highly limited by the lack of an extracellular matrix in most cell culture applications outside of tissue engineering [124], which is not used in virus production. It is possible, through some modification, to adapt adherent cells to growing without any anchorage [125]. This can be useful in certain specialized applications

There are advantages and disadvantages to both adherent and non-adherent cultures. The former makes cells easier to visualize using light microscopy as they grow in a two-dimensional manner [122]. This allows for easy monitoring of cell culture growth and health. Being most cells' natural growth pattern, it also removes the need for adaptation to different conditions. The main drawback to adherent cultures is the limitation of space in the two dimensions available.

20

Cells growing in suspension remain in contact with media even at very high densities while adherent cultures are limited to the available treated surface area [122]. This makes scale-up of a production process with anchorage-dependant cells more difficult and requires specialized technologies.

2.2.1.1 Traditional Adherent Cell Culture Scale-up

Scale-up is a necessity in any bio-manufacturing process. Methods which are efficient and effective at lab scale become unwieldy and expensive when the required quantities of product increase a hundred-fold or more. Suspension cultures can simply be handled using larger bioreactors, though mass and heat transport become more complex. With adherent cultures the product output is proportional to the surface area available to the cells and the footprint becomes a serious issue as the scale increases. The earliest scale-ups in the 1950's were done using large glass Povitsky flasks [120] and suffered for this very reason.

The disposable roller bottle (Figure 5) was developed in the 1970's and quickly became the main method for large-scale bio-manufacturing [120]. Cells are grown on a curved surface of a cylinder rather than a flat surface. This cylinder is rotated at a rate so that the cells all along its circumference remain wetted with media. The bottles come in a wide variety of sizes and scale-up involves the use of hundreds of such bottles at once. Besides allowing for simpler stacking and a better surface area to footprint ratio, the roller bottles also introduced media agitation to adherent culture which prevents concentration gradients from forming [120]. As a disposable technology, roller bottles also eliminate the need for in-line cleaning. Unfortunately, roller bottles are still labour-intensive as each must be seeded and infected individually. While roller bottles are no longer the golden standard for bio-manufacturing, they are still used for many of the processes which were initially validated for them. Modern set-ups have been optimized in terms of surface treatments and shapes.
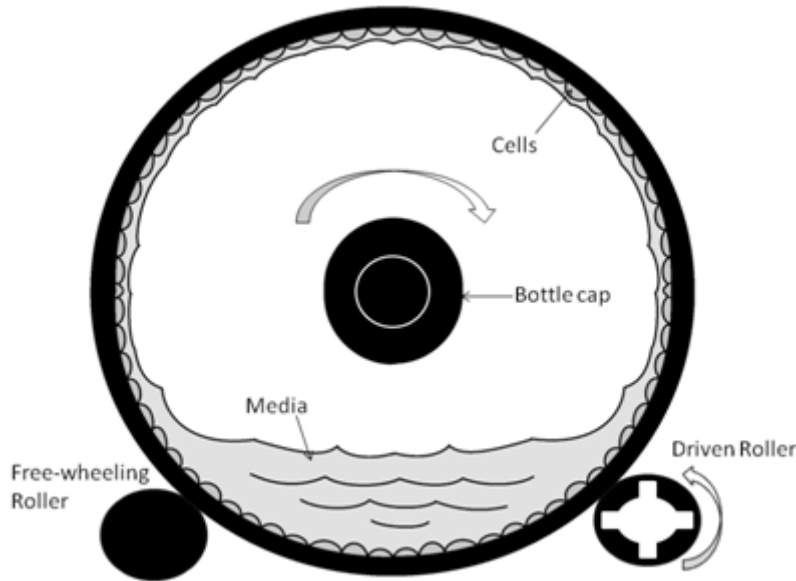
Figure 5: Roller bottle cross-section

Neatly stackable flat-bottom flasks can fit as many as 40 trays in the same space as a single basic flask. These are used extensively for the efficient culturing of cells. These flasks also come with valves and ports for attaching media pumps and can therefore be used in semi-continuous production processes. While these multi-trays can offer a much higher efficiency than even roller-bottles for lab work and small-scale manufacturing, they remain too limiting for the highest-volume applications [126]. To reach the same efficiency at larger scales, microscopic surfaces are often required.

2.2.1.2 Micro-carrier Cell Culture

Micro-carriers (MC) allow the efficiency of a suspension culture to be attained with a cell line dependant on anchorage, or at least come much closer than previous technologies allowed. They also allow the process to be carried out using stirred-tank bioreactors, some of the best-understood and most optimized equipment available for work with cell culture [120]. The result is a culture which can be easily controlled for culture parameters, can be easily adjusted for cell density by changing MC concentration, and for which perfusion is easily accomplished [127]. The basic concept is the culturing of adherent cells on microscopic particles which can then be suspended in media and cultured in a specially designed bio-reactor. This method is almost as old as the roller bottle, with the early development starting in the late 1960s [128], and has

22

undergone extensive development as new materials, coating, and morphologies became available.

Materials used for the main matrix of the carriers vary widely in their stiffness and application. Dextran, cellulose, polystyrene, glass, gelatin, and silica are all used in commercially available micro-carriers [127]. No matter what material is used, the density is always just above 1g/mL in order to be easy to suspend in culture media. The overall shape of the particles is usually spherical, although cylindrical and hexagonal particles are also used. Sizes range from 100μm to about 400μm with larger carriers available, although these are technically not on the micro scale. More unique morphologies exist within these general shape categories as well. For example, macroporous carriers have been developed which can protect the cells from shear stress within a bioreactor [129].

The actual process of culturing cells on micro-carriers is the same as for any suspension culture except for a few key differences. Since the cells are not actually in suspension the first step is to seed the MC. The methods developed are in many cases proprietary to the pharmaceutical company that developed them, but the basic concept is almost always the addition of the beads to a gently stirred suspension of cells [130]. The attachment occurs without any outside assistance in most cases and the cells spread across the surface of the beads if allowed sufficient time to replicate. Bead-to-bead transfer is also possible in some cases, allowing all beads to become seeded with smaller inoculums.

The mode of attachment depends on the micro-carrier used. Some are coated with positively charged functional groups (which facilitate up to 90% cell attachment but reduced growth) or a collagen-like protein (on which cells grow readily but attachment is less efficient) [127]. Once a sufficient density of cells is achieved, the micro-carriers can be used like any other suspension to produce virus stock.

2.2.2 Dextran Sulfate Treatment

The virus production methodology discussed so far has mostly dealt with the properties and requirements of the cell culture used. Once the cells are healthy and available in sufficient density, the virus is introduced to the system and it is the properties of the virus which drive the process. Multiplicity of infection, batch culture time, and virus collection strategies are all

optimized for the virus being produced. One property of the HSV specifically is its limited budding into the supernatant. The majority of viable particles infect in a cell-to-cell manner or remain membrane-bound on the host cell surface. If only the virus particles in the supernatant were collected the overall yield would be unacceptably low even before down-stream processing (which always comes at a cost to yield).

This issue can be addressed by simply lysing the cells to free the virus particles, but this causes several issues. First, the virus particles within the cells are not all mature and infectious and can be difficult to separate from viable ones. The second issue is that lysis increases the level of contamination in the process stream significantly. The regulation-mandated threshold on host cell proteins and DNA for vaccine candidates is very low and clearing this contamination would not only increase costs but also reduce yield [131]. Chemical treatment of the cells in order to elute the virus particles allows lysis to be avoided but requires a good understanding of the binding mechanisms of the virus particles to the cell membranes. As long as the chemical can then be removed from the production stream, elution is the optimal solution.

Early on in HSV-2 research it was observed that the polyanionic polysaccharide heparin had an inhibitory effect on the virus at high concentrations (10-20 mµg/mL) [132]. It was found to prevent the infection of cells at the very earliest stages, likely interfering with adhesion to the membrane or entry (at the time, researchers could not determine which). Later on it was discovered that this property is shared by other sulfated polysaccharides including Dextran Sulfate (DS) and chondroitin sulfate [133, 134]. Only a few viruses aside from HSV are inhibited in this way and all of these are enveloped viruses. These include cytomegalovirus, vesicular stomatits virus, and human immunodeficiency virus [133]. More interesting still was the observation that at lower concentrations the polysaccharides actually have the opposite effect with some viruses, increasing the infectivity of the viruses [135]. All of this evidence points to an interaction between sulfated polysaccharides and the membrane glycoproteins of the virus.

As discussed in detail in Section 2.1.2.2.1 Fusion and Entry section, viral adhesion to host cell membranes occurs through interaction of viral glycoproteins with various cell membrane receptors. The very first step of the adhesion process involves glycoprotein C interacting with "highly sulfated cell surface glycoaminoglycans, such as Heparin Sulfate" [135]. Both HSV-1 and HSV-2 bind to these receptors, and although both have alternative routes of entry, their

infectivity is severely impacted if a receptor of this type is unavailable [136]. Those virus particles which have yet to undergo further adhesion to the host cell membrane can be eluted back into solution with the addition of heparin or Dextran Sulfate (DS) [137] and this has been found to also be true for membrane-associated progeny virus particles [117].

Based on the evidence presented above, it has been deduced that a polysaccharide like DS can be used to recover membrane-associated virus particles from host cells through preferential binding. The reversible nature of this bonding eases purification of the virus particles in down-stream processing and since the method is non-disruptive to the cell membrane, there is no additional contamination of the product stream. Treatment with DS is used for the HSV-2/Vero cell vaccine candidate elution at Sanofi Pasteur on a large scale and the purification scheme which is made possible by the harvesting method yields a ~200 times more pure final product (in terms of host cell contaminants) [110].

2.2.3 Downstream Processing (DSP)

Once virus particles have been harvested from the cell culture, they are purified in order to remove contaminants. Contaminants can include host cell DNA and proteins, cell media and its components, and chemicals added to the product stream (like DS used in cell elution). The volume of the process stream is almost always reduced drastically as part of the down-stream processing, which concentrates the virus to the concentrations required for the particular application. Virus particles, and HSV in particular, are known to degrade and become non-viable fairly quickly so stabilizing agents are added [138]. Ultimately, this work should yield insights on how to process and recover HSV-2 from Vero cells. Although the downstream processing of HSV-2 is not within the scope of this work, a review of DSP of viruses and virus-like particles was conducted and is presented in Chapter 3 in order to round out the discussion of this work.

Chapter 3 – Downstream Processing of Virus Particles from Cell Culture

This chapter was originally written as a mini-review for a grant application with the help of other members of my research group. I would like to acknowledge Megan Logan, Steve George, and Stanislav Sokolenko who co-authored the original document, much of which was retained in this version. I was first author on the original document and am solely responsible for the work which was required to convert it from a 7-page mini-review to its current version for my thesis.

3.1 Outline

Virus particles are being manufactured in higher amounts than at any other time in human history. The demand stems from research into novel uses for these particles, from both large-scale and small-scale manufacturing of pharmaceutical products, and from numerous trials of novel therapeutic candidates. All require high yields of correctly assembled, and often ultra-pure, virus stock. The crude product stream (either lysate or supernatant) must undergo extensive down-stream processing (DSP) in order to meet purity regulations in a financially viable manner. Making up as much as 80% of overall per-dose cost, DSP represents a significant area for optimization and a very active field of research.

The entire process can be broken down into three main stages. The process starts with clarification, which aims to remove large-scale contaminants while maintaining the integrity of the desired product. Clarification is being done mostly by disposable filtration units including dead-end depth filtration and body-feed filtration. These allow for high throughput while minimizing the need for process validation. Aqueous two-phase systems are also being implemented, thereby combining clarification with the next step in DSP of virus particles, concentration and purification.

Concentration refers to the reduction of the process volume. Diafiltration can achieve this while also removing impurities from the process stream. Membrane technology has become more popular than resin chromatography in some applications. Where chromatography is still the method of choice, larger pore-size resins are being developed to purify larger molecular-weight biological products like virus particles. Monolith columns have also seen a rise in development recently.

The final stage of DSP is polishing, where the product is brought into compliance on purity without sacrificing yield. For this stage, chromatography remains the method of choice with research focused on development of more ideal stationary phases. Ion exchange, size exclusion, and metal affinity chromatography are currently in use. Diafiltration has also been shown to have potential, but may not be appropriate for all polishing applications.

DSP of virus particles is a field that is very much growing, and ongoing research is focused on making the production of high yield and purity particles more cost effective. Novel therapeutics and vaccines each come with their own set of DSP requirements and characteristics, meaning the field is unlikely to ever reach a point of stagnation and regular reviews of the methodology will continue to be required.

3.2 Introduction

The production of complex biological particles for use in vaccines and therapeutics is both technically difficult and financially restrictive. Any biopharmaceutical manufacturing process aims to produce at the lowest possible cost per dose while maintaining the highest standards for purity (in terms of host cell DNA, host cell proteins, and presence of chemical reagents [131]). This balance is even more difficult to achieve for the newest wave of vaccine candidates and therapeutics comprised of large complex biological compounds produced in cell cultures. Products like virus-like particles (VLPs), viral vectors, monoclonal antibodies, and various nucleotides all show tremendous potential, but come with inherent challenges for DSP. Since DSP commonly accounts for as much as 80% of the overall cost of vaccine production [139, 140], it is a prime candidate for optimization and the development of novel technologies. This review focuses on recent developments in the downstream processing of viruses.

Live viruses can be used to deliver genes of interest into a cell, thereby adding to the cell's genomic content, or resulting in the production of a desired cell product. When used in this way a virus is referred to as a viral vector. Viruses may also be produced in a less modified form for use in vaccines and for research purposes. Viruses are large for biopharmaceutical products (on the scale of 10^7 Da compared to monoclonal antibodies with a size on the order of 10^5 [131]), which has a significant effect on the DSP. Viruses can be enveloped (structural proteins are enclosed in a membrane layer of lipids and glycoproteins [2]) or non-enveloped and may be secreted or localize within the cells in which they were produced. In most cases, enveloped

viruses are found on the outside of the cell as they acquire their envelopes as part of a secretory pathway with membrane proteins trafficking to the plasma membrane [141, 142].

Challenges to DSP arise based on the nature of the virus production process. Enveloped virus particles may not require cell lysis for separation, but they can also be sensitive to shear stress and osmotic pressure due to the labile nature of the envelope [143]. When production of virus particles occurs in bacterial cells, endotoxins become a major concern and must be eliminated quickly to ensure protein stability [144, 145]. In insect cell systems, baculovirus may be co-produced and have a molecular weight similar to that of the desired product [146]. Other systems may be required to produce highly variable products, such as those producing different influenza vaccines every year to keep up with natural mutations [147]. It is clear that the processing of virus particles must be not only high resolution but also specifically tailored to the system in question.

DSP of virus particles can be broken down into three stages: clarification, concentration, and polishing (Figure 6). The advances in each area are covered separately below for a wide array of applications. The actual process steps used depend in large part on the properties of the product and process stream. As with any separation process, reduction of stream volume is done as early as possible to minimize overall costs and reduce the required equipment size.
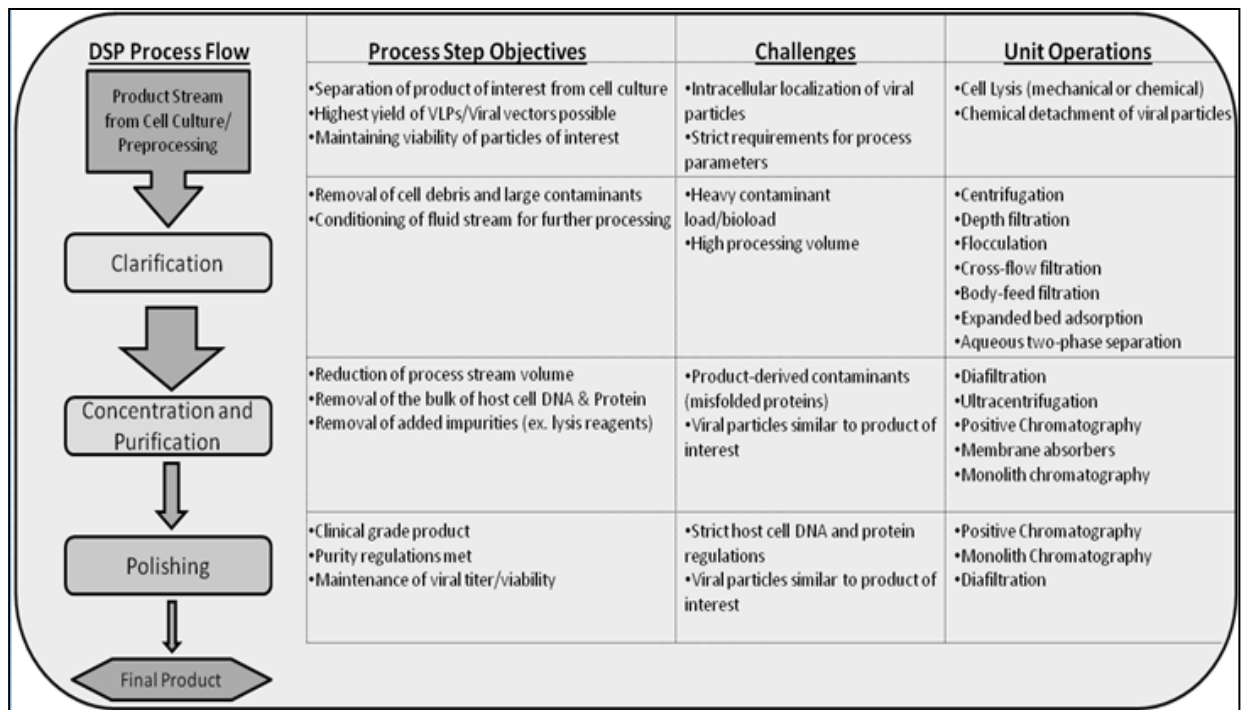
Figure 6: Summary of DSP of virus particles

3.3 Clarification

Every virus particle production process begins with upstream production in a cell culture. Once this step is complete, a preprocessing step may be necessary before clarification can begin; the virus particles must be separated from the host cell so they are released into the cell media. Cell lysis may be needed in case of intracellular products such as non-enveloped viruses e.g. adenoviruses [148, 149]. Additives can also be mixed with the starting solution to help with the freeing of virus particles from the cellular membranes, as with the case of HSV-2 where Dextran Sulfate is used to help dissociate the virus from the cell membrane [150].

Extracellular products have the benefit of being excreted from the cell and can be isolated in the supernatant without extra processing steps [151] and cell lines are even being genetically engineered to efficiently excrete the virus particle to aid in the downstream processing [131]. Protease inhibitors are another additive added at this stage in order to protect the final product from degradation[152, 153]. Those systems in which cell lysis is unavoidable almost invariably suffer from higher host cell protease concentrations. In general, while adding extra components may aid in the initial separation process, these compounds have to be removed in subsequent purification steps. This can add further complexity to the purification and polishing steps and the overall yield can suffer for it.

Flocculation can be used as a pre-clarification step to aid in the separation of cellular debris from the product. It involves the addition of other components such as inorganic salts, organic solvents, acids or bases to the cell media to precipitate out unwanted contaminants or to precipitate the product [149]. This has primarily been used for intracellular VLP's [154]. This step is usually followed by centrifugation of the flocculated material.

Clarification is the first major step in the downstream bioprocessing of a cell culture fluid solution. The main goals of this step are to remove cells, cell debris and other large contaminants and to condition the fluid for further downstream processing. Clarification usually follows a general 3-step process: centrifugation to remove cells and solid, depth filtration to remove smaller particles, colloids, and contaminants and a final filtration step to reduce the amount of biological material further. This is done to avoid filter or column clogging in later purification steps [155].

The mechanical separation of large particulates has traditionally been done by centrifugation. However, with the rise of single-use, disposable units for biomanufacturing centrifugation is in some cases replaced with a series of dead-end depth filters with diminishing pore size [131, 156]. Pore sizes start out fairly large (~3µm) and then decrease to about 0.45-0.8µm [157, 158]. Single use filters reduce the need for cleaning and validation, decreases the change-over time, and lowers the risk for cross-contamination in multi-purpose facilities [159, 160, 161]. Along with these benefits depth filtration has limitations such as filter blocking, turbidity breakthrough (the piercing of the membrane by contaminants due to the buildup of pressure), and required pre-flushing of the filter material [155]. For these reasons research has been directed at searching for alternative single-use methods for clarification: cross-flow filtration and body-feed filtration [162, 163, 164, 131, 165].

Cross-flow filtration is done by pumping the feed in a tangential direction across the membrane while having pressure applied to the system to allow the permeate to pass through the membrane. Particles that are too large to pass through the membrane remain in the retentate and are recirculated [164]. The principle of using cross-flow filtration is to avoid clogging of the membrane. There are different membrane configurations, such as hollow fiber, flat sheet, tubular, spiral wound and vibrating membrane systems and each has their own advantages and disadvantages [166]. Even though these methods can handle high solids loads, they can result in

poor yields due to polarization at the membrane surface and sometimes require excessive dilution of the product which can limit the use of this technology [149].

Body-feed filtration has been adapted from the plasma fractionation industry and it was originally used to fractionate human plasma into its components such as albumin, clotting factors and immunoglobulins [167, 168, 169]. It uses selective precipitation by adjusting pH, ionic strength, addition of alcohol and temperature changes to form precipitates that are then removed by depth filtration. It involves a two step process; 1) adding a precoat of the filter aid (for example diatomaceous earth or cellulose fiber) to the filter septum and then 2) continuously adding small amounts of the filter aid to the liquid so that a new filtering surface is continuously being added (Figure 4) [170]. The disadvantage of this technology is that by the addition of filter aids, there is an increased risk of product contamination and cross-flow membrane fouling, which would reduce the flux rates [154].
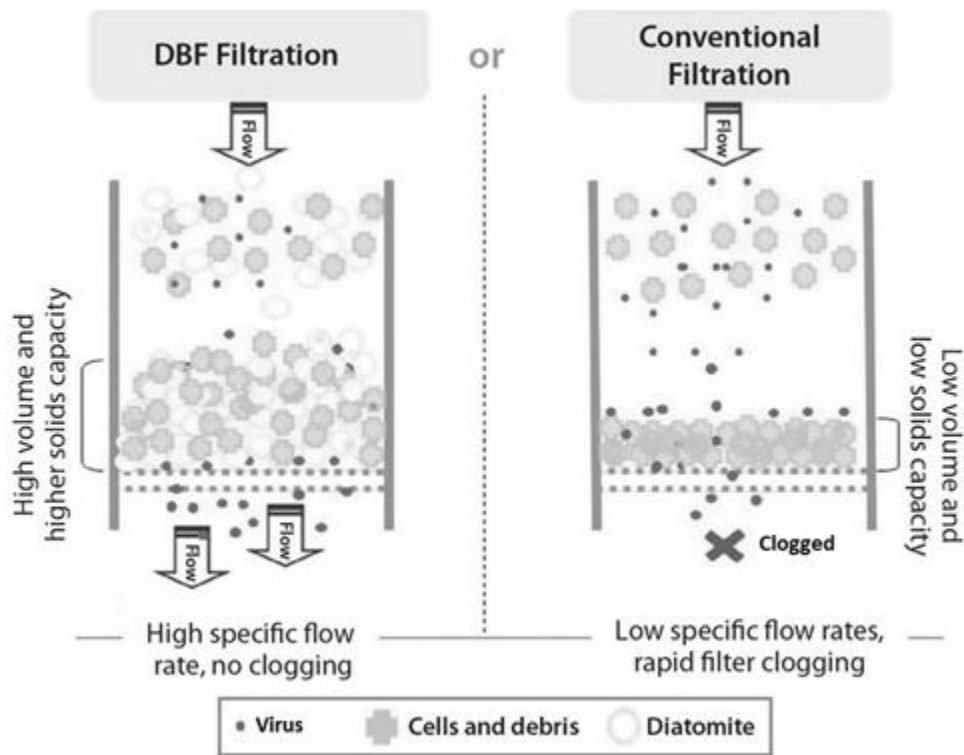
Figure 7: Comparison of dynamic body-feeding filtration and traditional depth filtration (image adapted from van der Meer et al. 2014)

One recent trend aimed at reducing DSP costs is the combination of clarification with concentration and purification. Some ways of accomplishing this are by doing a direct capture of the product with an expanded bed adsorber, by using a multi-stage aqueous two-phase extraction [166, 171], or by using disposable cross-flow filtration systems [165]. Expanded bed adsorption works like classical chromatography, but the solid resins are in a fluidized state which creates larger voids for whole cells, or cellular debris to pass through. In practice there is interaction between the biomass and the adsorbent phase, which causes increased buffer consumption and decreased sorption performance [172].

Aqueous two-phase systems (ATPS) are composed of either water soluble polymers (such as polyethylene glycol or dextrin) or a combination of a polymer and a salt [173] in a system composed mostly of water (making for a relatively bio-particle friendly environment) [174]. The process works by having the two phases separate the proteins/virus particles based on their surface properties. This has been successfully used for purification of many biological products including organelles, bio-nanoparticles, and genetic material [175, 176]. This method is easy to scale-up, can be low-cost (especially from the materials cost side), and has the ability to select particulate materials from the crude cell media [177]. There are still many disadvantages to this method due to its novelty (as a large-scale manufacturing DSP method) including large amounts of process development required, low capacities and limited mechanistic understanding [177].

Where implemented, ATPS has been found to carry the risks of loss in virus infectivity (in viruses sensitive to high ionic strength solutions), protein co-purification, and difficulty in recovering polymers [178]. On the other hand, most non-enveloped viruses can maintain infectivity under these conditions. It has already been demonstrated that ADPS can be used as a combined clarification-purification step for porcine parvovirus, achieving a high infectious yield and separating major contaminating proteins effectively [178]. Adenovirus [179], Adeno-associated virus[173], Poliovirus [180], and Malignant Catarrhal Fever Virus [181] have all been successfully purified with ATPS.

3.4 Concentration and Purification

The goals of this stage of DSP are to reduce the process volume as much as possible and to remove host cell proteins (HCP), host cell DNA (HC DNA), and other impurities such as lysis

reagents used to disrupt cells. While ultracentrifugation is the most established technology for this kind of processing, membrane and resin chromatography based systems have seen increased popularity due to the easy scale-up as well as advantages in selectivity and footprint. As a first step though, diafiltration is a useful method to remove small molecule impurities like detergents [182], to exchange buffers [183], and to concentrate the process stream.

Various modes of operation are possible, with constant volume diafiltration reported to give VLP recovery yields of about 78% with murine polyomavirus VLPs [183]. A further concern is the need for the removal of HC DNA to comply with federal regulations. This is currently done using the addition of benzonase to a concentrated stream prior to further purification, and can be integrated into a discontinuous diafiltration process, such that benzonase can then be removed during the buffer exchange step [184].

A major concern for filtration steps is the need to establish process parameters that would reduce membrane fouling, while providing acceptable concentration factors. For instance, a higher operating pressure and flow rate would increase the amount of liquid processed per unit time, and may provide higher concentration factors, but can cause membrane fouling [182, 183]. Diafiltration can be run in tangential flow modes to reduce this problem [185]. This process has been shown to remove up to 90% of the host cell proteins and DNA from a rotavirus VLP process stream [182].

The most common next step of the process involves the purification and concentration of the product of interest using "positive chromatography" in the bind-elute mode [131]. These processes can be classified into ion exchange chromatography, affinity chromatography, hydrophobic interaction chromatography, and size exclusion chromatography [186], with the type of purification strategy being used depending on virus characteristics such as size and surface charge.

Recently, some interest has grown in using biomimetic design for the development of new affinity chromatography ligands. By using binding structures from known receptor proteins, it has been shown that very high affinity can be achieved for specific proteins of a VLP. Such a custom ligand was developed for a VLP of murine polyomavirus (MPV) by Yanying Li and his group in 2014. This ligand was shown to be efficient enough to purify the VLP capsomeres from

crude cell lysate in a single separation step, followed by successful self-assembly of the particles [187]. While this approach shows great promise in challenging separation environments, using biological systems for the production of affinity ligands is expensive, time-consuming, and reduces their applicability for scaled-up manufacturing processes. Luckily, the fields of molecular modeling and combinatorial chemistry are growing quickly and can provide more cost-effective ligands without any threat of contamination for VLP and virus purification [188].

Traditional chromatography, using beads and absorptive resins as supports, depends on the transport of the product of interest into pores which are usually quite small, usually 60 - 100 nm [189]. In addition, high shearing forces can be present within the column [190]. This is difficult for bulky virus particles and these processes must be run at low flow rates [171]. In addition, fragile enveloped virus particles, and filamentous viruses can be especially sensitive to shear forces, and their purification by resin bead chromatography may be problematic. Large pore size membrane adsorbers are an excellent solution to these problems, and can be operated at higher processing rates. They also allow for lower pressure drops [191] and higher flowrates that can reduce process times up to 10% compared to traditional columns [192]. Monolithic columns, which are highly porous and contain uninterrupted and interconnected channels, offer the advantages of membranes, such as large pore size of up to 1500 nm [193], but with increased resolution, and lower dead volume [186]. Monoliths are more common in polishing and are discussed in more detail below.

There are many examples of column resin-based separation processes for the purification of virus particles [186]. Membrane technology, however, is relatively new, and the two most popular membrane devices are the Mustang® and Sartobind® resins from Pall and Sartorious respectively. Scale-up compatibility with this technology is also excellent, allowing for processing capacity of up to 100kg [194]. Ion exchange membranes have been used for the purification of AAV [195], Adenovirus [185], Baculovirus [196, 197], Lentivirus vectors [198, 199, 200], Retrovirus vectors [200] and Influenza vaccines [201].

Various affinity membranes have been used for virus purification, including the use of sulfated heparin membranes for the purification of vaccinia virus [202, 203] and influenza virus [204], and metal affinity resins for the purification of influenza virus [205] and adenovirus vectors [206].

34

The purification of biologics by monolith columns is even newer than that by membranes, and there is now much interest in their use for virus particle purification. These columns have been shown to be much superior to traditional resin bead columns in terms of virus particle recovery, and ease of operation, which stems from their open pore structure which provides increased accessibility to the interior [207]. Monolith columns also offer non-turbulent flow and low pressure drops even at high flow rates [190]. Ion-exchange monoliths have been used for the purification of bacteriophage [208], baculoviruses [209], enterovirus 71 [189], influenza viruses [210], tomato mosaic virus [193], and rubella virus [190], and for the purification of adenovirus VLPs [211]. In addition, hydrophobic interaction chromatography using monoliths has been used for the purification of Hepatitis B VLPs [207]. Affinity chromatography in monoliths has also been done for the purification of lentiviral vectors by metal ion affinity columns [212] and biotinylated retroviral vectors by strepavidin functionalized monoliths [213].

Monolithic column chromatography methods often report very high recoveries, especially when compared to traditional bead chromatography. Monolith columns have also been successfully used for the purification of filamentous viruses, albeit with lower recoveries of about 50% [208]. Other types of chromatography have also been used for virus purification including hydrophobic interaction chromatography [202] and hydroxyapatite pseudoaffinity chromatography [214]. A detailed review of chromatography-based virus purification strategies used for different viruses prior to 2010 can be found elsewhere [186].

3.5 Polishing

Polishing represents the final step in downstream processing. What that entails depends in large part on the global processing scheme and virus. However, clinical grade material will typically have stringent requirements on contaminating DNA or protein content as function of dose amount [215]. As the input material has already undergone one or more processing steps, polishing can involve more specialized approaches, tailored to the requirements of the overall process. Furthermore, a previous reduction in contaminating material and concentration facilitates applications that would be too costly to apply to crude cell supernatant or lysate. These factors combine to make chromatography one of the only practical polishing options [131, 215, 216]

Despite the strong focus on a single methodology, new polishing options are emerging with developments in chromatography technology. The biggest of these have been in the use of different stationary phases. The typical approach of using bead resin has significant issues with poor diffusion of large biomolecules such as VLPs and viruses due to small pore size and high pressure requirements. Decreasing bead size for improved diffusion only exacerbates the issue of pressure [217]. The result is a tradeoff between processing time and possible damage to highly sensitive membrane glycoproteins [216]. One solution to this problem has been to move to single-piece "monolith" or membrane stationary phases [217]. As previously mentioned, both feature much larger channels that allow greater access for large biomolecules. A recent monolith application has reported improved flow rate as well as capacity [207], with other reports of good DNA clearance [218]. In another case, an overall process yield of 38-45% was achieved for canine Adenovirus polished with anion exchange monoliths [219]. Apart from changes to the stationary phase, different chromatography configurations are also being explored [220].

Of the various available chromatographic techniques, two are commonly encountered in polishing applications. General polishing makes use of size exclusion chromatography to filter out small contaminating particles such as DNA or proteins. However, new developments in ultra and diafiltration make them competitive options in some applications [143]. While there are reports of using only diafiltration as the final processing step [221], it is difficult to generalize such reports to all polishing needs. For more specific applications, ion exchange and affinity chromatography remain the preferred options [215]. While ion exchange may not be enough to discriminate between two different virus capsids, there have been new developments in the use of various fusion tags such as polyionic insertions [222]. The insertion of a polyionic tag has been demonstrated for a polyome VLP, albeit not in the context of chromatography [223].

There has also been at least one case of using immobilized metal affinity chromatography for VLP separation, without the need for a His-tag [224]. The researchers argued that the natural occurrence of histidine and other protonated amino acids (such as glutamic and aspartic acid) was enough for electrostatic interaction with the metal-ion-matrix. While affinity chromatography offers the greatest sensitivity of all the polishing methods, elution can remain a challenge due to capsid sensitivity [215].

3.6 Conclusion

Downstream processing of virus particles is a fast-growing field of research in which well entrenched traditional separation methods are currently competing against emerging technologies. Traditional approaches have a higher breadth of research available into their implementation and more work has been done on their optimization. In many cases, the older technologies are in higher supply and can perform much the same tasks at a lower cost. On the other hand, newer methods offer many advantages including higher resolution of separation, lower diffusion mass resistance, and disposable units (no cleaning or validation required).

Many challenges and opportunities for research breakthroughs remain for the field of virus particle DSP. Separation of similar and/or closely related viral species with similar physical and chemical properties remains difficult. Depending on the application, viral activity is either a requirement or to be avoided resulting in process-specific challenges not easily solved. Viral inactivation during DSP is still not well understood in many cases [225]. Aggregation of viruses and viral proteins is an issue in almost every DSP technology and results in loss of overall yield of usable product if not carefully controlled [226, 225].

As with any manufacturing process the overall cost-effectiveness is a very important deciding factor. The lowest cost per dose possible while meeting all regulatory requirements for purity is the ultimate goal of many DSP schemes. Whether this means returning to the "golden standard" or investing in the state of the art depends on the product and the preference of the engineers designing the system.

Chapter 4 – Materials and Methods

4.1 Cell lines and virus stock

4.1.1 Vero cell culture maintenance and methods

Unless otherwise noted, all experiments described were conducted using a genetically modified HSV-2 strain and complementing cell line in which it is able to replicate. The virus, ACAM529, is deficient in two genes. The first, U_L29, codes for ICP8, which is required for binding of viral DNA and DNA synthesis. The second, U_L5, encodes a "component of a heterotrimeric helicase-primase complex"[2] that interacts with ICP8. Therefore, this virus cannot replicate in regular human cells. As a result ACAM529 has a reduced biohazard risk designation of Risk Group 1 (wild type HSV is designated Risk Group 2). ACAM529 is also referred to as *dl*5-29 in older literature.

The complementing cells are from a cell line called AV529-19 (also known as HSV2013-121), which is a Vero cell line that has been stably transfected with plasmids pCId. U_L5 and pcDNA.U_L29 (Dr. David Knipe, Harvard Medical School). This transfection enables the cells to "rescue" the virus and allow it to replicate. A second stable Vero cell line (HSV2012-121), based on AV529-19, transfected with another plasmid containing the gene for the enhanced Green Fluorescence Protein (eGFP) under the HSV-2 ICP10 promoter, was also used in the body of this work.

4.1.1.1 Vero cell culture maintenance

Vero cells were cultured in flat-bottom surface tissue culture flasks; either a T150 flask with ~$50cm^2$ surface area (Fisher Scientific, Whitby ON, CA, cat #:12556-011) or a T175 with ~$75cm^2$ (Corning Cellgro, Manassas MA, USA, cat #: 29186-105). Cells were grown in Dulbecco's Modified Eagle Medium (DMEM) with F12 supplement (Corning Cellgro, Manassas MA, USA, cat #: 90-090-PB), 4mM L-Glutamine (Fisher BioReagents, Loughborough, UK, cat #: BP379-100), and 10% Fetal Bovine Serum (Gibco Life Technologies, Burlington CA, SKU #: 12483-020). Initially, cultures were provided with 1mM Puromycin (Corning Cellgro, Manassas MA, USA, cat #: 61-385-RA) and 1% G418 Sulfate (Corning Cellgro, Manassas MA, USA, cat #: 30-234-CR) but both of these antibiotics were removed from the media for the majority of the work to reduce stress on the cells.

Cells were seeded in the culture flasks at between 1.0×10^5 and 1.5×10^5 cells/mL and allowed to grow to confluence (monolayer of cells completely covering the surface of the flask). Confluence was monitored visually using an inverted light microscope. To passage cells, media was aspirated and the cells washed using Dulbecco's Phosphate Buffered Saline (DPBS) (Life Technologies Inc., Burlington ON, Canada, cat #: 14190-144). Once washed, the cells were treated with TrypLE Select enzyme (Life Technologies Inc., Burlington ON, Canada, cat #: 12563-029) for 10 min to dislodge the cells from the culture flask surface. The cells were resuspended in media (containing FBS as described above) for aspiration (volume dependent on the flask size) which also deactivated the TrypLE thanks to protease inhibitors contained in the FBS [227]. The suspended culture was then centrifuged at 115 x g for 5min and the supernatant containing TrypLE was removed. Lastly, the cell pellet was resuspended in fresh media and the cells seeded into a new flask.

4.1.1.2 Cell banking

A cell bank was created by freezing cells in liquid nitrogen (-196 ℃). First, cells were grown to confluence in one or more T175 T-flasks. Cells were then recovered using TrypLE centrifuging at 115 x g for 5 min and resuspend the cells in a solution of cell media and 10% DMSO (Sigma-Aldrich, Oakville ON, CA, cat #: D2650) at $1.0 - 5.0 \times 10^6$ cells/mL and aliquoted into 1mL cryogenic vials (Thermo Scientific Nalgene, cat #: 5000-0020). The cryovials were then placed directly into liquid nitrogen for storage. The cell banks were maintained at around -196 ℃ in liquid nitrogen within a double-insulated Dewar flask once frozen.

4.1.1.3 Thawing cells

Thawing of the cells was conducted whenever a new culture was required. It was also done right after a batch of cells was banked to ensure freezing was conducted effectively and frozen cells were viable. To thaw out cells, one cryo vial was removed from the liquid nitrogen Dewar flask and placed in a 37 ℃ water bath. Once thawed, the cells were pipetted drop by drop into DMEM/F12 cell media. The suspension was then centrifuged at 1000rpm for 5min and the media aspirated to remove the DMSO. Lastly the cells were resuspended in fresh media and the whole suspension was used to seed a T150 culture flask. 24 hrs after seeding the thawed cells, the cell media was replaced to remove dead cells and any remaining DMSO. Post-thawing, the Vero cells were passaged at least twice before they recovered from their freezing and could be used in experiments.

4.1.1.4 6-Well plate cultures for transcript analysis

A 6-well plate was seeded at $2x10^5$ cell/mL, two wells with AV529-19 and four with HSV2012-121, and incubated overnight. A confluent monolayer was not required for this investigation given that the results were entirely qualitative and the infection compromised confluence regardless of initial cell density. The two wells containing HSV2012-121 had their media aspirated and diluted viral stock added for 1 hr. After replacing infection media with fresh media all wells were incubated for an additional 18 hrs to allow infection to progress.

4.1.1.5 Culture of Vero cells in the presence of sodium butyrate (NaBu)

4.1.1.5.1 Uninfected controls and protocol optimization

6-well culture plates were seeded with HSV2012-121 Vero cells at $1.5x10^5$ cells/mL. NaBu was either added immediately after seeding at 0, 1, 2, 3, 4 and 5 mM, or 24hrs after seeding, at 0, 1, 2, 3, 4 and 5 mM. At 48 and 72 hours after seeding, both plates were imaged with fluorescence and light microscopy. Light images were taken at 40x magnification to capture as much of the culture as possible while fluorescence images were taken at 100x magnification. The higher magnification allowed the images to focus on the more fluorescent sections of the culture. The images were analysed in a qualitative manner to determine the level of cell death and eGFP leakage. Cell death was easily discerned in the culture as dead cells become rounded and detached from the culture plate surface. eGFP levels were described by comparing them to the control well fluorescence.

4.1.1.5.2 Infecting cultures under optimal NaBu addition protocol

A 6-well plate was seeded with HSV2012-121 Vero cells at $1.5x10^5$ and spiked with NaBu at the time of seeding. NaBu concentrations of 2mM and 4mM was used. At 24hrs after seeding, the plate was infected with ACAM529. The viral infection medium contained no NaBu and was replaced with fresh DMEM media with NaBu at the proper concentrations after 1 hour was allowed for viral attachment to the cells.

4.1.1.6 96-well plate culture and infection of Vero cells

A 96-well culture plate was seeded with 100μL of HSV2012-121 cells at $2.5x10^5$ cells/mL and allowed 18-24hrs to attach at 37^oC and 5% CO_2. Of the 12 wells in each row of the 96-well plate, 10 were seeded with cells, while the 2 wells at the edges of the plate were filled with 150 μL of water. Similarly, the two rows of wells along each of the long sides of the 96-well plate were

also filled with water. This was done to reduce the effect of evaporation. Infection and EPDA quantification were conducted as per Section 4.3.

4.1.2 Insect cell system

4.1.2.1 Sf9 cell maintenance
Sf9 cells (ThermoFisher Scientific, Cat.# 12659-017) were cultured in 125 mL shake flasks (Pyrex Glasswear, Corning, NY, #4985) in an incubator at 27 $^{\circ}$C using Sf900 III serum-free media (Gibco Life Technologies, Burlington, CA, Cat.# 12658019). Each flask was maintained at between $1x10^4$ and $5x10^6$ cells/mL and any culture below a viability of 95% was replaced with a fresh batch of cells. For this investigation, a clear-bottom 96-well plate was seeded and infected.

4.1.2.2 Baculovirus Stock
The baculovirus construct used in the experiments presented in this thesis was created in our laboratory by my colleague Steve George. The GFP gene was isolated from the pcDNA3-GFP plasmid (Addgene, Cambridge, MA, Cat.# 13031) and was then cloned into Autographa californica multicapsid nucleopolyhedrovirus (AcMNPV) (BD Pharmingen, San Diego, CA) using overlap extension PCR. The full protocol is described in Steve's published work [228]. Viral stocks were kept at -80 $^{\circ}$C and thawed before each experiment in the 27 $^{\circ}$C water bath.

4.1.2.3 96-well plate culture and infection of Sf9 cells
The Sf9 insect cells were known for occasionally clumping and showing other signs of non-exponential growth so a clear-bottom plate was used to confirm that they still formed a uniform attached layer in the wells. For infection, 100μL of a $5x10^5$ cells/mL Sf9 culture suspension was distributed to each well of the plate. The plate was incubated overnight (18-24hrs) to allow for cell attachment. 96-well plates were always incubated within a BioTransport Carrier (Thermo Scientific Nalgene, cat #: 7135-0001) which maintained high humidity in order to minimize evaporation. Baculovirus stock (maintained as per Section 4.1.2.2) was then diluted and added to the wells for infection. The dilution was done serially as per Section 4.3. The wells in each row of the 96-well plate were infected with 10μL of the same dilution (12 replicates for each of the dilutions). The plates were then incubated to allow the infection to proceed before the EPDA quantification could proceed (Section 4.3).

4.2 Cell counting

Cells were diluted using a 0.5% V/V solution of Trypan Blue in DPBS (HiMedia Laboratories, Mumbai, India, cat #: TCL005) and counted using a Hemocytometer (Hausser Scientific Co., Horsham PA, USA, cat #: 3720).

4.3 Plaque assay

12-well tissue culture plates (Thermo Scientific Biolite, Korea, cat #: 130185) were seeded with AV529-19 Vero cells at 2.5×10^5 cells/mL (1mL per well) and incubated overnight to achieve confluence. Once cells were confluent, the media was aspirated and the cells washed once with DPBS prior to infection. Virus stock was serially diluted from its original concentration and 200 µL of each dilution was used to infect 3 wells. The cells and infection media were incubated for 1 hr at 37 ^{o}C and gently rocked every 15min to ensure even viral attachment. After 1hr the infection media was replaced with overlay media (DMEM culture media + 7.5% methyl cellulose (Sigma Aldrich, St. Louis MO, USA, cat #: 274429)).

The culture plates were incubated for 48 hours to allow plaques to form. The overlay media was removed and the plates were stained with 1% crystal violet solution in methanol (Sigma-Aldrich, St. Louis MO, USA, cat #: HT90132) for at least 30min. Plaques were counted after washing off the crystal violet solution and dried, yielding a titer in "plaque forming units" (PFU)/mL. Taking into account dilution, and using triplicates to establish reasonable statistical confidence, the initial infectious virus titer is given by:

$$\textbf{Equation 1: } Virus\ titer\ (\frac{pfu}{mL}) = \frac{Average(plaques) \times Dilution}{Volume\ of\ virus\ solution\ added}$$

4.4 End point dilution assay (EPDA)

HSV2012-121 cells were seeded at 2.5×10^5 cells/mL in a clear-bottom 96-well plate (Corning Costa, New York NY, USA, cat #:3603) and incubated overnight to achieve confluence. The virus stock was serially diluted with media up to a factor of 10^9. Plates were incubated for 24-48hrs to allow infection to progress and fluorescent protein to be produced. Each well was scored based on the presence of infection (fluorescence above baseline).

First, the cumulative positively and negatively scored wells at each dilution level were calculated. Infected wells were counted starting from the highest dilution while uninfected wells

were counted from the lowest dilution. The cumulative number at each dilution level was recorded and these values were then used to find the percentage of wells infected overall at each dilution. The "tissue culture infective dose" (TCID50), which corresponds to the virus dose that causes 50% of the cultures to be infected, was calculated according to Equation 2.

$$\textbf{Equation 2: } \log(TCID_{50}) = \log(Dilution_{>50\%\ infection}) - PD_{response}$$

where $PD_{response}$ is the proportional distance of the dilution giving greater than 50% infection to the dilution factor which corresponds to the $TCID_{50}$.

$$\textbf{Equation 3: } PD_{response} = \frac{(Percent_{>50\%\ value} - \textbf{50\%})}{(Percent_{>50\%\ value} - Percent_{<50\%\ Value})}$$

Multiplying the $TCID_{50}$/mL by 0.69 yields the plaque-forming units per mL (PFU/mL).

4.5 Spectrofluorometric analysis

EPDAs and other investigations involving the spectrofluorometer were conducted using black-bottom (Thermo Scientific Nunclon, Roskilde Denmark, Cat. # 137101) or clear-bottom (Corning Costar, Corning, NY, USA, #3603) 96-well plates. Most of the work was done using the clear-bottom plates which allowed visual tracking of the progress of infection. The spectrofluorometer was a BioTek Synergy 4 plate reader (BioTek, Winooski, VT, USA).

Before each 96-well plate was examined using the fluorescence plate reader (another name for the spectrofluorometer), the lid was removed and replaced with MicroAmp optical adhesive tape (Applied Biotech, Foster City, CA, USA, #4311971). Condensation was prevented from forming on the inside of the slip by allowing the plates to acclimatize in a biological safety cabinet for 20-30 min. The excitation and emission filters were set to wavelengths of 488 nm and 507 nm respectively to excite the eGFP and capture the resulting emissions of light. Values for relative fluorescence varied with sensitivity settings of the plate reader. Each plate was run using three different sensitivity settings and the highest-sensitivity data without any sensor overflow values (outputs of "overflow" rather than a quantitative measure of the fluorescence when the sensor is overwhelmed) used for analysis. Direct comparison was only possible with data collected using the same sensitivity.

4.6 Reverse transcription real-time polymerase chain reaction (RT-PCR) for gene transcript analysis

All Polymerase Chain Reaction (PCR) experiments started with AV529-19 Vero cells seeded in a 6-well plate and infected once they reached full confluence. The seeding density and length of time the infection progressed in each well was dictated by the experiment being conducted.

At 18 hpi, all wells' media was aspirated and 1mL of TRIzol® reagent (Life Technologies Inc., Burlington ON, Canada, cat #: 15596-018) added. The TRIzol® was pipetted repeatedly and aggressively to lyse the cells, after which it was transferred to 1.5 mL microtubes (Corning Axygen, Union City CA, USA, cat #: MCT-150-C). After 5 min of incubation at room temperature (to allow for DNA disassociation) 200µL of Chloroform (Midland Scientific Inc. EMD, Davenport IA, USA, cat #: EMD CX1055-2) was added and the microtubes shaken vigorously for 15 seconds. The sample tubes were then centrifuged for 15 min at 12000 x g and 4 $^{\circ}$C to separate the mixture into three phases. The top aqueous phase was transferred to another 1.5 mL sample tube without disturbing the other phases.

RNA was precipitated using 500 µL of isopropanol. Tubes were incubated for 10 min at room temperature and then centrifuged at 12000 x g and 4 $^{\circ}$C for 10 min. The RNA pellet was isolated by removing the liquid and washed using 75% ethanol. Once washed, the pellet was once again centrifuged at 7500 x g and 4 $^{\circ}$C for 5 min before the wash was aspirated and the pellet air-dried for 5-10 min. The pellet was resuspended in 50 µL of RNase-free water (Life Technologies, Burlington ON, Canada, cat #: 10977-015) and then placed in a 55-60 $^{\circ}$C water bath for 15 min to denature the RNA. RNA was converted to DNA using a High-Capacity cDNA Reverse Transcription kit (Applied Biosystems, Burlington, ON, Canada). 2 µL of each sample were mixed with 18 µL of reverse transcription (RT) mixture consisting of 2 µL RT buffer, 0.8 µL of "dNTP" mix, 2 µL of RT random primers, 1 µL Multiscribe Reverse Transcriptase, and 12.2 µL of nuclease-free water. The mixing was done using the same microtubes which were then placed in a Bio-Rad T100 Thermal Cycler. Reverse transcription was achieved by holding the sample at 50 $^{\circ}$C for 30 min followed by denaturation of the DNA for 5 min at 99 $^{\circ}$C, and then cooling to 4 $^{\circ}$C for storage.

The qPCR reaction itself was conducted using an Applied Biosystems StepOnePlus RT-PCR system ("StepOnePlus"). 2 µL of each sample were pipetted into the well of a MicroAmp

Optical 96-well reaction plate (Life Technologies Inc., Burlington ON, Canada, cat #: N8010560) containing 18 µL of primers and indicators. The exact composition of this mixture was 6.56 µL nuclease-free water, 10 µL of Power SYBR® Green PCR Master Mix (Life Technologies, Burlington ON, Canada, cat #: 4367659), and 0.72 µL of each of the forward and backward primers corresponding to the gene being tested (Table 1). The 96-well RT-PCR plate was then sealed using MicroAmp optical adhesive tape and placed in the StepOnePlus. The real-time PCR consisted of a pre-incubation at 95 ^{o}C for 10 min with a 4.4 ^{o}C ramp rate, followed by 40 cycles of denaturation at 95 ^{o}C for 10 sec with a 4.4 ^{o}C ramp rate, annealing at 58 ^{o}C with a 2.2 ^{o}C ramp rate, and elongation at 72 ^{o}C with a 4.4^{o}C ramp rate. The PCR was terminated with cooling at 40 ^{o}C with a 1.5 ^{o}C ramp rate.

Table 1: Reverse transcription primers used

Primer	Sequence	Description
RT GFP (forward)	5' – CCT GAA GTT CAT CTG CAC CA – 3'	Primers used to quantify levels of eGFP
RT GFP (backward)	5' – GAA GAA GTC GTG CTG CTT CA – 3'	
β-Actin (forward)	5' – GGC CAG GTC ATC ACC ATT– 3'	Primers used to quantify levels of β-Actin
β-Actin (backward)	5' –ATG TCC ACG TCA CAC TTC ATG –3'	

The amplification curves produced by the qPCR reaction were analysed using LinRegPCR software (available for free from www.hartfaalcentrum.nl). The software was used to set a common threshold fluorescence at which the gene amplification could be detected. The number of cycles required for each sample to reach this threshold was used as a "Cycle Threshold value" which could be used alongside the "effectiveness" of the amplification (factor by which each cycle increases the signal) to compare GFP and B-Actin expression. Ideal PCR reaction have an effectiveness of 2, meaning that the length of the cDNA chain increases two-fold with each cycle, but LinRegPCR allows the true effectiveness to be used for more accurate results. The equation below was applied to calculate an effective "initial" level of fluorescence for GFP RNA. This level is proportional to the amount of GFP RNA which was present in the initial sample:

$$F^o_{GFP} = F^o_{\beta-Actin} \frac{e^{Ct_{\beta-Actin}}_{\beta-Actin}}{e^{Ct_{GFP}}_{GFP}}$$

In the equation above, F_x^o is the threshold level of fluorescence of a given protein's RNA, e_x is the effectiveness of the reaction for that protein, and Ct_x is its threshold cycle value. The value calculated (F_{GFP}^o) was effectively the level of GFP fluorescence signal at the threshold cycle adjusted for the level of β-Actin signal. The F_{GFP}^o values were compared in a relative manner since the actual initial expression level of the GFP RNA was not being investigated here, only the relative degree of leakage.

4.7 Immunofluorescent staining (IS)

Vero cells were seeded on the surface of a glass cover slip (Globe Scientific Inc, Paramus NJ, USA, Item # 1404-15). This was accomplished by placing sterilized cover slips in the wells of a 6-well plate and seeding the wells with the AV529-19 Vero cells at 1.5×10^5 cells/mL. These were then incubated at 37 ^{o}C and 5% CO_2 overnight to allow for cell attachment. After approximately 24 hrs the cells were infected with the ACAM529 virus at an MOI of 0.6-1.0 (based on viral titers of 2-3 PFU/mL and a 1:10 dilution) and incubated for 1, 6, or 18 hpi. Cultures fixed at only 1 hpi were used to establish potential false-positive results as no progeny virus were expected to be observed at this time-point.

Once ready, the cells were fixed using 2 mL of 4% paraformaldehyde added to the well to cease all biological activity at the desired point in the infection (20 min fixation). Cells were then flushed 7 times with PBS to remove as much of the fixative as possible. All washes consisted of adding 2-5 mL to each well, tipping the plate gently to move the liquid and then aspirating the PBS. One final 1-2 min soak with 1 M Glycine in PBS was also done to quench any residual formaldehyde.

Cell membranes were permeabilized using Triton X-100 (Sigma-Aldrich, St. Louis MO, USA, cat. # X100-1L) at a concentration of 0.1% in PBS. 2 mL of the solution was added directly to the wells. Permeabilization lasted between 10 and 12 min after which the Triton X-100 solution was removed and the cells washed 7 times with PBS. Once permeabilized the cells were blocked and stained.

0.1% Tween 20 (Sigma-Aldrich, St. Louis MO, USA, cat. # P9416-100mL) and 1% Bovine Serum Albumin (BSA) (Sigma-Aldrich, St. Louis MO, USA, cat. # A1933-5G) in PBS (referred to collectively as PBS-T) was used to dilute all stains and blocking agents to maximize

their penetration into the Vero cells. Blocking was done using a solution of 10% animal serum (goat (Sigma Aldrich, Oakville ON, CA, cat. # G9023) and/or rabbit (Sigma Aldrich, Oakville ON, CA, cat. # R9133) serum depending on the antibodies used) in PBS-T for 45 min at room temperature. Enough of the blocking solution was added to each well to submerge the cover slips, which remained in the 6-well plate for this step to ease transportation.

The cover slips were inverted over 60-100 µL of a solution of antibody in PBS-T for 45 min at 37 ^{o}C to allow the antibody/stain to interact with the sample. The level of dilution was different for each antibody and was based on supplier recommendations, literature review, and personal experience. Between 100x and 500x dilution was the typical range used in this investigation. A separate staining step was required for each antibody and cell structure stain. Cells were rinsed 7 times with PBS after each staining step to ensure excess material was removed.

Once staining was complete, the glass cover slips were inverted onto a glass microscope slide (Fisher Scientific, Whitby ON, CA cat #:12-544-1) and into one or two droplets (roughly 80-120µL) of ProLong Gold Antifade reagent and mounting medium (Molecular Probes, Eugene OR, USA, cat. # P10144). The mounting medium was used to reduce bleaching, which can occur when the fluorophores are exposed to light. It also improved the refractive properties of the sample and ensured signal clarity. The mounting media required 12-18 hrs to cure before the cover slips could be sealed with nail polish (Extra Life No Chip Top Coat, Revlon Consumer Products Corporation, New York, New York) to prevent the samples from drying out. Once sealed, the slides were ready for imaging.

4.7.1 Establishing noise levels and assessing experimental controls for viral protein immunofluorescent staining

AV529-19 Vero cells were grown on glass slides as described in Section 4.4. ACAM529 HSV virus was used to infect half of the cells at an MOI of approximately 1 and infection was allowed to progress for 1 hour. The other cover slips remained uninfected. The cells were then fixed, permeabilized, and one of each slide was stained with each of the primary antibodies listed in Table 2 at the concentrations listed therein. Each staining step was conducted for 45 min at 37 ^{o}C. Cells stained with a-gE+FITC underwent no secondary staining while cells stained with a-gD, a-gB, a-gC, a-ICP5, a-ICP27, and a-Poly all underwent secondary staining with a-Mouse

AlexaFluor 488 for 45min at 37°C. Lastly, each cover slip was stained with CellMask at a concentration of 1:500 for 5min.

Table 2: Information on antibodies used in Section 6.2 experiments

Stain/Antibody Name	Target	Source Animal	Supplier	Code	Dilution
a-gD	HSV glycoprotein D	Mouse	abcam	ab6507	1:500
a-gE + FITC	HSV glycoprotein E	Mouse	abcam	ab24277	1:500
a-gB	HSV glycoprotein B	Mouse	abcam	ab6506	1:500
a-gC	HSV glycoprotein C	Mouse	abcam	ab46860	1:250
a-ICP5 monoclonal	HSV infected cell protein 5	Mouse	abcam	ab6508	1:200
a-ICP27 monoclonal	HSV infected cell protein 27	Mouse	abcam	ab31631	1:250
a-poly	HSV late structural proteins	Rabbit	abcam	ab20535	1:250
a-Mouse Alexa Fluor 488	Mouse primary antibodies	Goat	abcam	ab150113	1:500
a-Rabbit Alexa Fluor 488	Rabbit primary antibodies	Goat	abcam	ab150077	1:500

Imaging was done within 48 hours of the completion of the staining to minimize the risk of fluorescence degradation. Laser strength was not changed throughout the experiment to minimize inconsistencies between samples. Brightness and contrast modifications were made using the built-in settings of the Zeiss Zen 2009 software (Section 4.7).

4.7.2 IS antibody panel to determine efficacy at 6 and 18hpi
AV529-19 Vero cells were grown on glass slides as described in Section 4.4. ACAM529 HSV virus was used to infect the cells at an MOI of approximately 1 and infection was allowed to progress for either 6 or 18 hours. The cells were then fixed, permeabilized, stained, and imaged as per Section 4.4.1.

4.7.3 a-ICP5 and a-gE+FITC co-staining for mature viral particle identification
For this investigation, AV529-19 Vero cells were grown on glass slides as described in Section 4.4. ACAM529 HSV virus was used to infect the cells at an MOI of approximately 1 and infection was allowed to progress for 20 hours. The cells were then fixed, permeabilized, and stained with a-ICP5 (at a dilution of 1:100), a-Mouse AlexaFluor 405 (1:500), and a-gE+FITC (1:500). Staining steps were all carried out for 45 min at 37 $^{\circ}$C. The cells were also stained with either CellMask cell membrane stain (1:500 dilution, 5 min at room temperature) or Cytopainter Phalloidin-iFluor 647 Reagent F-actin stain (1:500 dilution, 45 min at 37 $^{\circ}$C). No infection and 2 hpi controls were also stained to capture the level of background and/or non-specific staining. Imaging and image analysis was conducted as per Section 4.4.1.

48

4.8 Microscopy

Two microscopes were used in this body of work. The first was a dual inverted light and fluorescence microscope that allowed a sample to be visualized under one of three fluorescence excitation filters or using white light. This was achieved using a Zeiss Axiovert 200 inverted light microscope with an attached Zeiss HBO 50 burner mercury lamp and filters. This microscope allowed for imaging at 50x and 100x magnification and was used to track cell confluence and the progress of infection. In cases were infection was expected to produce fluorescence, both light and fluorescence imaging could be carried out on the same sample. Images from this microscope were captured digitally using the ".raw" format.

The second microscope used was a LSM 510 META confocal microscope from Zeiss. The confocal microscope provides a clear image of a very thin cross-section of a sample. The images themselves are composed section by section digitally as a pair of scanning mirrors moves the excitation laser across the sample. The resolution was set manually and is inversely proportional to the time required for the image to be compiled.

The LSM 510 META was equipped with oil immersion objectives which allowed for imaging at 40x and 63x magnification. Images were captured using Zeiss Zen 2009 software in ".LSM" format.

Images taken using the Axiovert 200 were modified using ImageJ (National Institutes of Health, Maryland, USA, public domain software package), a free image processing and analysis software available online. The digital settings (brightness and contrast) were adjusted using Zeiss' Zen 2009 software for each image individually in order to capture the best images possible in terms of signal strength and clarity. The software uses several pre-set options which were used for fast and consistent processing. Each image was captured after a "Min/Max" or "Best Fit" adjustment had been made to ensure that signals of different strengths could be observed. Both of these adjustments are pre-set in the software and affect only the image's display options, not the data itself [229]. The "Min/Max" option provides the best balance of signal and background noise and is optimal to isolate strong signals. The "Best Fit" option attempts to capture as much of the signal possible, making weak signals easy-to-see, but also resulting in high background noise.

4.8.1 Quantitative image analysis

Several features of the ImageJ software were used to produce quantitative data for images which could then be compared in a more rigorous fashion. It allowed for high fluorescence intensity regions of images to be isolated and quantified. The qualitative data then allowed for more robust analysis.

ImageJ was used to set a threshold on signal strength on a pixel-by pixel basis. Once a threshold had been established (the criteria being subjective but consistent among the images analysed), the software set all pixels meeting the threshold to white and everything else to black. By determining what fraction of the pixels were "on" or "off", the program determined the percent of the image area which met the threshold criteria. As long as the brightness threshold remained consistent between images, this provided an accurate quantitative method of comparison between the infected and uninfected cell fluorescence. Displaying the entire image area to a binary colour-coded manner also benefitted quantitative analysis by simplifying the image and ensuring consistency (through consistent thresholds).

4.9 Vero cell culture insert culturing, infection, and staining

All cell culture insert experiments involved the culturing of HSV2013-121 Vero cells in both 1.0 µm PET transparent cell inserts (Millipore, Switzerland, Cat. No. PIRP30R48) and in wells of a 6-well cell culture plates (Thermo Scientific Nunclon, Roskilde, Denmark, Cat. No. 140675). The two were seeded concurrently in separate 6-well plates and then allowed to adhere and grow to confluence. Both the well culture and insert culture could be tracked visually using an inverted light microscope in order to ensure confluence. Once the monolayer has completely formed, the cell in the insert could be infected with ACAM529 HSV.

The insert and well cultures remained separate when the "primary infection" was conducted. 1mL of diluted viral stock (dilution based on experiment goals) was added to each cell insert and 1 hr was allowed for viral attachment. After 1hr the infection media was aspirated and replaced with sterile DPBS. The inserts were then moved to another cell culture plate containing only DPBS. DPBS was used to remove as many un-fused virus particles from the cell monolayer, insert membrane, and insert surfaces as possible. After being washed two more times with fresh DPBS the insert culture was covered with plaque overlay media (standard DMEM Vero cell culture media with 0.75% methyl cellulose) to prevent virus particles from travelling

through the supernatant. Once this was done the insert was moved to the 6-well culture plate containing the well cultures.
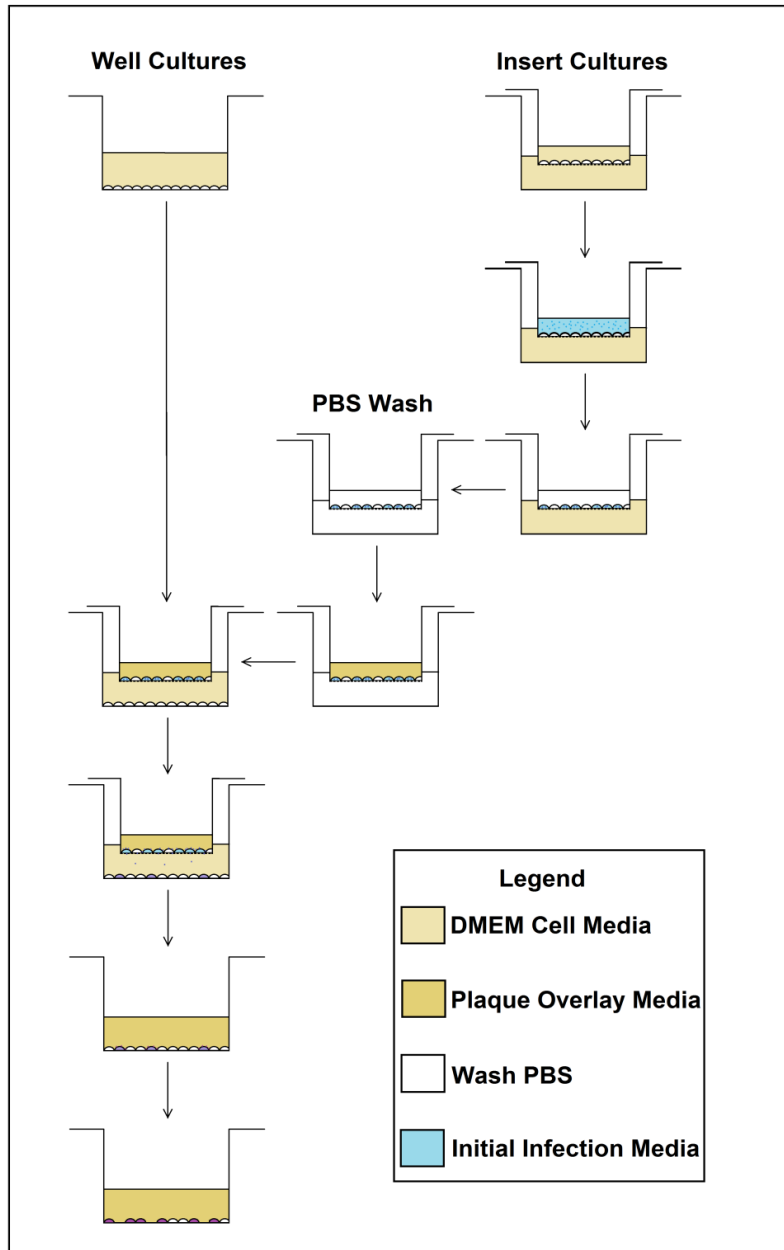
Figure 8: Cell culture insert experimental protocol diagram

4.9.1 Validation of cell culture insert membrane as a valid Vero cell substrate

A 6-well cell culture plate and set of cell culture inserts were seeded at $2x10^5$ cells/mL as per Section 4.8. 2mL of cell suspension were added to each culture plate well and 1.5mL to each cell

insert. After 24hrs of incubation both sets of cultures were imaged using an inverted light microscope after which the insert cultures were infected at a 1:10 dilution of viral stock. The exact viral titer was not determined for this investigation. Once the one-hour virus attachment step was complete, the inserts were washed and moved to the well culture plate.

One of the insert cultures was not infected (as a control) and imaged immediately instead of being transferred to the well culture plate. The remaining inserts were allowed to remain in the well culture plate for 12, 15, 18, and 20 hrs. At each time point the corresponding cell culture insert was removed from the well culture plate and both well and insert cultures were imaged.

4.9.2 Determining infective titer reduction between primary and secondary infection for infected cell culture inserts

Two 6-well culture plates and 12 cell culture inserts were seeded at 2.5×10^5 cells/mL, 2 mL into each culture plate well and 1 mL into cell insert. An additional 12-well culture plate was seeded at the same density for a concurrent plaque assay. The cells were incubated for 24 hrs and the confluence of the monolayers was confirmed visually prior to initial infection. Virus serial dilutions were prepared within 30 min of infection to minimize degradation. The serial dilutions used for infecting cell culture inserts were 10^{-1} (1:10), 10^{-3}, and 10^{-5}. Six inserts were infected at 10^{-1} and three were infected with each of the other two dilutions. Three wells (one column) of the plaque assay plate were infected with each of no virus, 10^{-4}, 10^{-5}, and 10^{-6}. 200μL of the corresponding viral dilution was used to infect each plaque assay well, and 1 mL was used to infect each cell insert.

The plaque assay's uninfected wells served as a negative control for viral infection the experiment. Three of the six cell culture inserts infected at 10^{-1} were allowed only one hour in their corresponding well culture (after the one hour of virus attachment and washing steps). This "2hpi" control served as a measure of how many virus particles from the initial infection could be found in the well cultures. Two hours was not enough time for progeny virions to form, meaning all plaques formed in these wells had to be formed by viral particles added to the cell culture insert and not removed by washing. Plaque overlay media was added to the plaque assay plate at 1hpi and to the 2hpi well cultures at 2hpi.

All other cell inserts were removed from their corresponding well cultures at 20hpi. Plaque overlay media was added to these wells and the cell culture inserts were moved to another

6-well culture plate. All cultures (both insert and well) were then allowed 48hrs for plaque formation before being stained with Crystal Violet for 30min. Plaques were counted using visual inspection and the viral titer calculated as per the plaque assay protocol.

The length of time for which infected inserts remained in the well culture plate was dictated by the goals of the experiment being conducted. During this time, any viral particles budding in a direction of the force of gravity towards the well culture could infect its cells. As long as the infected inserts were removed before this secondary infection could produce further (tertiary) progeny viruses, the number of virus particles descending from the insert could be quantified by removing the insert and replacing the cell culture media with plaque overlay media. Both insert and well cultures were stained with Crystal Violet 48hrs after plaque overlay media was added, allowing the same amount of time for plaque growth as in the methodology (Section 4.2). Counting these plaques (along with those in control wells) allowed the number of infective virus particles that budded downward to be quantified.

Chapter 5 – Virus Infection and Quantification using Fluorescent Protein Expression

HSV2012-121 is a Vero cell line capable of allowing the replication of ACAM529 that also contains the gene for enhanced green fluorescence protein (eGFP) under the viral promoter which controls ICP10. In theory, eGFP expression should only occur upon infection of the cell with a virus encoding a viral polymerase that recognizes the infected cell protein 10 (ICP10) gene's promoter sequence. The objective of this chapter was to establish protocols to monitor the infection of HSV2012-121 with ACAM529, and determine the feasibility of using these protocols as part of an end-point dilution assay (EPDA). The motivation for this work was the time and labour-intensive nature of the current best method for virus quantification (the plaque assay) which makes investigating the system more difficult.

Protein expression can be achieved by stably transfecting a cell line with a reporter protein gene under the control of a viral promoter. Viral promoters, as referred to here, are sequences that "promote" gene expression but that require a viral RNA polymerase that is only brought to the cell by means of the virus. Thus, under normal conditions (i.e. no virus infection), the cell does not express an RNA polymerase that recognizes the promoter sequence. Upon infection, the viral polymerase becomes available and the reporter protein is expressed in the cell. This type of system is one that can then be used to understand how the cell becomes infected and how long it takes for expression of genes under particular promoters or, alternatively, can be simply used in virus titration.

The importance of measuring virus titer accurately in research and industry applications cannot be overstated. The extremely small size and unstable nature of virus particles present an interesting challenge for enumeration, which has resulted in the development of many assays. In most cases, the virus is enumerated in an indirect manner and the titer is expressed in plaque-forming units or $TCID_{50}$ rather than the actual particle density.

Alternative titration methods are always being sought to replace the Plaque Assay, which is still the most relied upon titration method used in industry. The protocol, outlined in Section 4.2 requires four days to complete and relies on operators to recognize individual plaques. Plaques are generally visualized using Crystal Violet (ammonium oxalate), which can damage aquatic environments if improperly disposed of, and can be carcinogenic [230]).

5.1 Determining fluorescence threshold indicative of infection

A known high-fluorescence system composed of SF900 insect cells and a GFP-producing Baculovirus construct was used as a positive control for the use of the Spectrofluorometer (as per Section 4.1.2). In this investigation, a 96-well plate was seeded with Sf9 cells and infected as per Section 4.5.1. This was done to determine the extent to which wells showing fluorescence could be differentiated from uninfected ones using a spectrofluorometer. This effectively served as a positive control for EPDA experiments using this methodology.

Daily observations of the fluorescence under the light microscope showed that the infection spread very slowly in low MOI wells. While some fluorescence was observed within the expected 20 hpi, the wells infected at 1:1000 (referred to as "10^{-3}" wells) dilution and below did not show pervasive infection until 3 days post infection (dpi). Those wells infected with 1:10,000 (10^{-4}) and 1:100,000 (10^{-5}) viral dilutions showed signs of infection by 3dpi but required up to 10 days before the fluorescence spread to a significant portion of the well.

By 6dpi, high cell death and lysis were observed in those wells infected at 10^{-2} and 10^{-3}. This was in line with what had been observed in infected cell culture time course experiments in which high to moderate MOI resulted in almost complete culture death by 4dpi (Figure 9). The level of fluorescence in the highly infected wells was substantially lower than those in the well infected at lower MOIs (Figure 10). However, the eGFP was sufficiently stable in the extracellular environment to remain easily detectable and the loss in overall fluorescence did not result in false negatives in these wells.
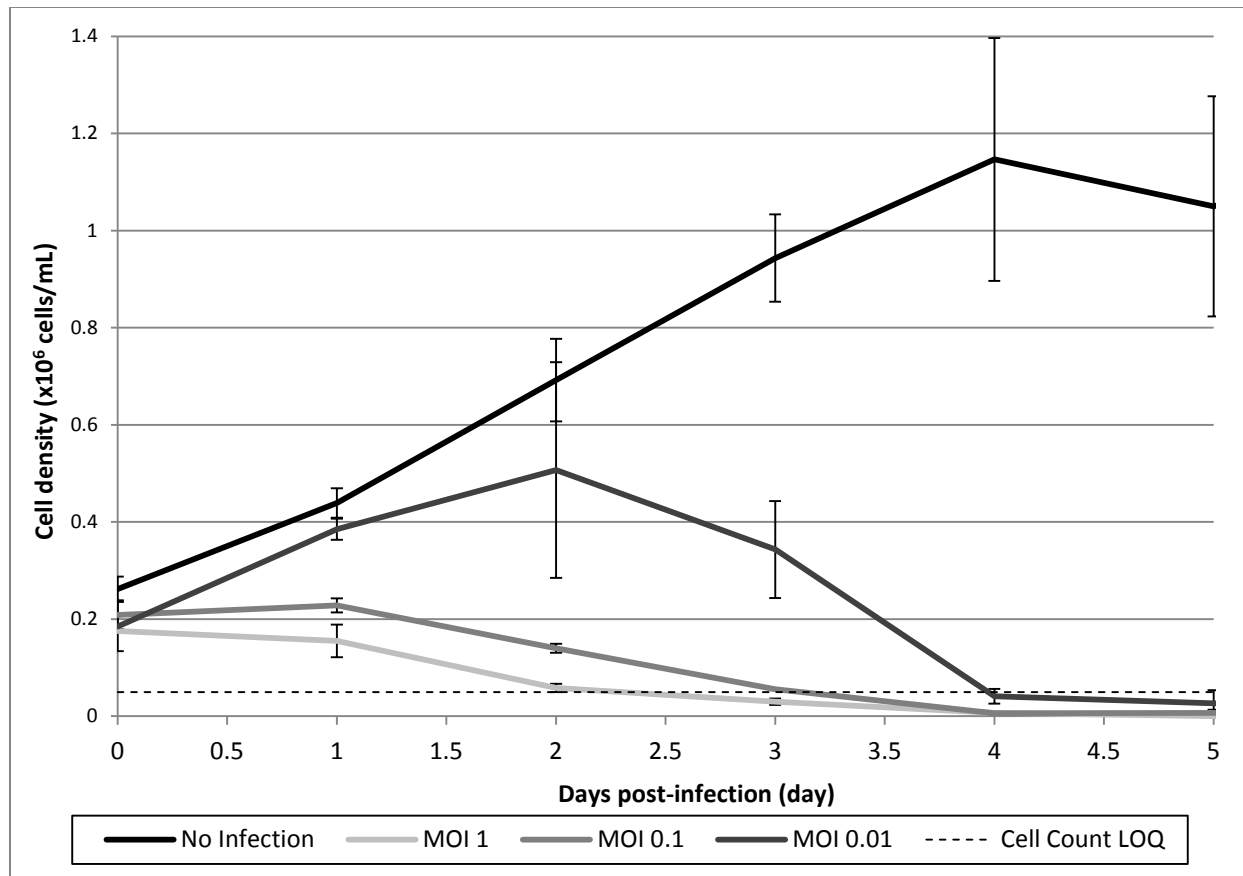
Figure 9: Viable cell count over time for an infected adherent Sf9 cell culture according to MOI (n=3)

At 10 dpi, the plate data was analysed to establish the level of fluorescence which could be deemed "positive" for infection. The data was split into "infected" and "uninfected" categories using visual observation of cytopathic effect and fluorescence, after which the two sets of data were used separately in the analysis.

Two outliers (over two standard deviations from the mean) were found at 10 dpi in the infected wells. The average fluorescence level of the remaining 48 infected wells (excluding the outliers) was 2.4×10^7 relative fluorescence units (RFU) with a standard deviation of 6.7×10^6 RFU, which represents 27.3% of the total average fluorescence. The average uninfected well fluorescence was 3.7×10^6 RFU, which was roughly an order of magnitude lower than the infected average and lower than the standard deviation of the infected wells. The deviation of the uninfected wells (n=46) was much tighter at 2.8×10^5 RFU or 7.7% of the average level.
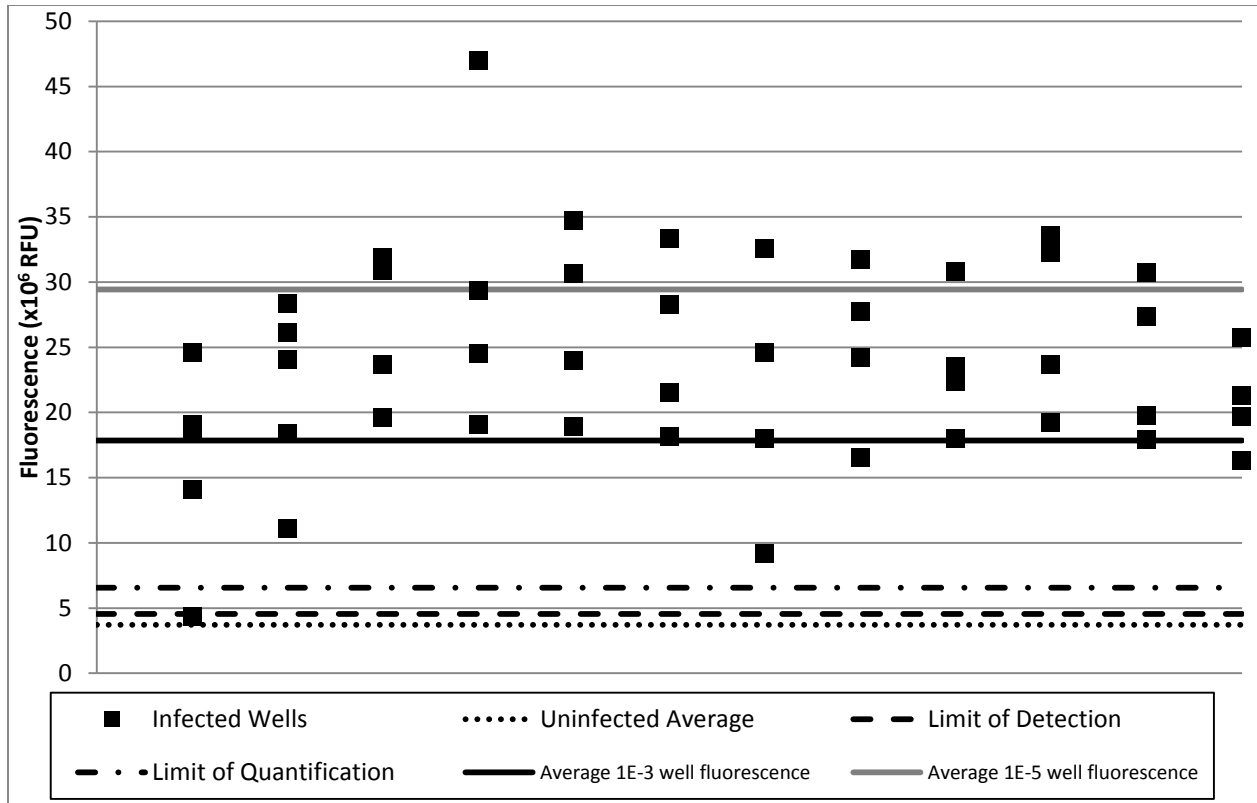
Figure 10: Sf9/Baculovirus EPDA Infected well fluorescence with LoD and LoQ

The limit of detection (LOD) and limit of quantification (LOQ) for the assay were calculated using the RFU measurements in the uninfected wells at 10dpi in order to determine the level of fluorescence which can be said with statistical cetainty to differentiate them from the infected wells. The low variability in the uninfected wells, these limits were very close to the average uninfected well RFU, indicating an effective assay. Only one of the outliers identified in the infected well data fell below the limit of quantification. This meant that even with the relatively high variability observed in the infected well fluorescence, this assay could distinguish all but one of the wells correctly at 10dpi.

Applying the LOD to the data collected at 3, 6, and 10dpi, the viability of the assay was determined at earlier time points. Comparing the titers to the one caclucated using visual inspection it was found that even at 10dpi the titer calculated from RFU data was 11.8% below the actual titer of the assay. At 3 and 6dpi this difference was much higher at -69.15% and -55.3% error respectively. The errors in titer were all negative, indicating that only false negatives were observed in the data (infected wells not exibiting high enough RFU values for the assay to

indicate an infection). Due to this oberved one-sided nature of the error, the use of a single criterion for determining the presence of infection (the LOQ) was justified.
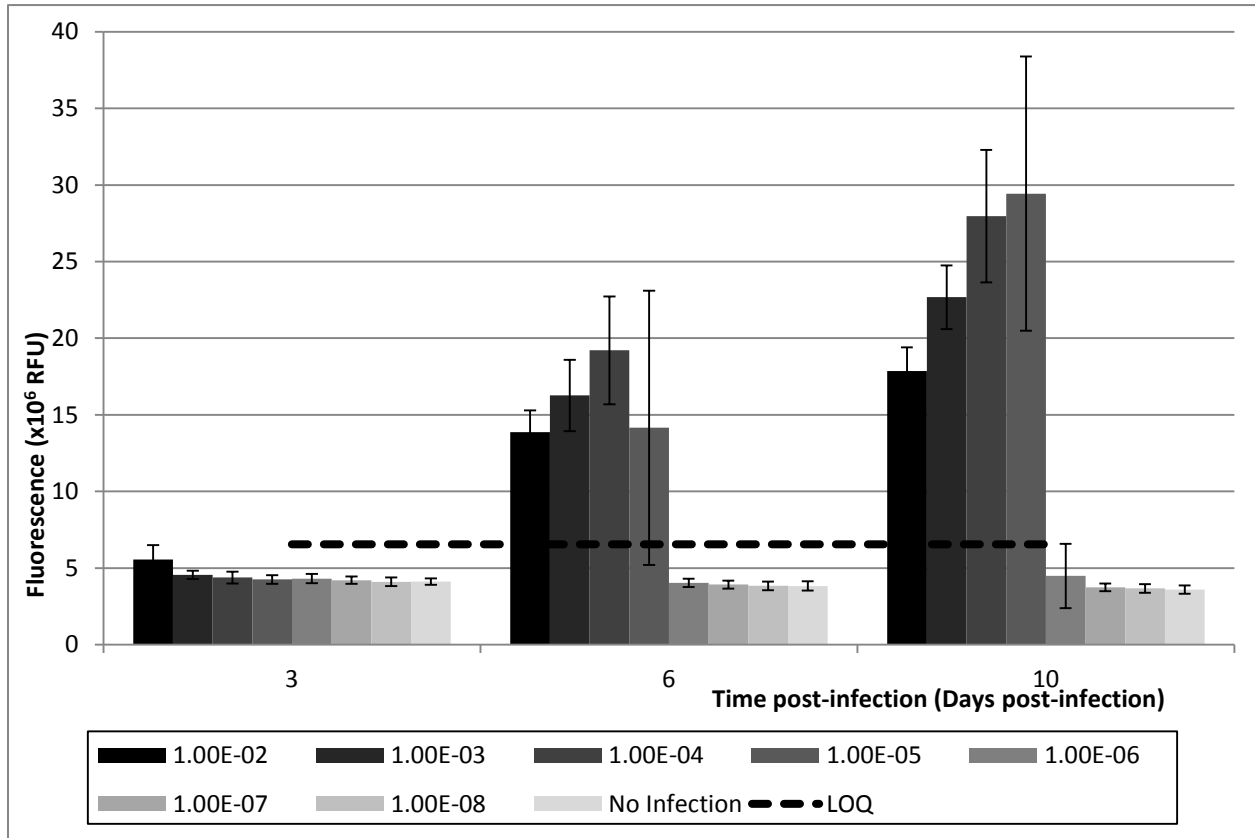
Figure 11: Sf9/Baculovirus EPDA Average Fluorescence (n=12 for each infection titer, titers expressed in scientific notation depicting the dilution (1E-02 = 10^{-2})

While eGFP was found to be fairly stable over the 10 day period, the wells in which it was evident later on were found to be more fluorescent at 10dpi. The difference was only statistically significant between the highest MOI wells (10^{-2}) and those infected at 10^{-3}, 10^{-4}, and 10^{-5}, with the latter three not completely differentiable from each other. The increase in the standard deviation of the RFU values with decreasing MOI was noticeable between the first four MOIs (as seen in Figure 12). These results were attributed to differences in the infection spread, with high MOI wells infected much more synchronously while lower-MOI wells required several viral replication cycles to become highly infected. The results also indicated synchronous infection resulted in lower RFU readings at 10dpi. Large differences in MOI are inherent in the EPDA, meaning that this trend was expected for all such assays.
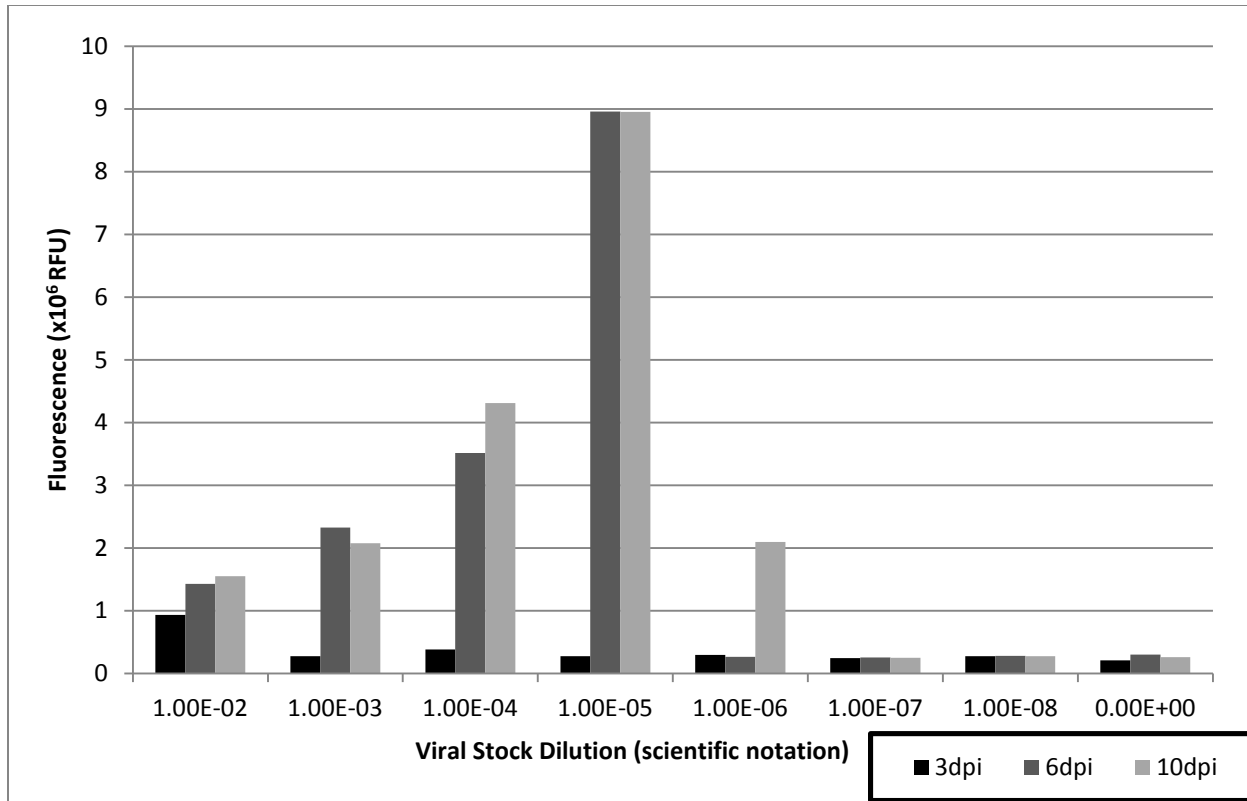
Figure 12: Sf9/Baculovirus EPDA fluorescence standard deviation values (n=3 for original fluorescence data)

The original intention was to use the high-fluorescence Sf9/baculovirus system to establish a positive control for the EPDA. This system yielded relatively accurate titers at 10dpi and validated the use of a spectrofluorometer in this assay. Some issues did exist applying the results of the above experiment to a completely different virus/cell system. Not only does the manner in which infection spreads vary between viruses, but the autofluorescence of the cell culture can also be quite different. Whether this was due to differences in the cells themselves or in the cell media it could result in issues for the assay.

5.2 Quantifying HSV2012-121 and media autofluorescence

To establish appropriate negative controls for the HSV2012-121/ACAM529 system, a closer examination of the fluorescence of the cell culture media and cells was conducted. In particular, the background fluorescence of the mammalian culture media and the cells themselves needed to be established.

Cell culture media can contain a wide variety of additives with fluorescence of their own including tryptophan, pH buffers like Phenol Red, and others. A first hypothesis which was to be

tested was that it may be possible to overcome media autofluorescence in the assay by removing the media and replacing it with a liquid that had lower autofluorescence.

Cells can also contribute to the fluorescence signal through what is known as "DNA leakage", or the production of a gene product without active stimulation of its promoter. It is possible for eGFP to be produced in the HSV2012-121 Vero cells even without an HSV infection. The level of the background fluorescence has to be quantified for a given system before its usefulness in an assay can be determined. Otherwise, it is difficult to say what level of fluorescence corresponds to an infection rather than to naturally occurring fluorophores. Furthermore, the background fluorescence and internal variability of the plate reader itself also has to be considered.

Using a clear-bottom 96-well plate, different combination of cells and liquid were examined for their fluorescent properties. The volume of liquid in each well was kept at 100μL except in the empty control wells. The wells containing cells and media were prepared roughly 24 hrs before the rest of the plate to allow for cell attachment. Wells already filled had their media aspirated and replaced to ensure that evaporation did not cause changes in volume.

Vero cells in DMEM were considered the "standard condition" given that this was the initial setup for the EPDA. Vero cells in overlay DMEM media (as per the Materials and Methods) was investigated as an alternative for regular DMEM. DMEM and overlay DMEM alone were investigated toprovide information on their autofluorescence. Dulbecco's Phosphate Buffered Saline (DPBS) and highly purified (MQ) water respectively were also investigated. This was done so that the autofluorescence of each liquid to be determined and compared both to the DMEM and overlay media and to the Vero cell autofluorescence calculated.
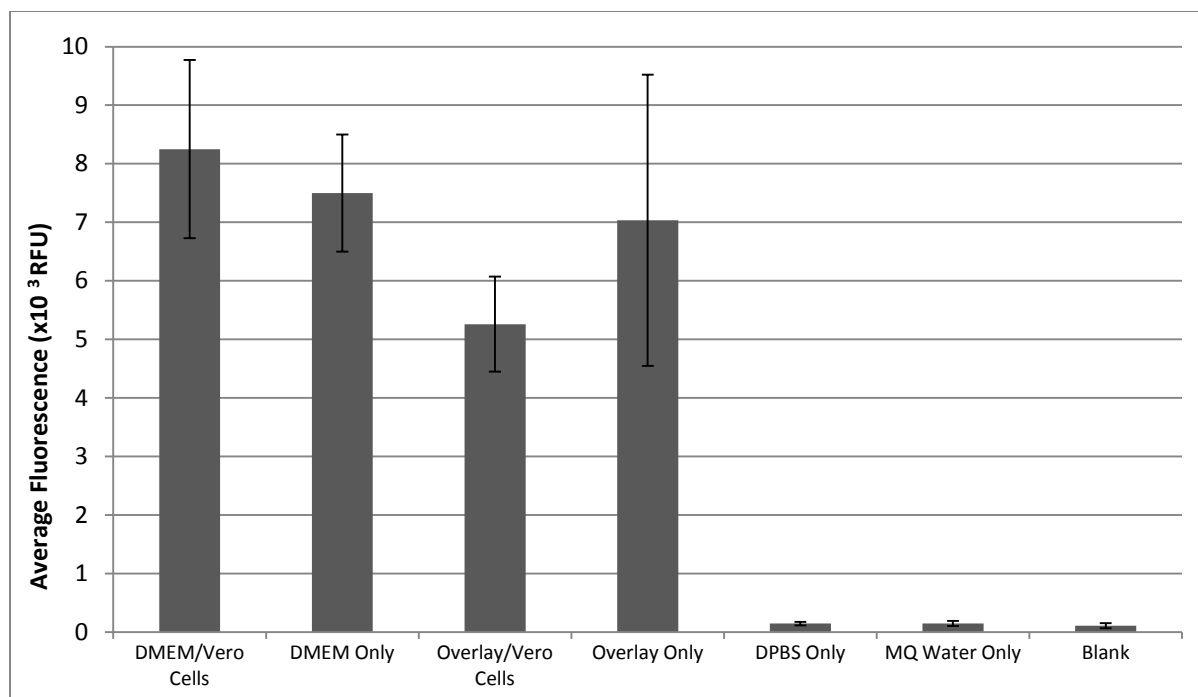
Figure 13: Average background fluorescence of Vero cells, cell media, and media alternatives (n=3, blank indicates the fluorescence in well that were empty)

Figure 13 shows the average fluorescence of media compared to other potential liquids that could be used to cover/host the cells. Replacing the DMEM media by either DPBS or MQ water could enhance the ability to detect eGFP significantly. However, there is a chance that replacing the media could result in loss of the protein released into the media through lysis, as well as loss of the cells themselves which have detached from their substrate as a result of infection(as seen in the insect cell infections where most cells have completely lysed).

As observed in Figure 13, the presence or absence of Vero cells did not affect the RFU values in DMEM and overlay media to a statistically significant degree. While the overlay media displayed a lower level of fluorescence than the DMEM in the presence of cells, the same could not be said about fluorescence of the two types of media in the absence of cells. For this reason, neither of the DMEM media variations had a statistically significant higher level of relative fluorescence.

5.3 Monitoring ACAM529 virus infection of HSV2012-121 cells using eGFP expression

The purpose of this experiment was to determine if the level of fluorescence of infected Vero cells could be discerned within a single cycle of infection and whether varying the MOI would result in detectable variations in fluorescence. Vero cells (HSV2012-121) were infected with ACAM529 at three different MOIs, diluting a virus stock with an approximate titer of $2\text{-}3\times10^6$ pfu/mL by a factor of 10^{-1}, 10^{-2}, and 10^{-3}. The expected MOIs were between 0.8 and 1.2, meaning that ~37% of cells would remain uninfected after the initial round of infection [2]. While the MOIs used could not be expected to result in synchronous infection (all cells infected at the same time rather than through multiple cycles of infection and virus replication), eGFP production was expected throughout the plate by 24hpi (since 24hrs is sufficient for the virus to undergo a single replication cycle and for a secondary infection cycle to begin).

An additional row of wells was seeded with Vero cells but not infected, which was used as a negative control for infection. Two rows of wells were filled with DMEM media (no Vero cells) and one row with MQ water to minimize evaporation and provide a gauge for the level of experimental (equipment) noise. The fluorescence of all wells was then read at 24 hours post-infection.
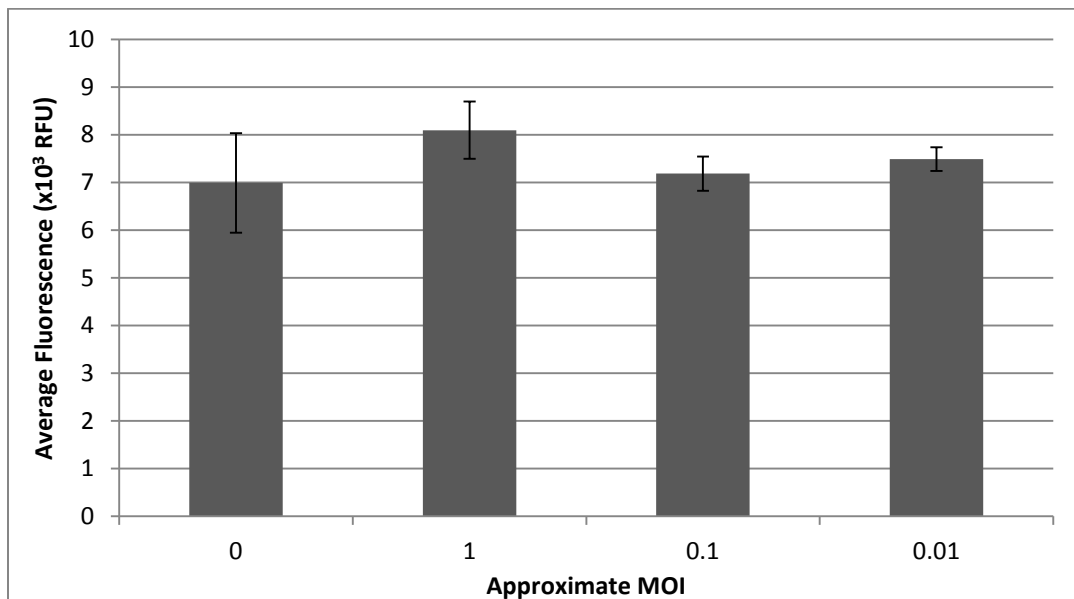
Figure 14: Average fluorescence of infected HSV2012-121 cells at 24hpi (n=8)

Unlike in an EPDA protocol, the MOIs used for this experiment resulted in most cells being infected, showing signs of cytopathic effect, and fluorescing by 24hpi. There was no statistically significant change in the RFU values observed at this time (Figure 14).

In an attempt to simplify the analysis, the fluorescence associated with infection was isolated by subtracting the average fluorescence of uninfected wells from that of the infected wells. Only those wells infected at the 10^{-3} dilution of virus stock had a difference in fluorescence from the uninfected wells that exceeded one standard deviation of the original data. As demonstrated in Figure 14, the infected wells could not be differentiated from the uninfected wells with any degree of statistical certainty. Whether this was caused by high autofluorescence or expression of eGFP in uninfected wells needed to be determined.

5.4 Alternative culture and infection conditions to enhance detection of eGFP

To determine if smaller volumes of media could be used to reduce the effect of background fluorescence Vero cells were infected with identical virus solutions in either 50 or 100 μL DMEM or DMEM Overlay media. Fluorescence data was collected using the spectrofluorometer at 24, 48, and 96hpi. As with the previous experiment, the majority of the cells were expected to become infected and fluoresce within 24hrs. Readings at later time points were taken to test this hypothesis and determine if any conclusions could be made about eGFP stability.

Uninfected wells containing Vero cells and each one of the media/volume combinations tested were used as negative controls for autofluorescence as well as evaporation (given that there were no changes occurring in these wells due to infection). Several rows of wells were filled with MQ water providing a control for internal variability of the equipment.

The 4-day changes in fluorescence were either negative or negligible in spite of adjustments made to minimize and account for evaporation. All changes were within a single standard deviation of the average RFU and were therefore not statistically significant even in the most lenient sense.
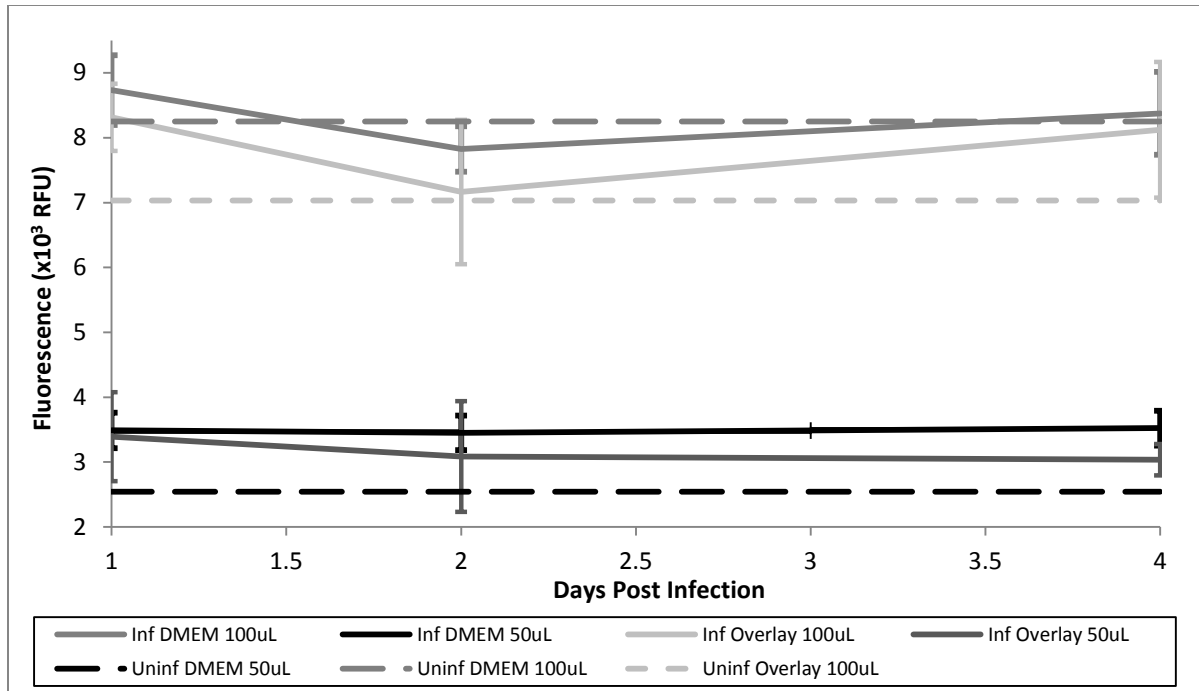
Figure 15: Fluorescence of infected and uninfected Vero cells in DMEM and overlay media (inf = infected, uninf = uninfected, n=3)

When 100μL of DMEM was used, the presence of infection was completely indiscernible from the uninfected control. Reducing the volume improved the separation slightly, but even in the best case scenario the fluorescence of the infected wells was not better than the established background. This together with the data presented above points to a weak level of eGFP expression that does not allow for the tracking of infection under the conditions used.
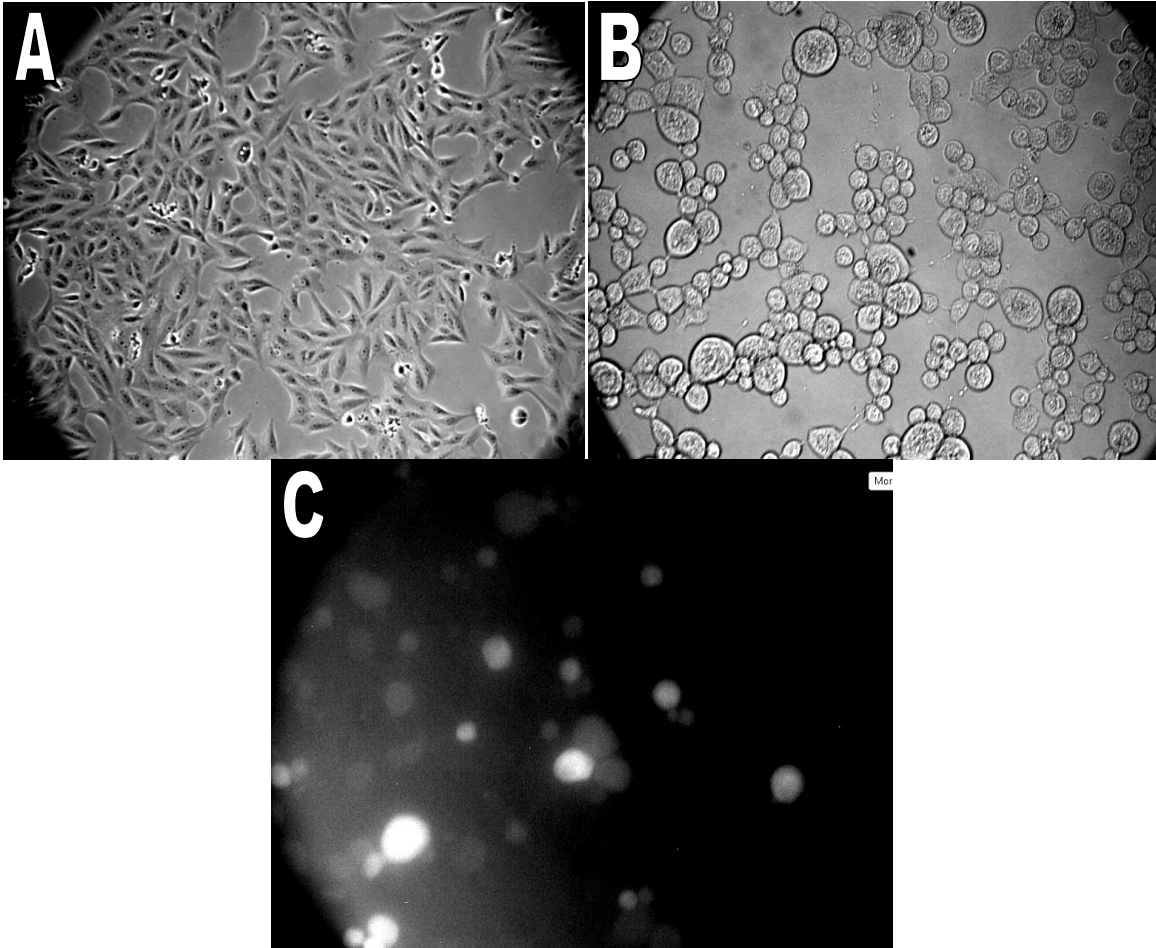
Figure 16: Uninfected Vero cells light (A), infected Vero cells light (B) and infected Vero cells fluorescence (C) images (images B and C are taken of the same section of the sample)

Images of the infected cell culture plate were taken at 24 hpi using the light and fluorescence microscope (Figure 16B and C) to ensure that the level of infection was as high as expected and that it was not a lack of infection that was causing the weak fluorescence signal. As the images show, by 24 hpi, all the cells showed extensive cytopathic effect (the visible effect which a virus has on the host cell which it is infecting) and the culture was unmistakeably altered from its healthy state (Figure 16A). The rounding and enlargement of the cells indicated a mid to late-stage infection with HSV-2. The fluorescent protein (eGFP) was being expressed, but the majority of the fluorescence in the image would not have been visible if the brightness and contrast had not been adjusted.

Given that an EPDA involves non-synchronous infection in which evaporation and cell lysis has been seen to lead to further reduction in signal strength, the issues described would be

further compounded if the Vero/HSV system was titrated with this method. Unless eGFP signal strength could be improved in some way, this system is not suitable for the EPDA.

5.4.1 Enhancing eGFP expression

Section 5.1 demonstrated the spectrofluorometer's ability to identify separate infected from uninfected wells based on their fluorescence in an EPDA with Sf9 cells as a positive control. Unfortunately, the same instrument was unable to discern a statistically significant difference in the RFU values of infected and uninfected HSV2012-121 Vero cells, as seen in the previous section. Several approaches were considered for overcoming the issue of weaker fluorescence signal. Given that fluorescence was detected by inverted fluorescence microscope it was known that some increase in fluorescence did indeed occur. Using more sensitive equipment could have allowed this difference to be quantified, but such equipment was neither available nor known for certain to exist.

The other logical way to detect the infection's effect on fluorescence was to increase this effect. One substance which has been used to enhance GFP transcription in adherent cell culture without altering the genetic information is Sodium Butyrate (NaBu) [231]. While high concentrations of this compound are lethal to the cells, at low concentrations it causes increased stationary phase nutrient consumption and hyperacetylation of the cells' histones, which results in increased protein production [232, 233]. The challenge in my work was then to balance the signal enhancement with the health of the cells.

A major concern with the use of a compound like NaBu stems from its inherent indiscriminate nature in terms of protein production enhancement. "Expression leakage", resulting from the cell's ability to transcribe from the viral promoter, can result in eGFP being produced in cells not infected by HSV. This undesired expression could be enhanced too, resulting in higher background levels of fluorescence not associated with infection. Balancing this background noise enhancement against the improvement of the actual fluorescent signal was therefore a priority in this investigation.

5.4.1.1 Fluorescence Protein Expression Leakage

To quantitatively determine the extent of the 'leakage' of eGFP, the transcription levels of its gene in infected and uninfected cells were analyzed. Reverse transcription real-time polymerase chain reaction (RT-PCR) was used to amplify and detect any ribonucleic acid (RNA)

corresponding to the eGFP gene. Ideally, no eGFP RNA would be present in any cells not infected with ACAM529.

β-Actin, a major structural component of animal cells, was used as a control to account for the number of cells from which RNA was being extracted. Since genes coding for β-Actin should be expressed at comparable levels in all Vero cells, β-Actin mRNA was used to standardize the eGFP readings. Both infected and uninfected HSV2012-121 along with uninfected AV529-19 were analysed for both eGFP and β-Actin.
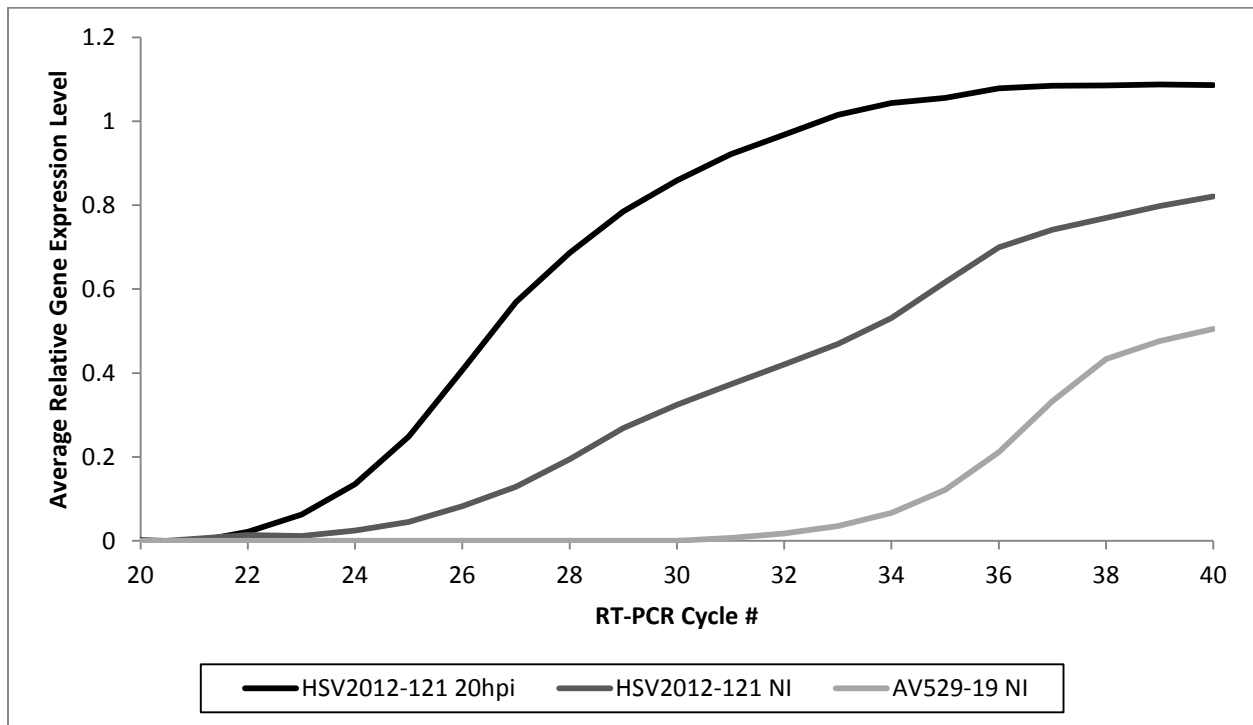
Figure 17: Translated and Normalized Reverse Transcription Polymerase Chain Reaction Data (Cycles 20-40) (NI = No infection, hpi = hours post-infection)

Figure 17 shows the portion of the RT-PCR data in which the signal became detectible (the point where it becomes detectable is known as the Cycle Threshold). AV529-19, the cell line containing no eGFP, was used as a control and shows the level of background noise in the experiment. The sample with no eGFP expression reached the detection threshold at roughly 32 cycles. The uninfected HSV2012-121 Vero cells reached the same threshold at about 24 cycles, only 2 cycles after the infected HSV2012-121. The LinRegPCR data analysis yielded similar results. The estimated level of GFP ribonucleic acid (RNA) in the infected HSV2012-121 cells was 595.28 times higher than that of the uninfected AV529-19 control (based on the cycle

67

threshold). The uninfected HSV2012-121 cells had an estimated level of GFP RNA 50.63 times higher than the control. The difference between infected and uninfected HSV2012-121 cells was only 11.74 times the GFP RNA.

The RT-PCR provided evidence of GFP gene expression leakage in the ACAM529/HSV2012-121 system. This leakage resulted in data not matching the negative control (a cell line completely devoid of GFP expression). While RT-PCR could differentiate between the infected and uninfected fluorescent cells' GFP expression, the levels of expression were much closer between the infected and uninfected HSV2012-121 cells than they were to the control.

5.4.1.2 NaBu Addition Window and Concentration Optimization

Since cell death due to NaBu toxicity would become confounded with viral cell death in an infected Vero cell system, uninfected cells were used for establishing an optimized protocol. This approach allowed differences in the health of cells to be more accurately attributed to the presence of NaBu and the level of eGFP expression leakage could also be monitored. Without the presence of ACAM529, fluorescence detected could be attributed to the leakage.

Two addition (or "spiking") times were tested for the NaBu, at the time of Vero cell seeding and 24 hrs after seeding. The cells were imaged using both fluorescence and light microscopy and the images compared to determine the optimal conditions. While spiking on seeding may integrate more easily with the existing protocol, it does not allow time for the cells to attach and become confluent before exposure to the toxicity of the NaBu. On the other hand, spiking at 24hrs after seeding would extend the protocol a further 24 hrs to allow for the NaBu to enter cells before infection with the virus.
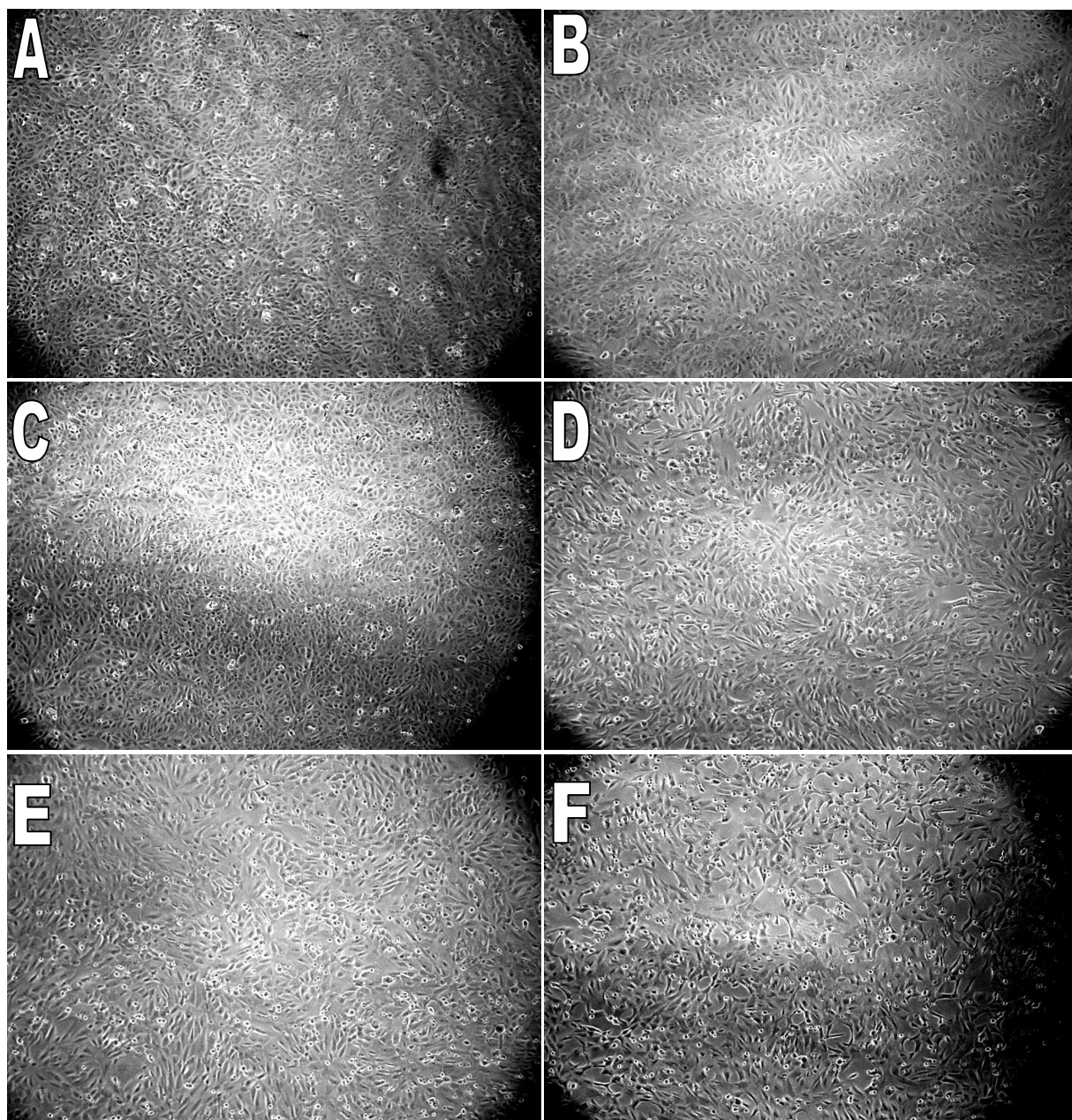
Figure 18: Cell Culture Spiked at Seeding Light Images 48hrs after seeding (0mM (A), 1mM (B), 2mM (C), 3mM (D), 4mM (E), 5mM (F)) (40x magnification)

The effect of the NaBu was apparent in Figure 18. The culture was completely confluent and the cell density was very high when no NaBu was present (Figure 17 A). Very few of the cells were rounded and detached, as is expected of a healthy Vero cell culture. As the concentration of NaBu increased the cells become more and more affected by the toxicity with a higher number of detached cells (Figure 18 B-F). Full confluence as maintained at NaBu

concentrations below 3mM despite this toxicity, indicating that the majority of the cells were still attaching to the culture plate surface normally and replicating. At concentrations above 3mM the cell death becomes significant and confluence was not full. In spite of this, the cells which remained attached remain healthy.

Figure 19: Cell Culture Spiked at 24hrs after Seeding Light Images 48hrs after seeding (0mM (A), 1mM (B), 2mM (C), 3mM (D), 4mM (E), 5mM (F)) (40x magnification)

Figure 19 shows the cells spiked with NaBu at 24hrs after seeding. The amount of cell death in the high NaBu concentration wells of the 24hrs after seeding plate was much higher than those seen in Figure 18 B-F. In fact, the adherent culture was difficult to distinguish past all of the detached cells in Figure 19F. At NaBu concentrations of 2mM and below, the culture was similar to the ones spiked at seeding. Full confluence was maintained until 4mM NaBu (Figure 19E), which was slightly better than the cells spiked at seeding (which were only confluent to 3mM).

The light images in Figure 18 and Figure 19 demonstrate the significant toxicity of NaBu to Vero cells at concentrations of 3mM and above. Both methods of adding the NaBu showed this toxicity with those cells spiked at 24hrs after seeding having the larger number of dead cells at 48hrs. NaBu addition 24 hour post seeding maintained confluence at slightly higher concentrations of NaBu, likely because the cells were given time to attach to the cell culture plate. After 48hrs, the cells were analyzed for fluorescent protein expression using inverted fluorescence imaging.
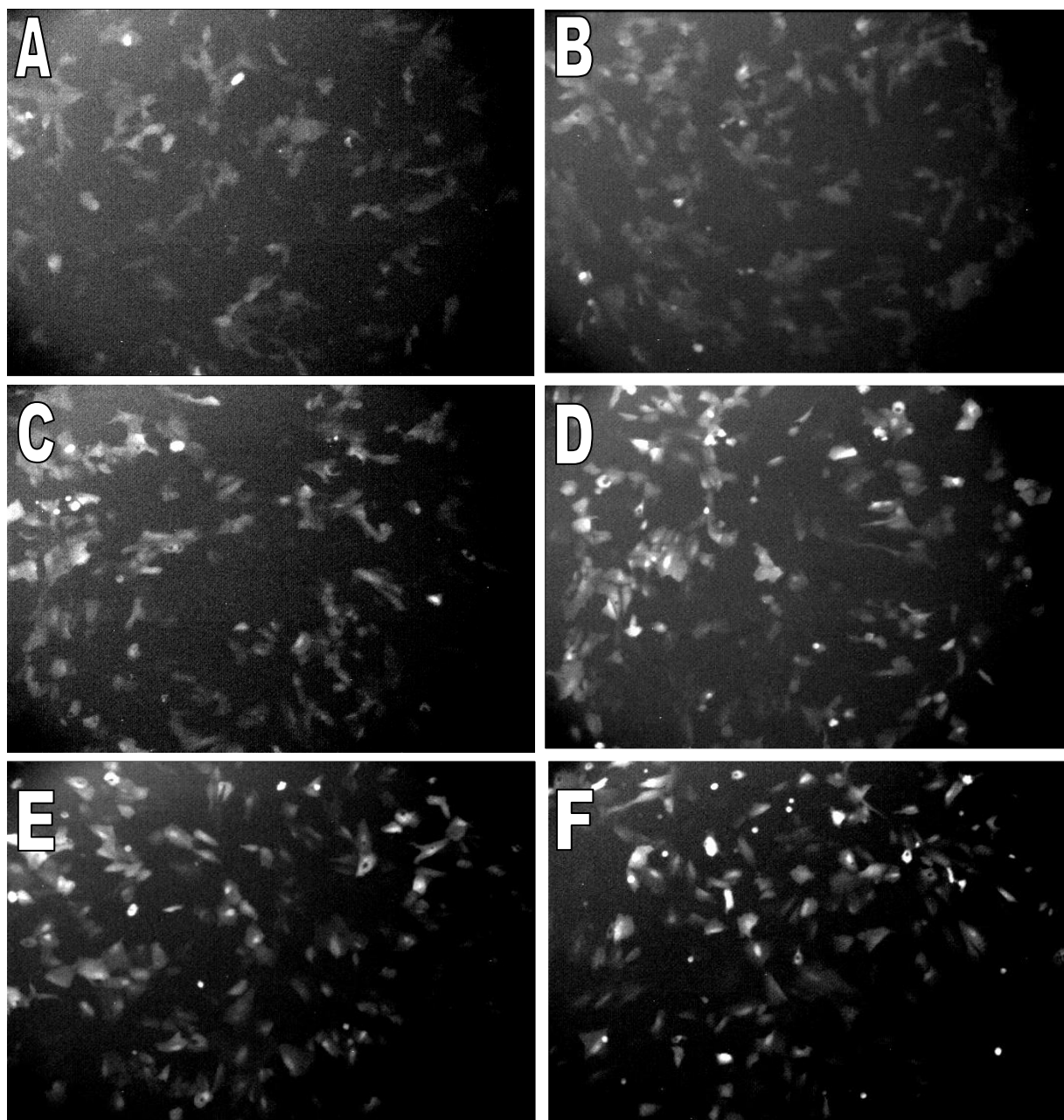
Figure 20: Cell Culture Spiked on Seeding Fluorescence Images 48hrs after seeding (0mM (A), 1mM (B), 2mM (C), 3mM (D), 4mM (E), 5mM (F) NaBu) (40x magnification)

The images in Figure 20 were highly altered in terms of brightness to clearly visualize the fluorescence. The fluorescence was strongest (relatively) in the 5mM NaBu well (Figure 20F). Expression leakage was present in the control well and its brightness increased with NaBu concentration. The fluorescence did not increase observably until 2mM NaBu, with a sharp rise in the fluorescence around 2mM or 3mM NaBu. The increase in fluorescence mirrored the

increase in toxic effect on the cells observed in Figure 18. By 5mM NaBu, the level of fluorescence was comparable to that of infected cells (Figure 16C). While not every cell in any image of Figure 20 displayed a high level of brightness, those that did would definitely create a high level of noise in an End Point Dilution Assay.
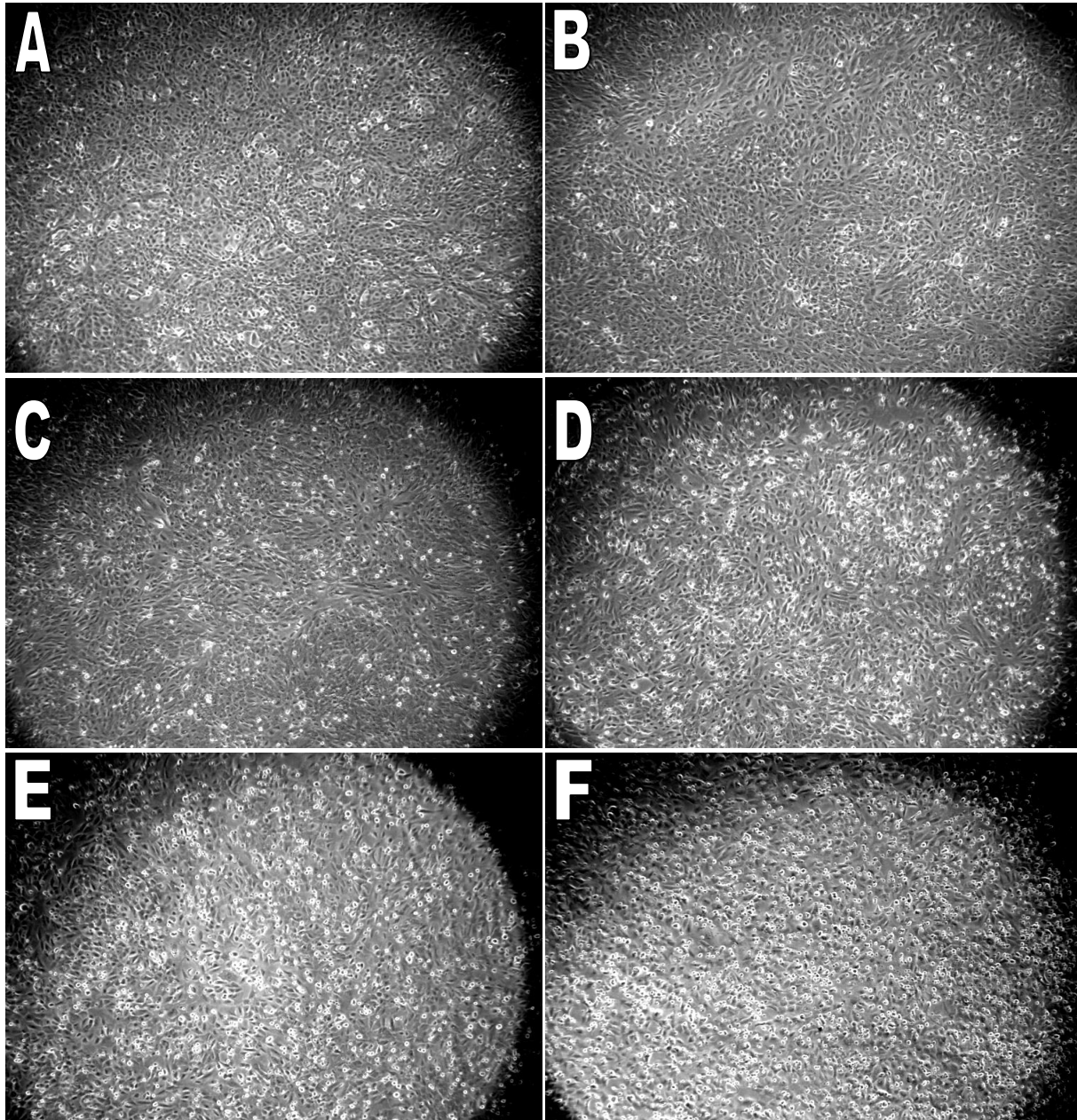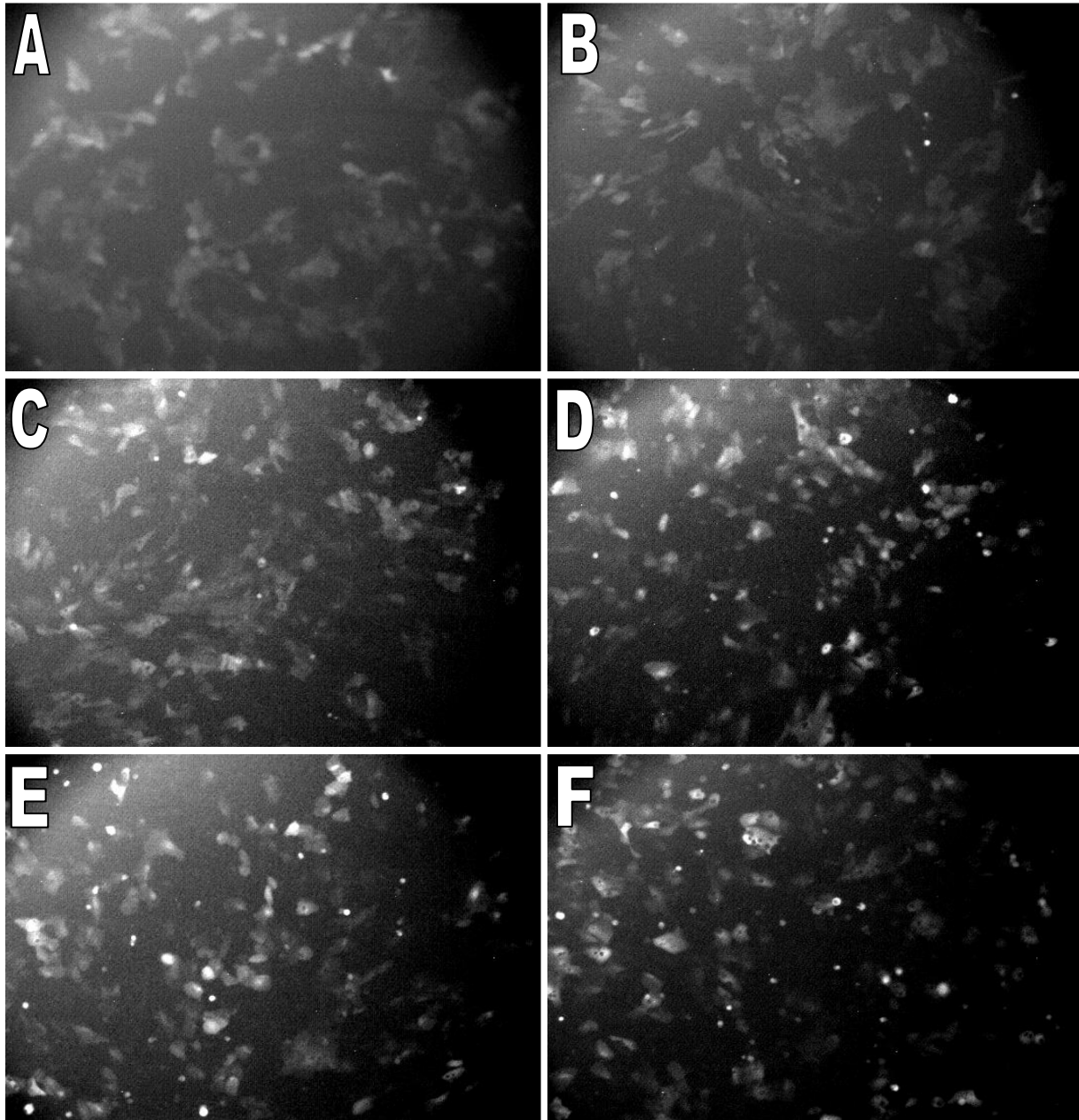

Figure 21: Cell Culture Spiked 24hrs after Seeding Fluorescence Images 72hrs after seeding (0mM (A), 1mM (B), 2mM (C), 3mM (D), 4mM (E), 5mM (F) NaBu) (40x magnification)

The increase in leakage was also observed in samples spiked with NaBu 24hrs after seeding. The increase seemed more gradual than the wells spiked on seeding (Figure 20) and the highest fluorescence (at 5mM NaBu) was less bright than for samples spiked at the time of seeding. Figure 21 also did not demonstrate the same leap in increased fluorescence between 2mM or 3mM NaBu that was observed in Figure 20 and both sets of light images. There was very little observable difference between the fluorescence at 4mM and 5mM NaBu for this plate (Figure 21 E and F).

The eGFP production of this system was significantly leaky with fluorescence detectable in the absence of HSV infection or NaBu. The leakage was most noticeable at concentration of 3mM and above, where it became almost as bright as that which was observed in infected cells without NaBu. NaBu's effect on the cells was most notable at concentrations of 3mM and above. Adding the NaBu at the time of seeding resulted in the more notable enhancement in protein production.

The toxicity of the NaBu resulted in high cell death at 4mM and 5mM NaBu after 24 hours. Although those samples spiked with NaBu 24 hours after seeding showed higher number of dead cells, they also had a higher degree of confluence at the highest concentrations of NaBu. Given the higher level of protein production enhancement when NaBu spiking at seeding coupled with the comparable cell death and confluence, it was judged that NaBu spiking at seeding was the more effective method. Concentrations of NaBu between 2 and 4mM were selected to be the best balance between protein production enhancement and cell death. As long as the enhancement of the fluorescence was more significant for infected cells than it was for uninfected leakage, NaBu spiking of the media showed potential for being the signal enhancement which was required for the EPDA to be effective.

5.4.1.3 NaBu Response in Infected Cell Culture

Having established the NaBu concentrations and NaBu spiking method which seemed to result in the best balance of protein production enhancement and cell death, the NaBu spiking could be applied to infected cells. Higher eGFP production was only useful for the improvement of the EPDA if infected cell fluorescence was improved more than uninfected eGFP expression leakage. This would make the infected wells more easily discernible from the uninfected wells using the plate reader.

The cells were imaged using fluorescence microscopy at 12hpi (36hrs after seeding). This was enough time for eGFP to be expressed in infected cells and as close to the time after seeding. The fluorescence of the infected Vero cell culture was far more easily imaged than the leakage which was analyzed in the experiment, allowing for the larger magnification to be used. Even without any digital optimization the infection could be easily tracked using the fluorescence microscope and the bright fluorescent signal.
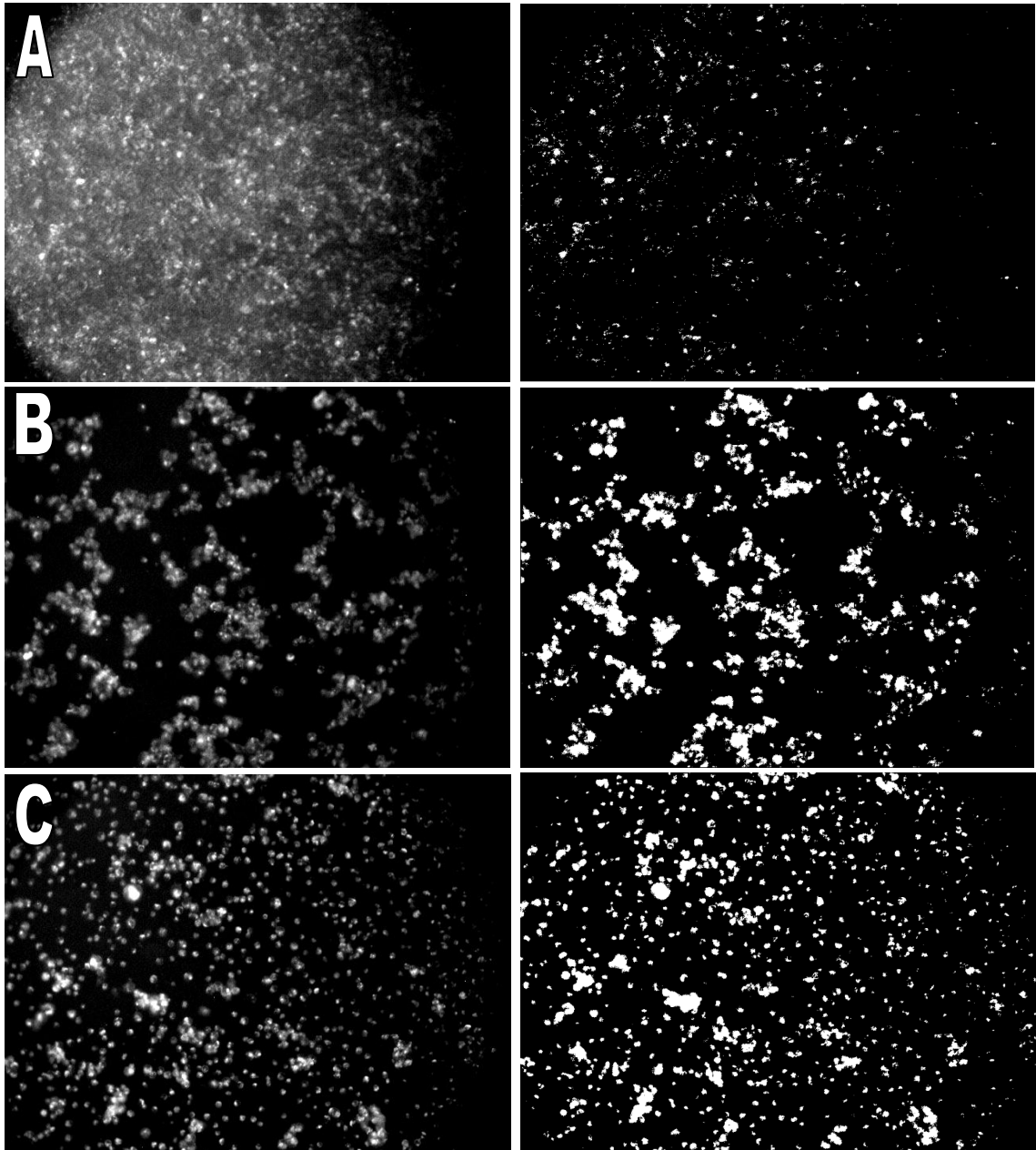
Figure 22: Infected Vero Cell Culture at 12hpi with Original Image on the Left and White/Black on the Right (0mM NaBu (A), 2mM NaBu (B), and 4mM NaBu (C)) (40x magnification)

The Vero cells showed a synchronous infection with a high level of eGFP expression even at 12hpi. Figure 22 can be used to make observations on the culture in general and not just the fluorescence. The health of the cells was seen to deteriorate significantly as the concentration of the NaBu increased. Cells are more detached, and even stop adhering to each other as their structure breaks down. Without NaBu, the cells showed a high level of confluence expected early on in the infection. At 2mM NaBu the cells appeared to be detaching from the culture plate and clumping up, a state usually observed at 20hpi or more. The cells in the culture spiked at 4mM NaBu displayed almost complete detachment and an almost complete lack of cell junctions. NaBu seemed to accelerate the process of cell death due to infection.

The fluorescence was likewise clearly influenced by the NaBu concentration. Figure 22A shows a fairly low level of fluorescence with only a few points meeting the level in Figure 22B and C. The latter two cultures on the other hand had a much more consistent level of fluorescence. The more spread out nature of cells in the culture spiked with the 4mM NaBu made a qualitative visual comparison more difficult, but its fluorescence seemed to be more pronounced than that of the culture spiked with 2mM NaBu. These images were subjected to further signal intensity gating using ImageJ to only capture higher intensity fluorescence provided much more convincing evidence of this higher fluorescence in Figure 23.
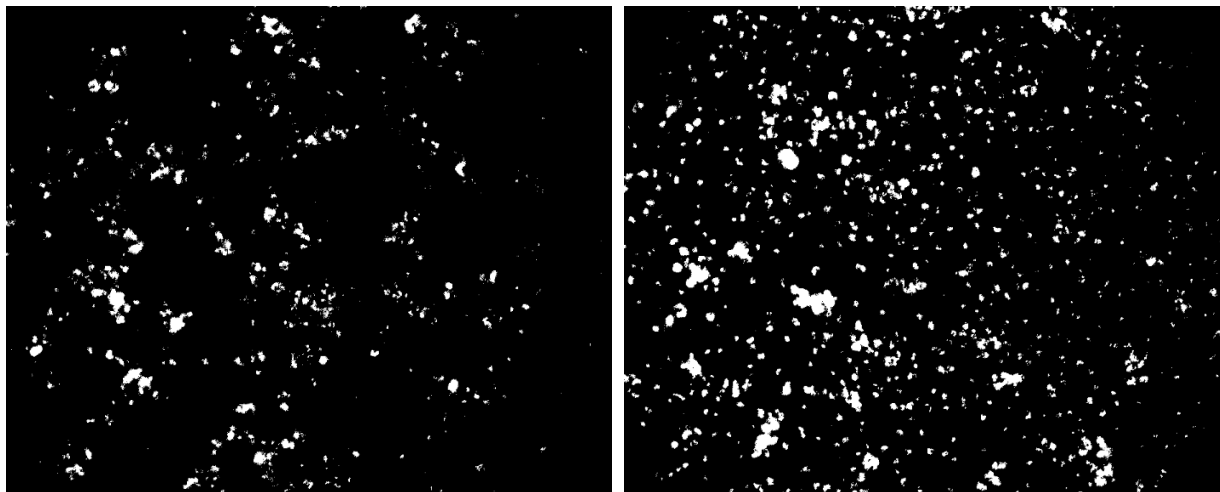
Figure 23: High Threshold fluorescence of infected cells with 2mM (left) and 4mM (right) NaBu (40x magnification)

The increase in fluorescence with NaBu concentration was established at this point and it was the degree to which it improves the detection of the infection that needed to be investigated.

The factor by which the infection of the cells increased the level of fluorescence was therefore calculated by dividing the 12hpi fluorescence by the fluorescence in the absence of HSV.
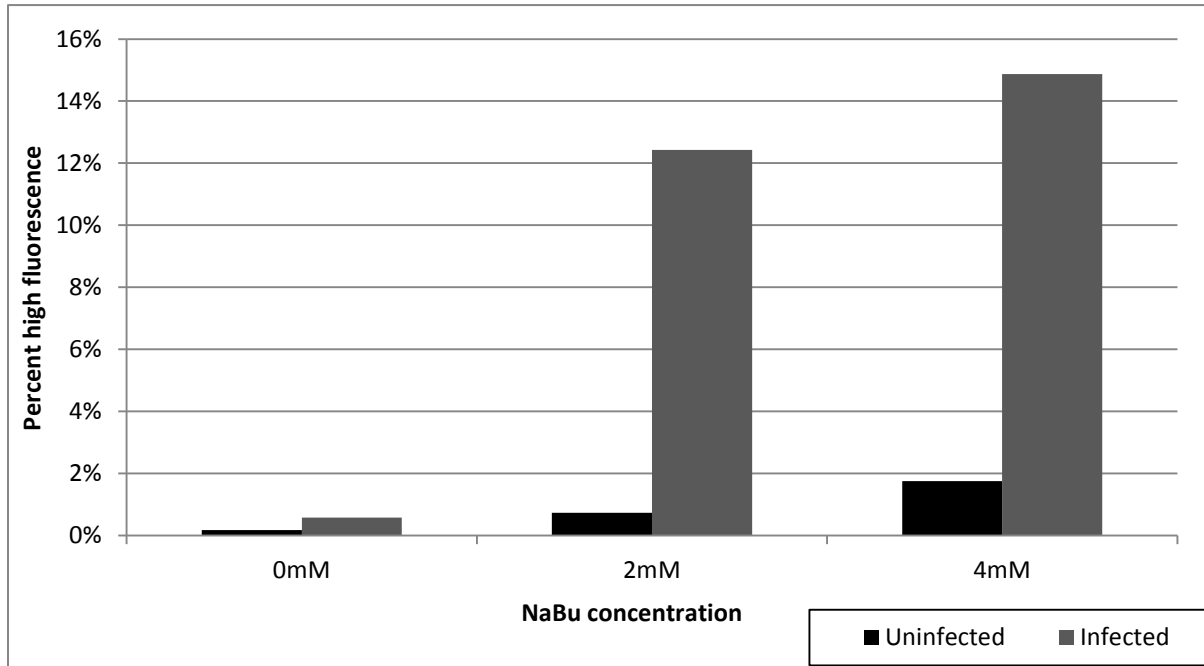
Figure 24: Percent of pixels in the image of each culture over the "high fluorescence" threshold in infected and uninfected HSV2012-121 Vero Cells (n=1)

Figure 24 shows the significant increase in fluorescence resulting from infection with ACAM529. The background (uninfected cell) fluorescence was low at all concentrations of NaBu, but the addition of 4mM of NaBu increases the percentage of the imaged culture fluorescing brightly by a factor of 9.7. The effect on infected cells was far more significant, with a 25.6-fold increase in area fluorescing brightly (between 0 and 4mM NaBu). Comparing infected and uninfected cell fluorescence at each concentration of NaBu, it was at 2mM that the difference between the infected and uninfected cells' fluorescence was the most pronounced with a factor of 16.9. The scale of this increase was almost twice that of the 4mM cultures in spite of the lower fluorescence area overall and lower intensity shown in Figure 23.

5.4.1.4 Conclusions

While the increase in fluorescence with increased NaBu concentration was shown for both infected and uninfected cells, the optimal concentration was 2mM. At 2mM NaBu the difference between infected and uninfected fluorescence was highest. At the same time, the percentage area of the images which corresponded to high intensity fluorescence was comparable to that of the

4mM NaBu culture. Given that the cell death was lower at this concentration (both for infected and uninfected cells) this level also kept the system closer to un-spiked culture conditions. Given the 16.9-fold increase in fluorescence that the cells displayed in the presence of the 2mM NaBu, there is definitely potential for NaBu spiking to improve the accuracy of EPDAs with the HSV2012-121 Vero cells and ACAM529 HSV line. Only one replicate was analysed for each condition and so further investigation is required to ascertain the true statistical significance of the results.

Chapter 6 – Viral Protein Cellular Co-Localization: Virus Production and Egress

In this investigation, immunofluorescent staining combined with confocal microscopy were used to image AV529-19 Vero cells infected with the ACAM529 HSV and to examine the localization and co-localization of viral proteins and cellular features. The motivation for this work was the lack of information on the location of mature virus particles within infected cells which could not be reached by current harvesting methods. The localizations of individual virus proteins could provide important information towards this goal and locating the co-localization of particular proteins could point to mature virus particles within the cells.

6.1 Background

Capturing images of virus particles by microscopy is a difficult proposition for several reasons. The first and most basic of these are the scales involved. Infected host cells are roughly three orders of magnitude larger than the 120-200 nm virus particles they are infected with (in the case of HSV specifically, other viruses may be larger or smaller). It is impossible to locate HSV virus particles using light microscopy. Electron microscopy offers a higher resolution and can be used to image individual virus particles or clusters of particles within cells. Unfortunately, at this scale a lot of the context (in terms of location within the cell and what organelles are involved) is lost unless specialized correlative microscopy equipment and techniques are used.

A method commonly employed to bypass these issues involves fluorescence staining of viral proteins. If a fluorescent tag can be attached to a viral protein then it can be located within a cell at lower magnifications using fluorescence microscopy. If the protein or set of proteins tagged in this way are those which indicate the presence of mature virus particles then their localization can be determined without the use of electron microscopy. Locating individual proteins rather than only whole virus particles can also yield other information which is useful for virology research. Since fluorescence microscopy only images fluorophores, fluorescent staining of major cell structural components (such as actin fibers or cell membranes) is usually used in conjunction with viral protein tagging to locate the host cells and their organelles.

Fluorescence staining of viral proteins requires the delivery of the tag directly and exclusively to the protein in question, all within an infected host cell. There are naturally occurring molecules that can be used to target and tag proteins i.e. antibodies. Antibodies are proteins produced naturally by B cells in vertebrates. These proteins have the ability to bind to foreign molecules (antigens), including viruses. This power can be harnessed and used *in vitro*, to bind to specific antigens. Combined with different fluorophores, the antibody can be used 'stain' specific antigens, a process referred to as immunofluorescent staining (IS).
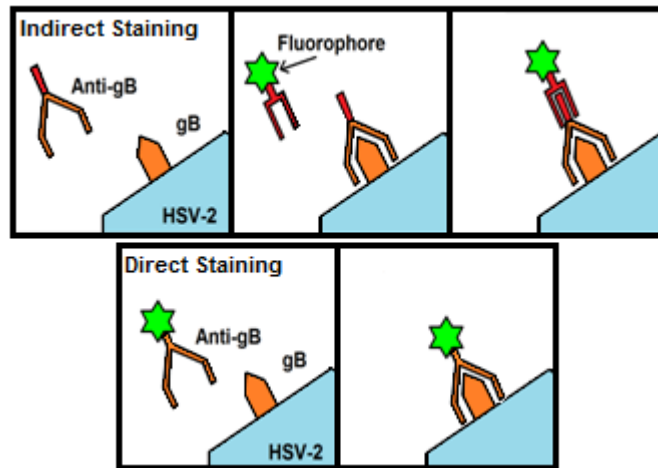
Figure 25: Indirect and direct immunofluorescence staining

The staining itself can be done using two methods (Figure 25), "Direct" and "Indirect" IS. Direct IS is the simpler but more restrictive of the two methods. The antibody targeting the viral protein (called the "primary antibody") is conjugated directly to a fluorophore and a single staining step is required. Conjugated antibodies are expensive to develop and can only be used in very specific systems. The selection of fluorescence-conjugated primary antibodies is therefore limited and creating a new antibody of this type is often too costly for a single project. There is a broader selection of unconjugated antibodies commercially available which can be used in indirect IS.

Indirect IS utilizes an unconjugated primary antibody and a fluorophore-conjugated secondary antibody. The staining is done in two steps, with a primary antibody added first to bind to a target, in this work, a viral protein. Once the cells have been washed of any excess (unattached) primary antibody, a secondary antibody, which targets a primary antibody, is added

to complete the tagging of the protein with a fluorophore. The secondary antibody is less specific and is designed to tag any antibody produced in a given source animal (anti-mouse, anti-goat, etc.). As long as the primary antibody is produced in the animal system that the secondary antibody targets, the indirect staining method can achieve similar results as direct IS without the need for conjugated primary antibodies.

6.2 Determining the efficacy of primary and secondary antibodies for IS of infected AV529-19 cells

The use of antibodies in IS creates some unique challenges for experimental design. The antibodies must be selected carefully both in terms of being able to achieve the goals set out for the experiment and in terms of being compatible with each other and the system being stained. Reviewing the literature and supplier recommendations can provide some information on the compatibility of the antibodies for a given system. However, since the ACAM529/AV529-19 system is genetically modified and unique, experimental results were also required to ascertain the viability of various antibodies. The goal of this experiment was to stain infected Vero cells with potential antibodies and image the staining to determine which antibodies could be used in future experiments.

Antibodies were selected based on availability from known suppliers, literature references of the specific products being purchased, and knowledge gained through literature review of the HSV virus itself. Due to the specialized nature of the experiment, only one conjugated primary antibody was identified. The remainder of the staining was accomplished using indirect IS. The conjugated antibody was anti-glycoprotein E attached to an FITC fluorophore, or "a-gE+FITC". The unconjugated antibodies were also named after the proteins they target and were designated as "a-gB", "a-gC", "a-gD", "a-ICP27", "a-ICP5", and "a-poly".
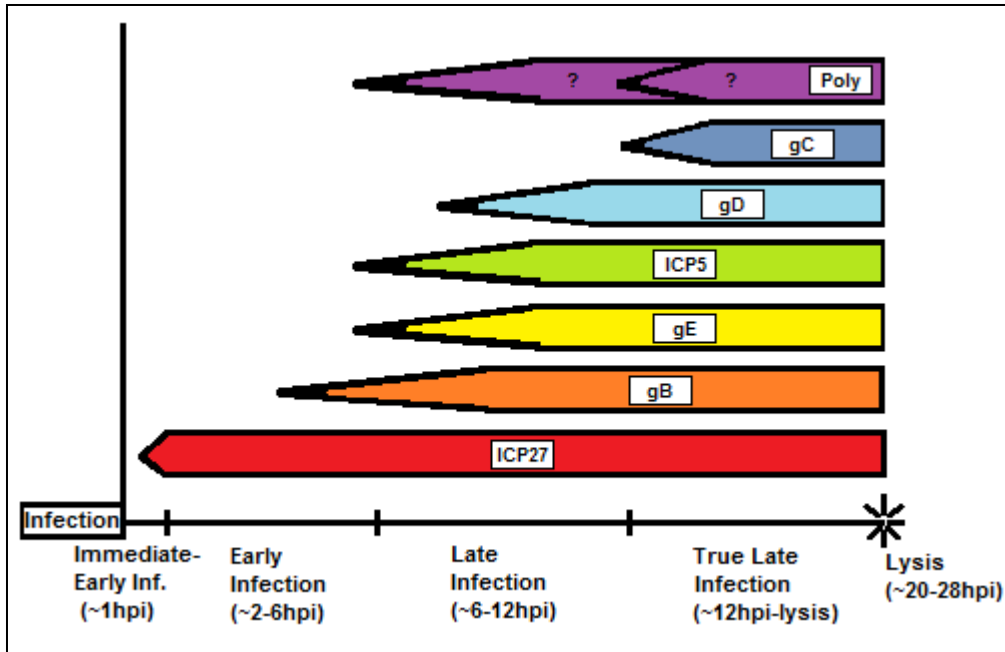
Figure 26: Expected gene expression timing

During infection, gB, gC, gD, and gE, which are all envelope glycoproteins, are produced at later stages of infection (Figure 26) and can be found at sites where virus particles become enveloped and bud out from the cell [2]. These proteins were targeted because co-localization of these proteins could indicate sites of mature virus particles. Finding them together with ICP5, which is a major viral capsid proteins, would be evidence of fully formed virus particles. "Poly" refers to a polyclonal antibody which targets the capsid proteins and other late structural components of HSV virus particles, much like a-ICP5. ICP27 is an essential multifunctional protein which could provide an earlier indication of infection (Figure 26).

6.2.1 Determining noise levels and assessing negative controls for viral protein IS

Controls are an essential part of any experiment, allowing the system's background noise to be quantified and exposing false positive signals. In fluorescence staining, controls are even more important, and without them, differentiating between true signals and non-specific binding is nearly impossible. The IS conducted in this investigation was aimed at identifying proteins produced through viral infection, and so two controls were necessary: a "no infection" control to show non-specific binding of the stains, and a "1 hpi" control to identify any proteins from the infecting HSV particles which were stained.

With no virus present, any staining which occurred in the no infection control could be attributed to non-specific binding with absolute certainty. At 1hpi the infection is just beginning and no progeny viral proteins should have been created in significant quantities. Any signal at 1hpi above and beyond the "no infection" background could be considered a false positive for this reason, as it does not represent progeny viral protein being stained.

Three representative proteins were chosen from the full panel to determine the extent of the non-specific binding which could be expected. A-gE+FITC and a-Poly were both unique, with the former being the only direct staining antibody and the latter being the only polyclonal antibody used. They were included in the control experiment alongside a-ICP5, which was used as a representative indirect staining antibody.
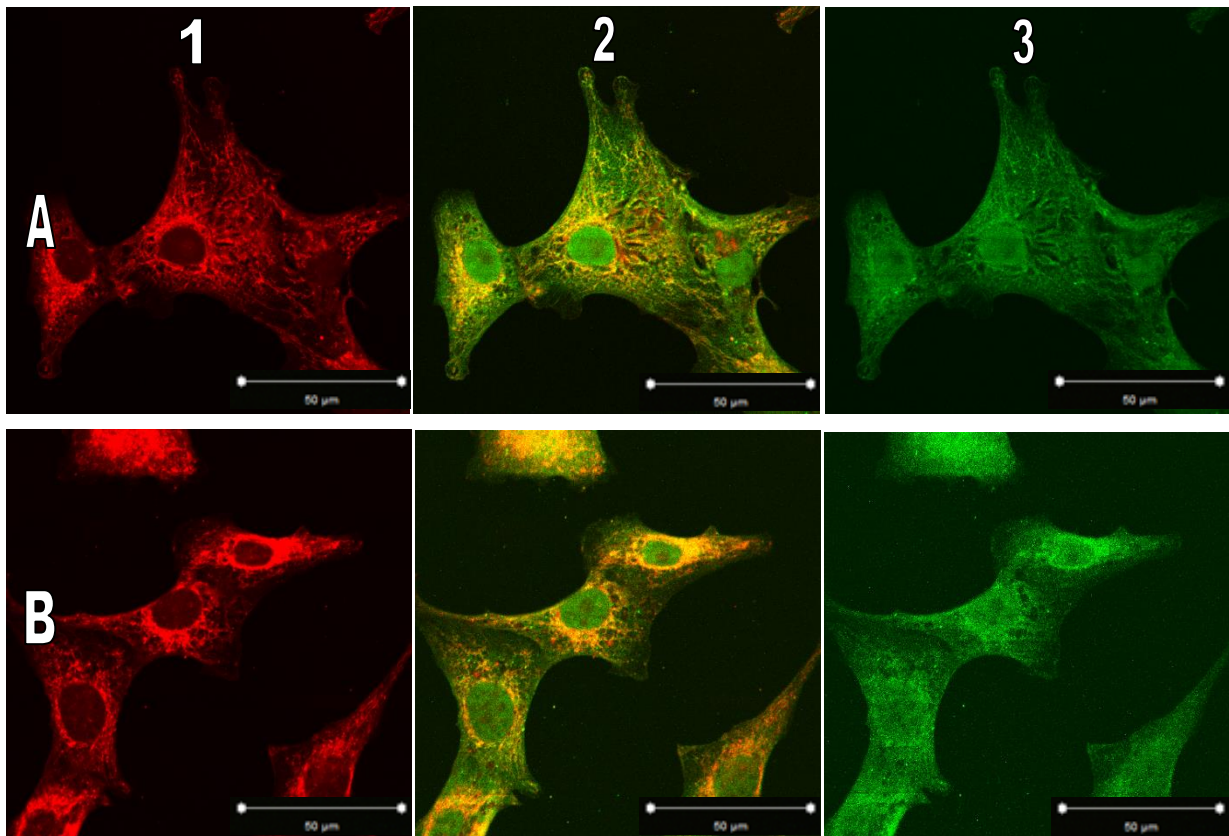
Figure 27: Infected AV529-19 cell a-Poly staining, no infection (A: no infection, B: 1hpi, 1: Cellmask (647) channel only, 2: 488/647 channel overlap 3: Alexafluor 488 channel only)
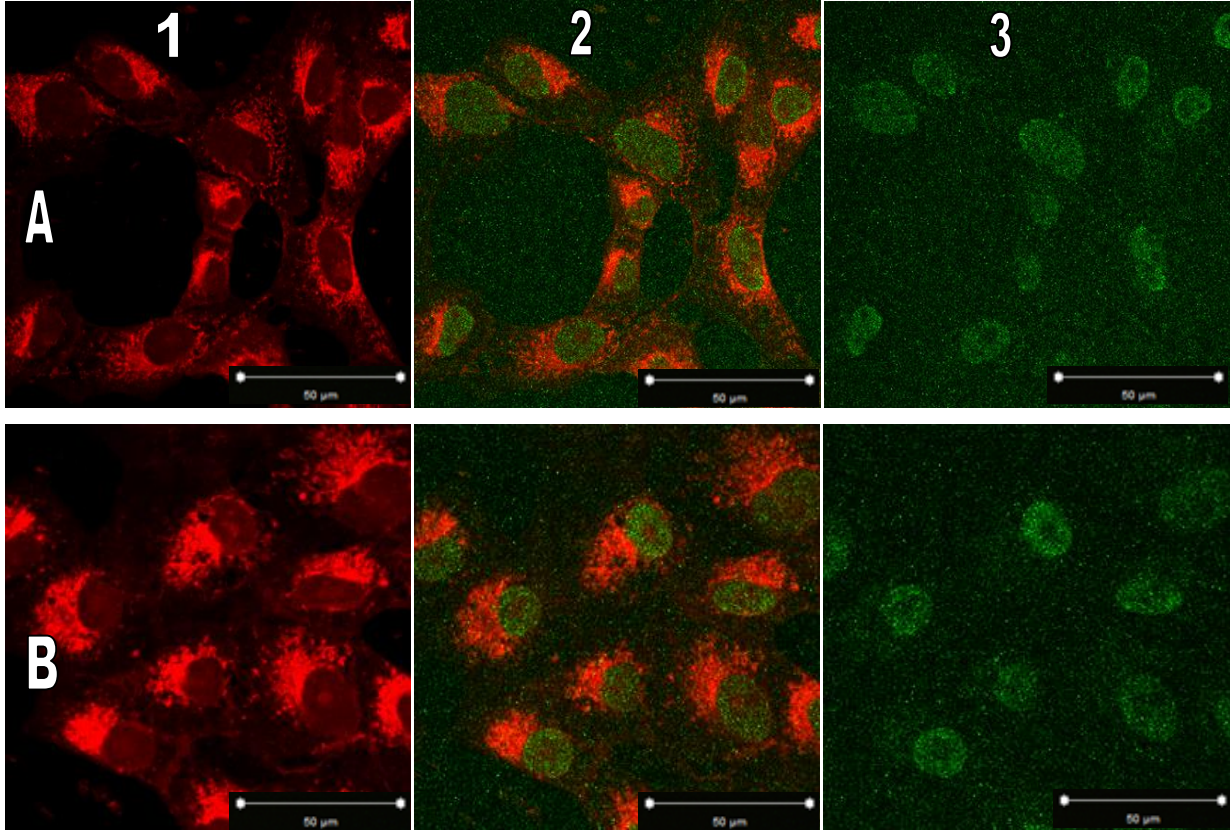
Figure 28: Infected AV529-19 cell a-gE staining, no infection (A: no infection, B: 1hpi, 1: Cellmask (647) channel only, 2: 488/647 channel overlap 3: Alexafluor 488 channel only)
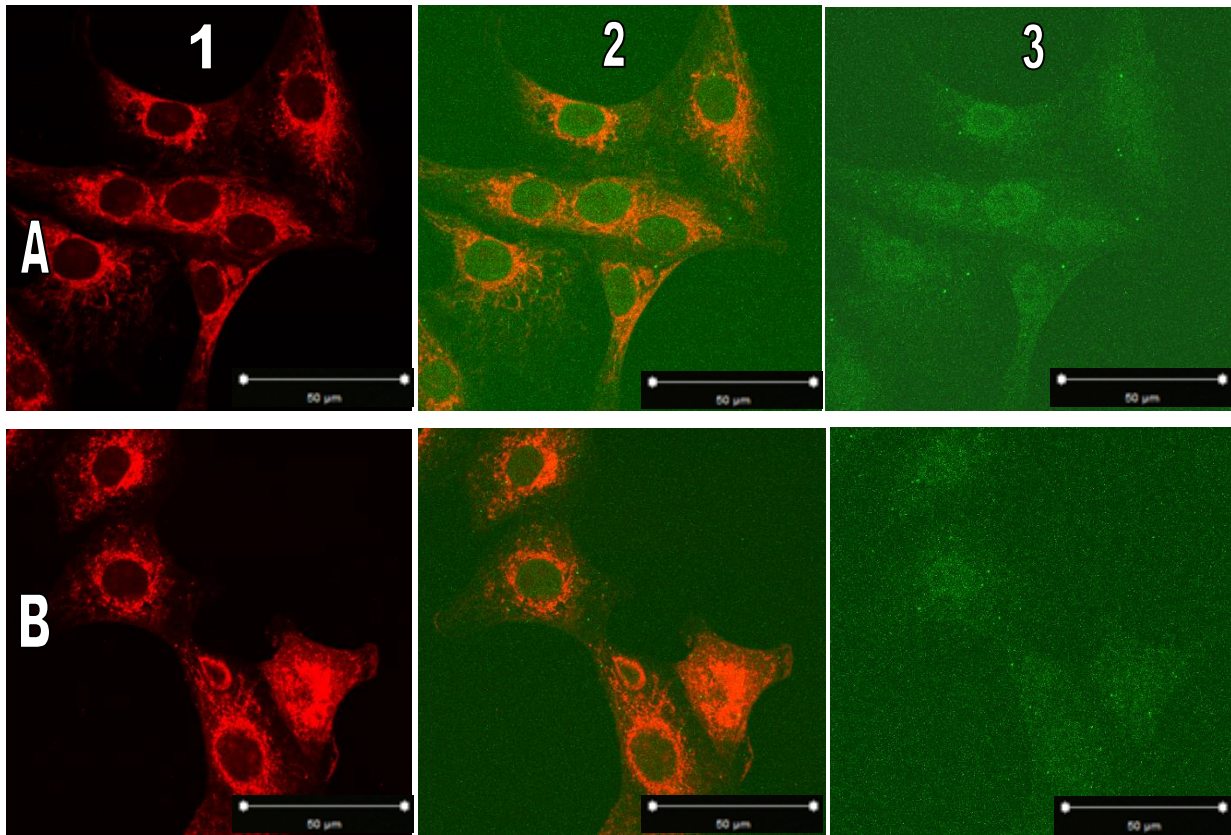
Figure 29: Infected AV529-19 cell a-ICP5 staining, no infection (A: no infection, B: 1hpi, 1: Cellmask (647) channel only, 2: 488/647 channel overlap 3: Alexafluor 488 channel only)

The images in Figure 27 indicated the very high level of non-specific binding in the a-Poly antibody indirect staining. The no infection and 1hpi control conditions showed a high intensity of staining even compared to the CellMask membrane stain. The pattern made by the Cellmask stain (Figure 27 1A and 1B) is almost exactly the same as that in the second channel (Figure 27 3A and 3B). It was not clear whether the primary or secondary antibody were primarily responsible for the non-specific signal. However, given that neither was used in combination with any other antibody and no other secondary antibody was available for use with the a-Poly this question could not be resolved within the scope of this investigation.

Staining with a-gE+FITC also showed significant fluorescence signal in the control images (Figure 28). This signal (Figure 28 3A and 3B) was significantly weaker than that which was observed for a-Poly in Figure 27 and was observed primarily in the cell nuclei (which can be seen in Figure 28 1A and 1B as rounded features surrounded by higher CellMask staining).

Of the antibodies investigated the a-ICP5 antibody had the highest specificity. The AlexaFluor 488 signal in the control images (Figure 29 3A and 3B) was faint and required significant enhancement to be visualized. What signal was observed in these images did not match the CellMask signal (Figure 29 1A and 3B) as closely as it had in the case of a-Poly (Figure 27). These findings were positive in light of the use of a-Mouse AlexaFluor 488 secondary antibody in the majority of the staining conducted on infected cells and validated the use of indirect staining in spite of the issues encountered in the a-Poly controls. None of the antibodies showed increased intensity or distribution of fluorescent signal in the 488nm channel of their 1hpi control (Figure 27, Figure 28, and Figure 29 B3) as compared to their respective 0hpi control (Figure 27, Figure 28, and Figure 29 A3).

6.2.2 IS antibody panel of infected cells at 6 and 18hpi

6hpi and 18hpi time points were stained to capture events both early and late in the infection. Only a few of the proteins stained were expected to appear within 6 hours of infection, namely ICP27, gE, and potentially gB and ICP5 (Figure 26). 6hpi staining was conducted in the hopes of testing the stains' lower limit of detection as well as provide insight on which antibodies may be suitable for early-infection work. By 18hpi all proteins were expected to have been expressed and visible as long as the primary antibody (and secondary where applicable) were effective.

6.2.2.1 Infected Cell Protein 27 (ICP27)

ICP27 is a multifunctional protein essential for viral replication. It is expressed in the "immediate early" (α) stages of infection and is involved in translation of viral genes [2]. It has also been implicated in late gene expression enhancement and progeny virus particle release from the extracellular surface of host cells [234]. The protein is known to be present in the nucleus and cytoplasm of infected cells, and to shuttle actively between the two locations [2].

Figure 30: Infected AV529-19 cell a-ICP27 staining (A: 6hpi, B: 18hpi, 1: Cellmask (647) and 488 channel, 2: Alexafluor 488 channel only 3: Alexafluor 488 channel with high brightness and contrast settings)

The staining with a-ICP27 was weaker than all of the other antibodies' in this investigation. The 6hpi images in Figure 30 A showed almost no signal even with adjustment to brightness and contrast. ICP27 is coded for with an α or early gene, meaning that this lack of signal was not expected. The 18hpi signal was weak as well, barely visible in Figure 30 B2. The staining observed was very diffuse throughout the cells rather than focused within the cell. The multifunctional role of ICP27 justified some signal diffusion, but the weakness of the signal remained an issue in terms of using a-ICP27 for staining experiments.

6.2.2.2 Glycoprotein B (gB)

Glycoprotein B is a trans-membrane protein that is the product of a gene expressed in a "leaky late" (γ_1) fashion. This means that while it was expected that the majority of the expression would occur after 6 hpi, some level of expression was expected earlier in the infection. gB has been detected as early as 2 hpi in some studies [51]. The main function of gB is fusion of the virus membrane with the host cell membrane on attachment through its interactions with the gH/gL complex as well as gD [2]. It has also been found to promote cell-to-cell fusion and

transmission [235], and was therefore expected to be found at cell junctions. It was also expected at sites of HSV envelopment and localizations of mature virus particles

Figure 31: Infected AV529-19 cell a-gB staining (A: 6hpi, B: 18hpi, 1: Cellmask (647) and 488 channel, 2: Alexafluor 488 channel only 3: Alexafluor 488 channel with high brightness and contrast settings). The circles indicate localizations at (by colour): cell outer membrane (red), envelopment sites (yellow), and cell/cell junctions (blue)

At 6hpi, a-gB was the most successful of all antibodies used. The localizations seen were dispersed but not diffuse with low background noise levels (Figure 31 A). Given that gB was expected to be detectable within 2 hours of infection, it was not unrealistic that it could be seen at 6hpi. This, along with heavy gB presence at cell-to-cell junctions and outer cell membranes, meant that the signal was very likely to be specific to gB. The signal only grew in strength for the 18hpi staining of gB (Figure 31 B), with strong localizations observed at the same expected regions as well as in pockets within infected cells. This was consistent with glycoprotein B's known function as an essential protein for viral attachment and fusion.

6.2.2.3 Glycoprotein E (gE)

Like other glycoproteins, gE is found on the outer membrane of mature HSV-2 particles and is multifunctional. Similar to gB, is connected to cell-to-cell transport [104] and has additional

functions in anti-host defense of the virus [2]. The gene coding for this protein is expressed under a γ_1 promoter like that of gB, but there is no evidence to support that it could be detected as early as gB in the infection. Nevertheless, it was anticipated that some expression could be detected by 6 hpi.

Figure 32: Infected AV529-19 cell a-gE+FITC staining (A: 6hpi, B: 18hpi, 1: Cellmask (647) and 488 channel, 2: Alexafluor 488 channel only 3: Alexafluor 488 channel with high brightness and contrast settings). The circles indicate (by colour): cell non-specific binding in nuclei (red) and possible non-nucleus localization (yellow).

Staining with a-gE+FITC at 6hpi (Figure 32 A) was consistent with the 1hpi and no infection negative controls (Figure 28 A3 and B3) with high levels of staining in the cell nuclei and diffuse background noise. Given the lack of evidence for gE presence in the nucleus, this was likely to be non-specific staining. The low specificity of the staining made the presence of gE impossible to determine in Figure 32. At 18hpi the signal strength increased and several non-nuclear localizations were observed (Figure 32 B3). These localizations were consistent with the known functions of gE, appearing near cell junctions and within the infected cells. The intensity of the positive signal reduced the effect of the diffuse background noise but did not eliminate it.

6.2.2.4 Infected Cell Protein 5 (ICP5)

ICP5 is also known in the literature as viral protein (VP) 5. Transcription of its gene is controlled by a γ_1 promoter [236]. ICP5 is a major structural component in HSV-2 viral capsids [236] and is known to localize at sites of capsid assembly within the nucleus. As part of the capsid, ICP5 is expected to spread throughout the cell with virus particle envelopment and egress at later stages of infection.
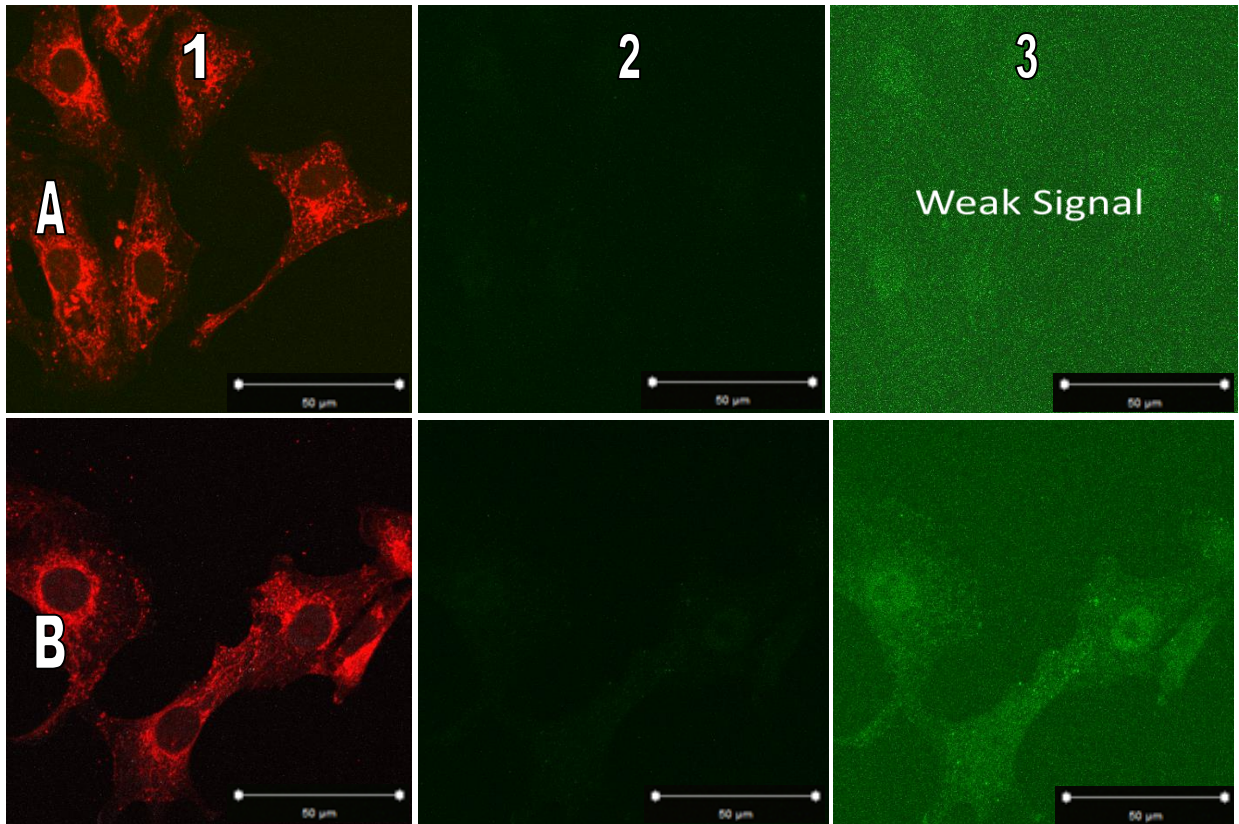

Figure 33: Infected AV529-19 cell a-ICP5 staining (A: 6hpi, B: 18hpi, 1: Cellmask (647) and 488 channel, 2: Alexafluor 488 channel only 3: Alexafluor 488 channel with high brightness and contrast settings). The red circle indicates strong localizations in infected cell nuclei.

The 6hpi Alexafluor 488 signal for a-ICP5 was non-existent (Figure 33 A) which was expected for a protein expressed under a γ_1 promoter. The 18hpi signal was strong, with very no brightness/contrast adjustments required. This pointed to a very high specificity of the antibody and validated the 6hpi results (poor antibody binding would result in weak signal in all samples). The majority of the staining in Figure 33 B was concentrated in the nuclei of certain cells but not others, which was further evidence of high specificity (otherwise all nuclei would have been stained). Furthermore, the non-uniform staining of infected cell nuclei was consistent with the

90

known formation of distinct occlusions at which viral DNA encapsulation occurs [2, 43, 44]. By 18hpi the capsids were expected to be at sites of mature virus particle egress, but this was not reflected in the images taken (Figure 33 B3).

6.2.2.5 Glycoprotein D (gD)

gD is another glycoprotein involved in the fusion of virus particles to host cell membranes. It signals the gH/gL + gB fusion complex when a compatible receptor is detected and initiates the conformational changes required for fusion to begin [20]. This protein has also been implicated in control of host cell apoptosis [237]. The gene coding for gD is expressed under a late (γ) [2] promoter. gD was not expected to appear until after the 6 hpi timepoint. Like other glycoproteins, gD was expected to localize at sites of virus envelopment and egress within infected cells. No specific staining was expected in the cell nuclei given this protein's functions.
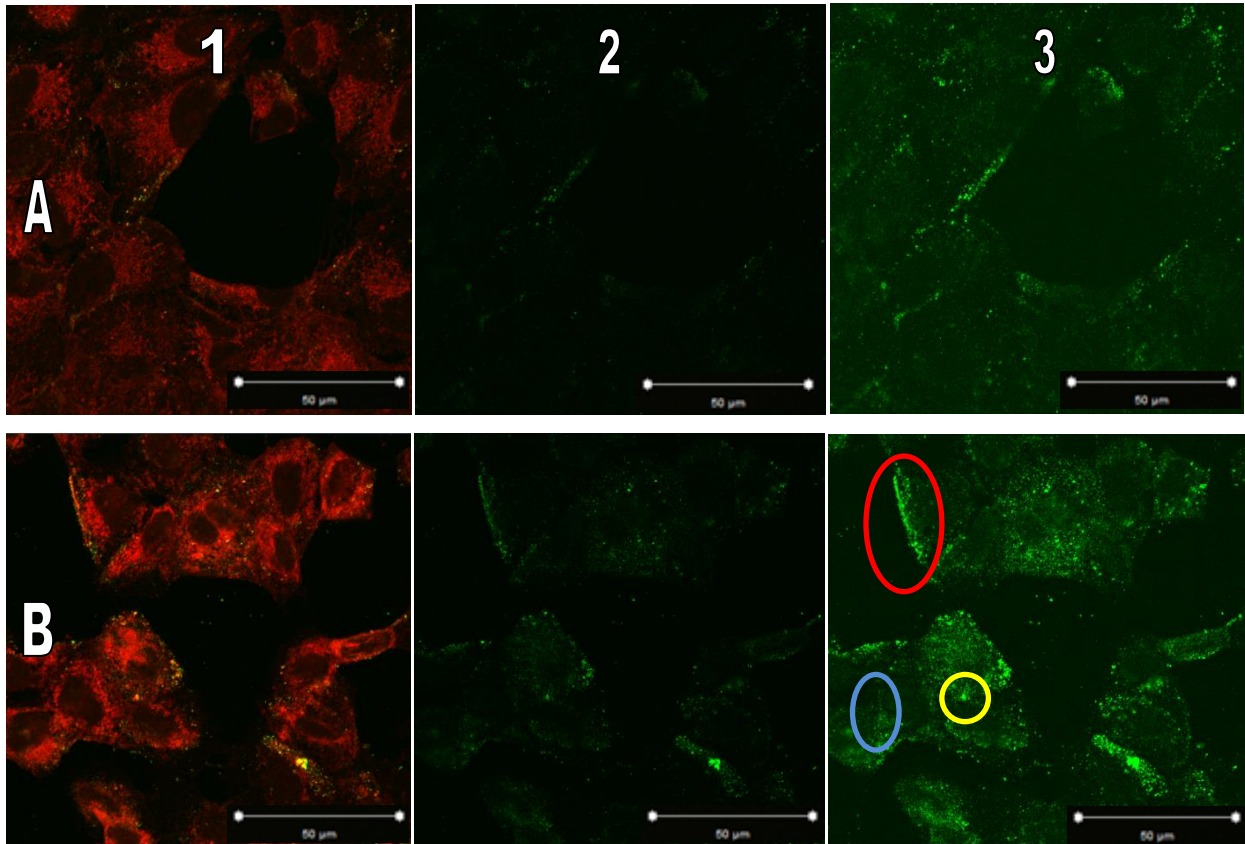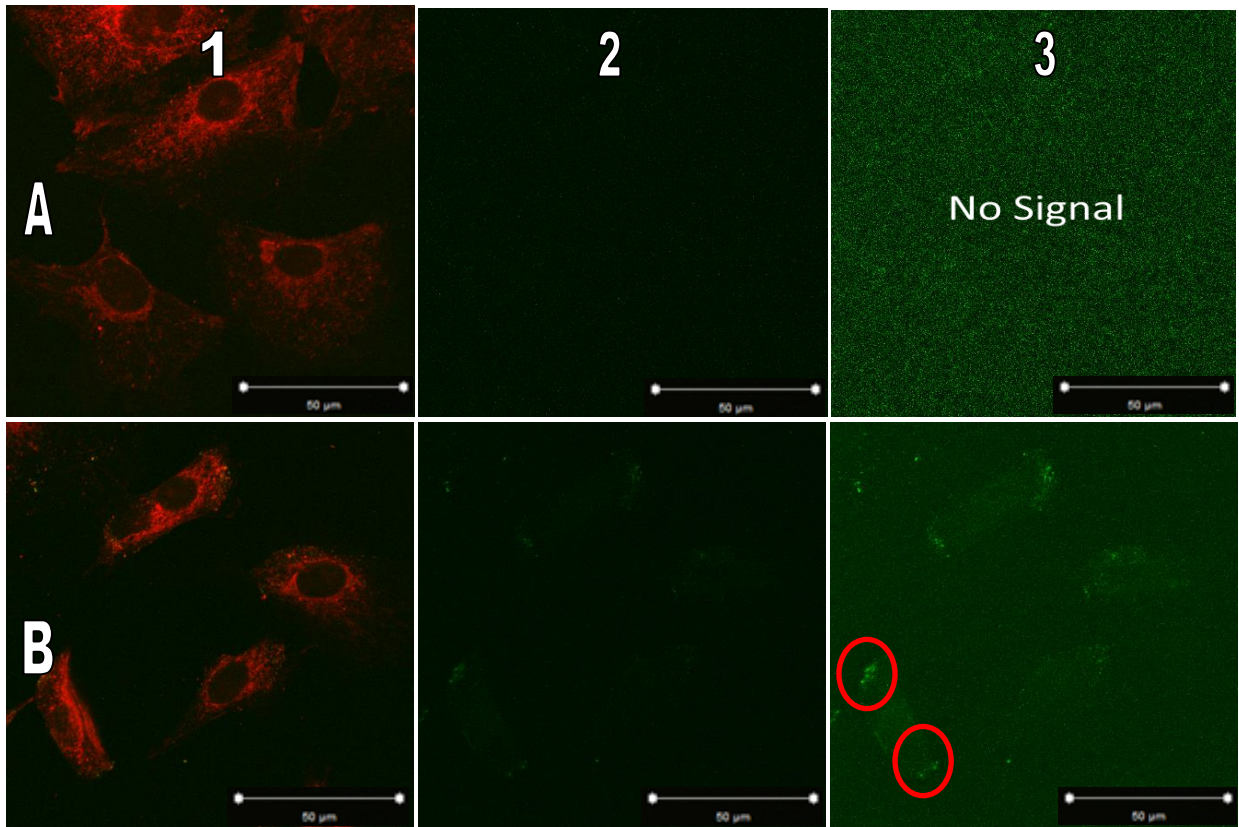

Figure 34: Infected AV529-19 cell a-gD staining (A: 6hpi, B: 18hpi, 1: Cellmask (647) and 488 channel, 2: Alexafluor 488 channel only 3: Alexafluor 488 channel with high brightness and contrast settings). The red circles indicate polarized localizations at outer cell membranes.

The 6hpi signal of the a-gD antibody was undetectable. The lack of non-specific binding in Figure 34 A2 and A3 was encouraging and the complete lack of staining was expected. The

staining in the 18hpi images (Figure 34 B) further established the efficacy of the a-gD stain. While the signal at 18hpi was not strong, it remained discernible. The protein was seen to accumulate near the outer cell membranes and in pockets within the cell. This along with the lack of staining in the nucleus was in agreement with literature for the localization of glycoproteins.

6.2.2.6 Glycoprotein C (gC)

gC is a viral protein that is expressed under a true late (γ_2) promoter and was not at all expected to appear until the 18 hpi timepoint. The 6hpi timepoint was stained for consistency and as a control to ensure specificity. The distribution of gC throughout the host cell was expected to be the same as that of gD and gB as it too is implicated in fusion of the virus particle membrane to that of the host. gC contributes by binding to heparin sulfate, an outer membrane structure found in all animal tissues, with a an affinity higher than that of other HSV-2 protein-receptor interactions [238].
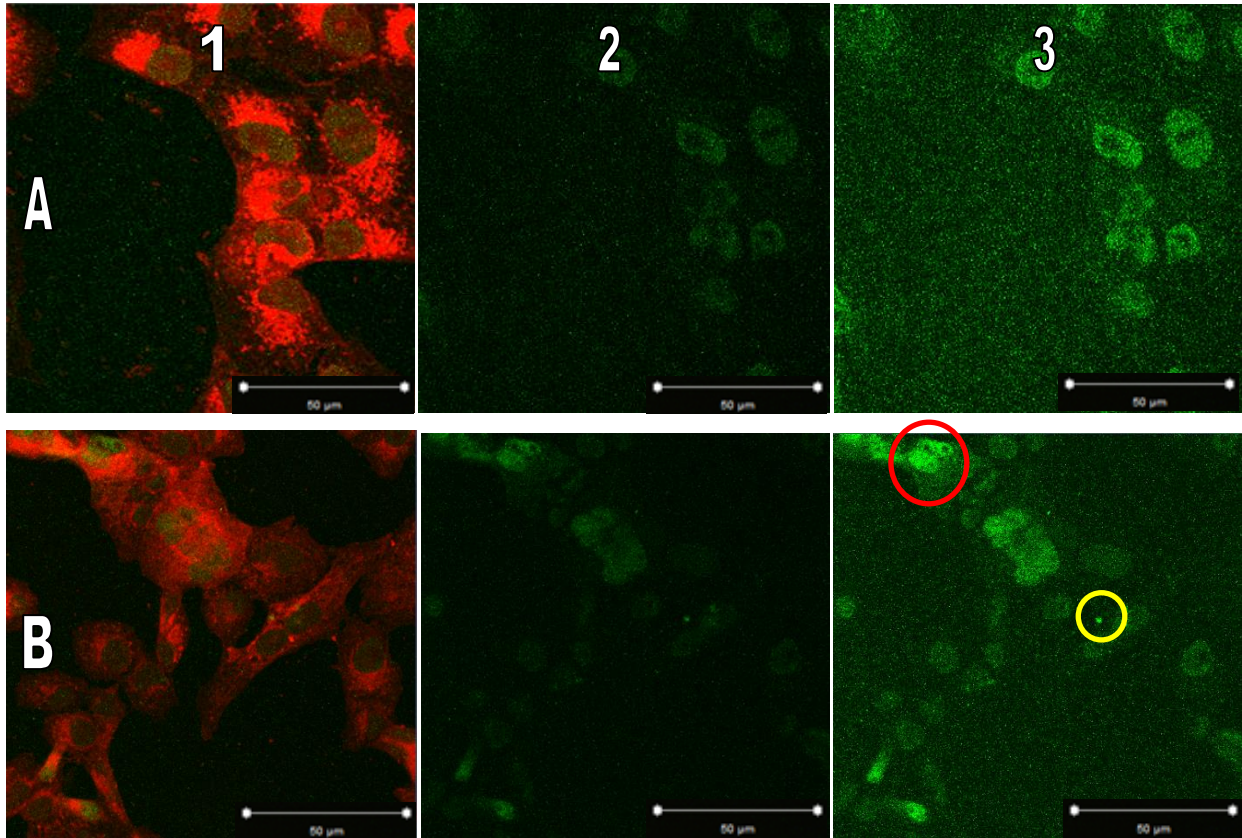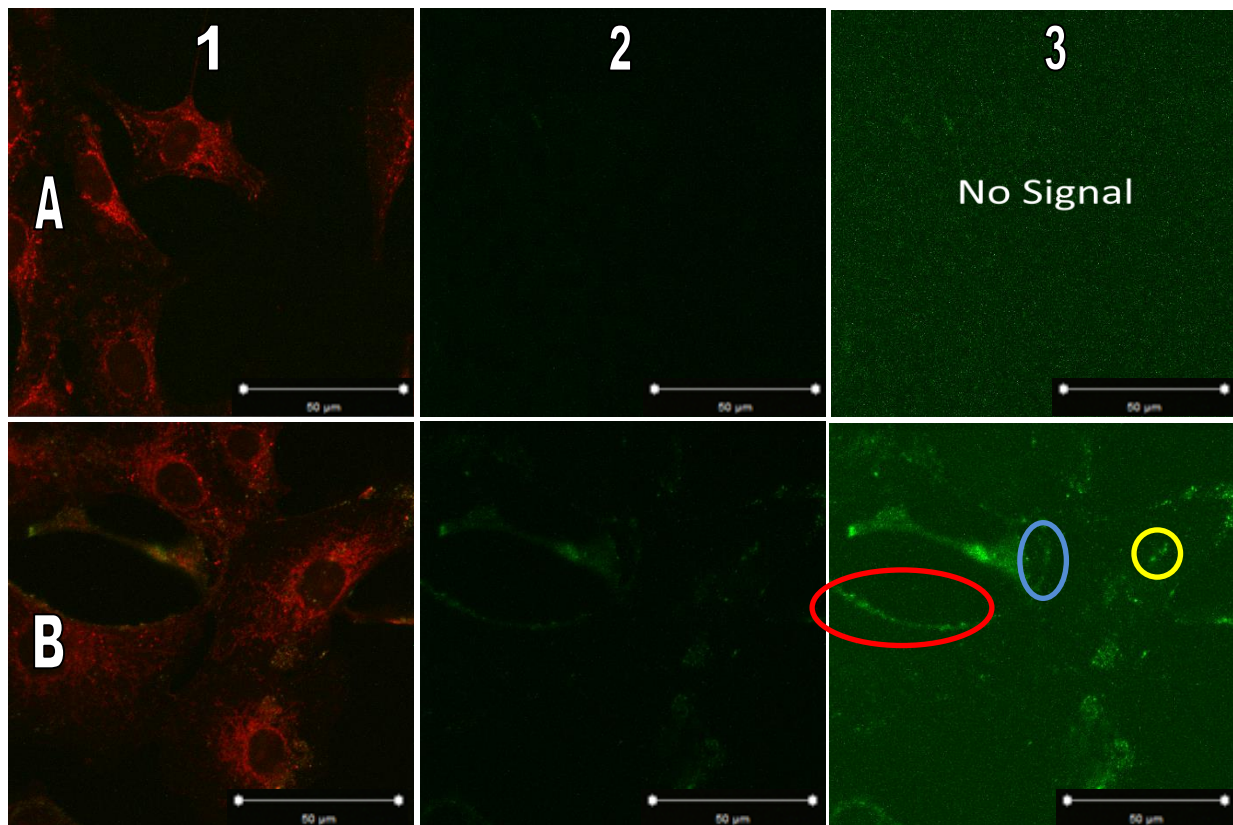

Figure 35: Infected AV529-19 cell a-gC staining (A: 6hpi, B: 18hpi, 1: Cellmask (647) and 488 channel, 2: Alexafluor 488 channel only 3: Alexafluor 488 channel with high brightness and contrast settings). The circles indicate localizations at (by colour): cell outer membrane (red), envelopment sites (yellow), and cell/cell junctions (blue)

92

The 6hpi signal was effectively undetectible for gC as anticipated (Figure 35 A), while the 18hpi staining was visible even at lower brightness and contrast (Figure 35 B). The a-gC signal did not seem to co-localize with the cell nuclei or the regions with strong Cellmask staining, further evidence of specific binding. The gC signals seem to be localized either on the edges of the infected cells, or in diffuse regions within the cell which was consistent with the known properties of this protein.

6.2.2.7 Polyclonal antibody against HSV-2 late structural proteins (Poly)

The proteins stained by a-Poly were not known and so the time of expression could not be determined. It was know, however, that the proteins were structural in nature and so were not expected until mid to late infection (6-12hrs). This was based on the known expression patterns of HSV-2 structural proteins. Capsid proteins like ICP5 and VP23 were known to be produced by expression of genes under γ_1 promoters, while tegument proteins like VP1-2 and VP26 are produced through expression of genes under a γ_2 promoter [2]. However, given the poor specificity displayed by a-Poly in Section 6.2.1 this antibody was not anticipated to perform well at any time post-infection.
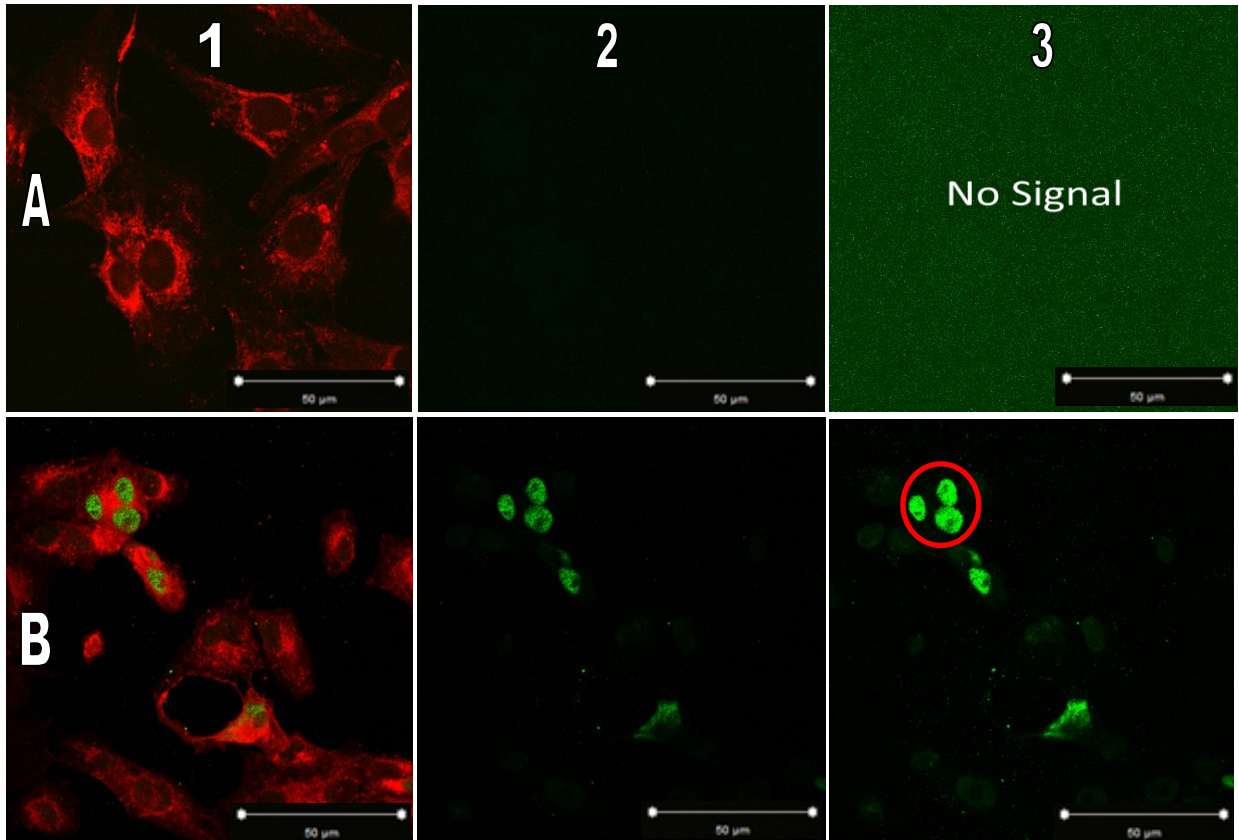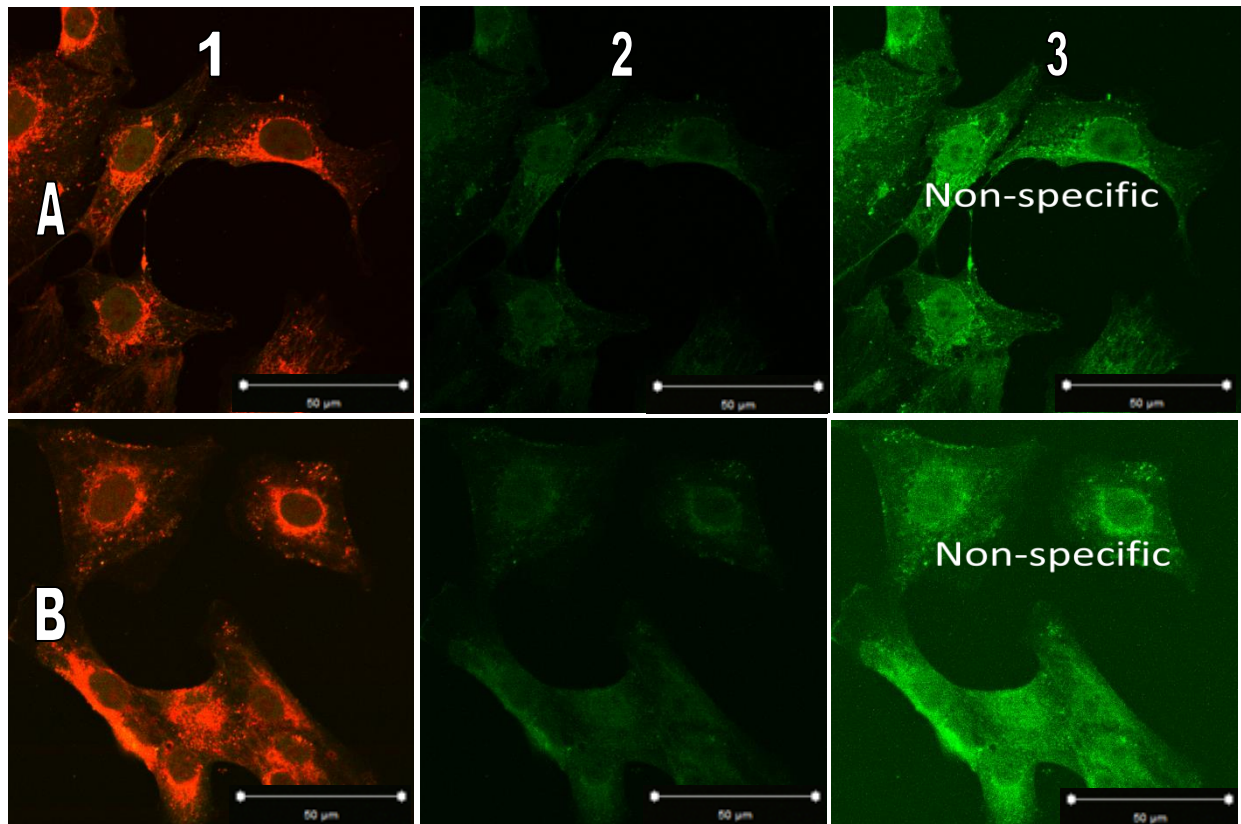
Figure 36: Infected AV529-19 cell a-Poly staining (A: 6hpi, B: 18hpi, 1: Cellmask (647) and 488 channel, 2: Alexafluor 488 channel only 3: Alexafluor 488 channel with high brightness and contrast settings)

The a-Poly staining in Figure 36 A and B was similar to the control images (Figure 27). In addition, the 6hpi staining was nearly identical in strength and distribution in the cells to that of the cells 18 hpi. With the continued strong mirroring between CellMask and a-Poly staining, all these observations pointed towards non-specific binding. The extent of the similarity between infected and uninfected cell staining also pointed towards very low levels of specific staining or expression of the proteins being targeted.

6.2.3 Conclusions

This investigation provided information on the interactions of a range of antibodies with the system being studied. Knowing what tools can be used to attain useful information can save time in future experiments. 1 hpi controls showed no significant differences from "no infection" controls for any of the antibodies tested. While viral proteins from the infecting virus may be present in the cells, their effect was seen to be minimal. a-Poly was the only antibody for which staining was deemed too non-specific for further experiments. a-gE+FITC also produced non-

specific binding, but this was for the most part limited to the cell nuclei and did not affect the antibody use where direct IS is required.

Table 3: Summary of Individual Protein Immunofluorescent Staining Results

Viral Protein	Results and Findings		
	Controls	6hpi	18hpi
ICP27	N/A	Weak, diffuse signal	Weak, diffuse signal
gB	N/A	Strong signal, locations supported by literature	Strong signal, locations supported by literature
gE	Non-specific signal in nucleus	Non-specific signal in nucleus	Non-nucleus localizations present
ICP5	Weak non-specific signal throughout	No signal	Very strong signal in infected nuclei
gD	N/A	No signal	Moderate strength signal, polarized localizations
gC	N/A	Weak/No Signal	Strong signal, locations supported by literature
Poly	Strong non-specific signal throughout	Strong non-specific signal throughout	Strong non-specific signal throughout

All 5 antibodies tested, except for a-ICP27, performed relatively well at 18 hpi with good signal strength and staining patterns supported by literature. a-ICP27 produced no signal and was therefore discarded as a candidate for future work alongside a-Poly. Of the remaining 4 antibodies, a-gB and a-ICP5 provided the strongest signal at 18 hpi with localizations which agreed with the literature in terms of their location relative to infected host cell features. All other antibodies produced weaker, but still discernible, signals at 18 hpi. At 6 hpi, only a-gB produced a strong and protein-specific signal. As a result, a-gC, a-gE+FITC, a-ICP5, a-gB, and a-gD are acceptable for future work in staining cell in late infection. Only a-gB was found to be useful in staining cells in early and intermediate stages of infection.

6.3 Mature virus particle identification through co-localization of fluorescently tagged proteins

Locating virus particles within infected host cell is a difficult proposition. Confocal microscopy and IS allow viral proteins to be identified and imaged. Unfortunately, viral proteins do not only

exist as part of a mature virus particle. Proteins can be found by themselves at the sites of their synthesis, together with other proteins being ferried around the cell, at the sites of viral egress, on incomplete virus particles, and on non-infectious virus-like particles. As a result, the imaging of a single viral protein can only be used to study that protein's localizations. To gain more concrete evidence on the location of mature virus particles, more than one protein must be stained.

The concurrent staining of more than one virus protein is a challenging proposition for several reasons. Firstly, if indirect staining is used then the antibodies must be selected very carefully to avoid cross-contamination of the signals. If the source animals of the two antibodies are the same then any secondary antibody used will bind to both equally and the signals become convoluted. The secondary antibodies and/or fluorophores must be selected such that their emission and excitation wavelengths are as far apart as posssible. This improves the ability of confocal microscopy to separate the signals Lastly, the antibodies must be chosen so that their co-localization provides valuable information. Staining multiple proteins which are expected to co-localize at all stages of infection does not point to mature virus particle localization.

For this investigation, infected Vero cells were stained using a-ICP5 and a-gE+FITC to determine the efficacy of this co-staining for investigating the HSV/Vero cell system. Both of these antibodies were derived from mice, but the fluorophore-conjugated a-gE+FITC allowed only one secondary antibody to be used. As long as a-ICP5 and its secondary antibody were added before the a-gE+FITC all cross-contamination was avoided. A co-localization of the two proteins had a very high likelihood of indicating the presence of complete (and hopefully infectious) virus particles given their roles in the assembly of HSV-2. In order to observe the location and condition of infected cells, they were also stained with either CellMask or Cytopainter Phalloidin-iFluor 647 Reagent F-actin stain. While the CellMask staining was significantly brighter and covered a larger portion of the cells' surface area, Cytopainter obscured other signals less and outlined individual cells more neatly.

Controls were examined first to determine the level of background fluorescence, whether from non-specific binding or from other sources of error. Each of the antibodies used was analyzed in Section 6.2 and the staining in this section used much of the knowledge gained from those experiments.
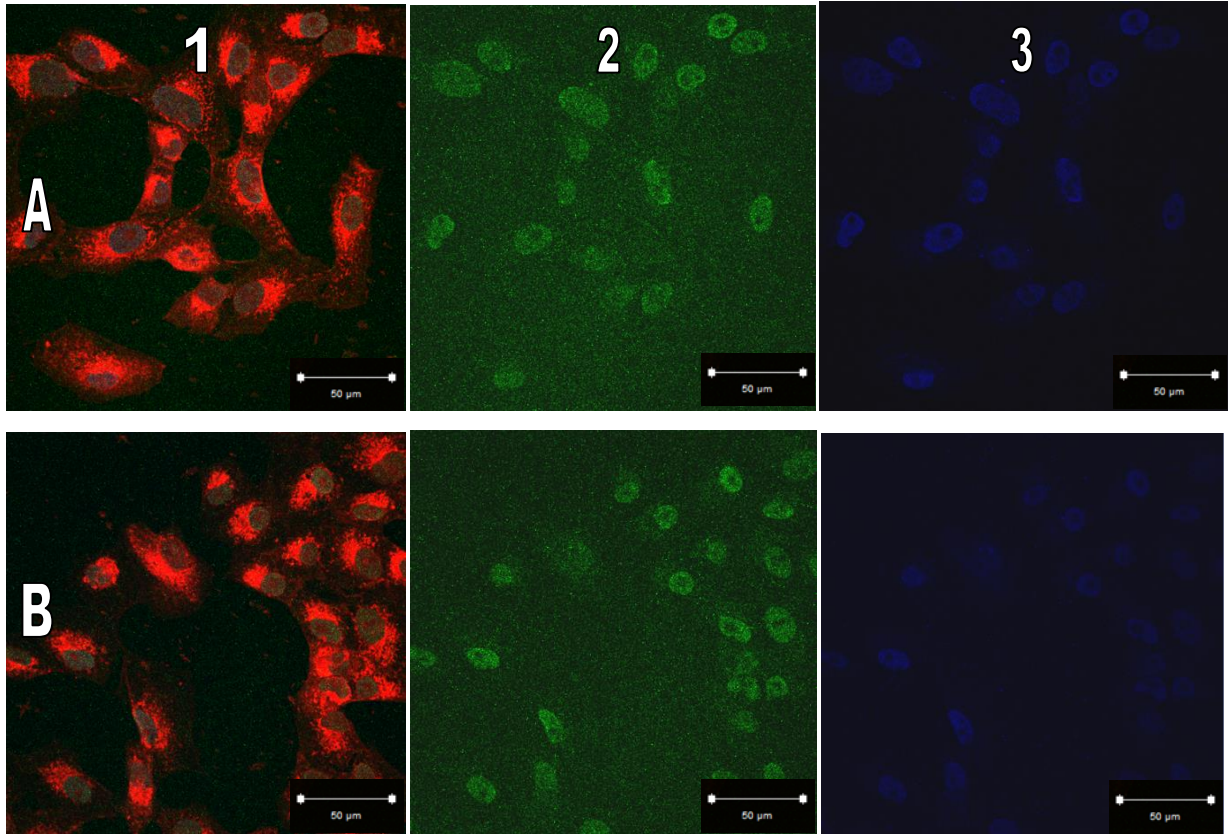
Figure 37: Infected AV529-19 cell a-ICP5, a-gE+FITC, and CellMask staining, no infection (A: no infection, B: 2 hpi, 1: All channels 2: a-gE+FITC staining only (488 channel), 3: a-ICP5 staining only (405 channel))

Figure 37 A2 showed that a-gE+FITC had negligible fluorescence outside of the non-specific nucleus staining already observed in 6.2.1 (Figure 28). a-ICP5 staining was also observed primarily in cell nuclei (Figure 37 A3) which indicated a possible issue for this protein's staining in particular (given that as a viral capsid protein stain it was expected to be seen in the nucleus). Specific a-gE+FITC staining was not expected in cell nuclei and that staining was therefore ignored in the analysis of further images.

The 2hpi control staining in Figure 37 B showed non-specific staining that was not noticeably different from the no infection control. Both antibodies showed no increase in prevalence due to the presence of infecting virus particles. This same observation was made in Section 6.2. As a result, the 2hpi control provided no additional information but did reinforce the findings from the controls in that section and eliminated any concerns over infecting virus particle protein staining.
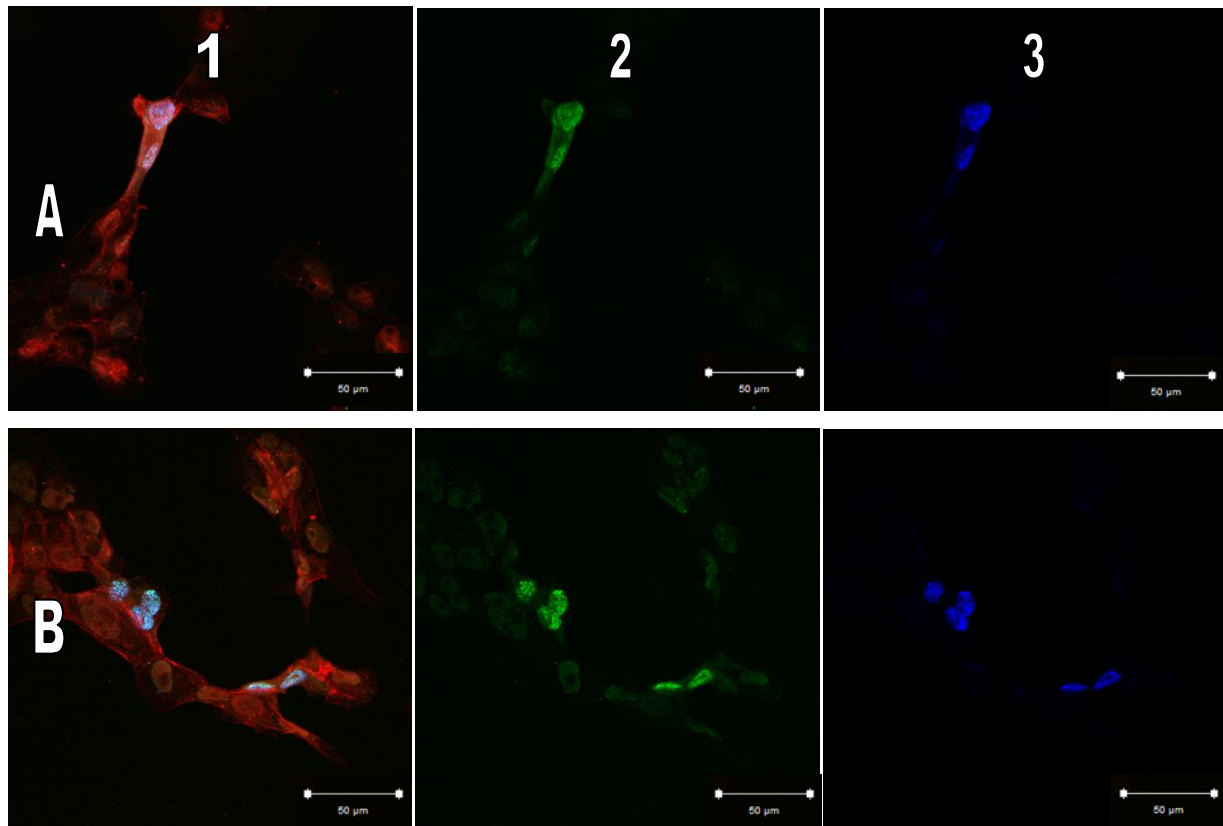
Figure 38: Infected AV529-19 cell a-ICP5, a-gE+FITC, and Cytopainter staining at 20hpi (A/B: two different samples, 1: All channels (405, 488, 647), 2: a-gE+FITC only (488 channel), 3: a-ICP5 only (405 channel))

Figure 38 shows the staining of cells at 20hpi. The signal for both ICP5 and gE were much more easily discernible than they were in the controls (Figure 28 and Figure 29). The F-actin staining (Figure 38 A1 and B1) provided information on the state of the cells with much less polyhedral shapes in some cells. AV529-19 Vero cells are known to become less polyhedral and detach from their substrate when infected (Figure 16). The strength of both the a-gE+FITC and AlexaFluor 405 antibodies varied significantly between the cells which appeared infected and those that did not. Unfortunately, the regions in which each channel showed the strongest signal overlapped completely.

While the a-gE+FITC was slightly more diffuse in its staining and maintained its low level of non-specific staining in cell nuclei, all other features were identical between the two antibodies. Given the different natures of the viral proteins being stained this observation was unexpected and pointed to cross-contamination in the staining or imaging. The order in which the two proteins were stained should theoretically have eliminated cross-contamination due to binding of the AlexaFluor 405 to both primary antibodies. Another feasible explanation for this

level of cross-contamination was leakage between the fluorescence channels during imaging. While the emission and excitation wavelengths of the two fluorophores were theoretically far enough apart for concurrent imaging (roughly a 100nm difference between the peaks for both excitation and emission), some level of leakage was reported with this combination of wavelengths [239].

Another concern was the low level of gE staining outside of the seemingly cross-contaminated infected cell nuclei. The glycoprotein was expected to be localized at cell-to-cell junctions and throughout the host cells, and none of this was evident in the results. ICP5 was also seen almost exclusively (and most strongly) within the infected cell nuclei. Granted, ICP5 was expected to have a strong presence in the nuclei. The highly stained localizations within the nuclei were in line with literature pertaining to the formation of viral capsids (Section 2.1.2.2). Unfortunately, its absence from other regions in the cell indicated a potential issue. If the presence of a tegument layer or envelope prevented the a-ICP5 antibody from tagging the viral capsid then the goal of the experiment could not be achieved.

6.3.3 Conclusions

Although the non-specific binding and background noise were at an acceptable level in this experiment and the staining seemed to result in a strong signal, the co-staining of ICP5 and gE was deemed unsuccessful. The two signals (from FITC and AlexaFluor 405 fluorophores) overlapped precisely in all stained regions, likely indicating that bleeding of the signals between channels was occurring. The lack of significant staining of either protein outside of the cell nuclei was also an issue given that both are expected throughout the cells at later stages of infection. The possibility that viral capsids could not be stained once they have acquired a tegument and/or envelope was concluded to be the most likely cause of this issue for ICP5. Given this combination of issues it was difficult to properly gauge the efficacy of the a-gE+FITC staining alone in this investigation.

Chapter 7 – Development of a Directional Assay to Probe ACAM529 Egress

In this investigation, a co-culturing (of cell lines) protocol was developed to separate infected and uninfected populations of cells from each other, and then observe if and how virus spread from one population to the other through downwards budding (Figure 39). The protocol is described in detail in Section 4.9. The goal of these experiments was to determine the quantity of infective virus particles that bud downwards (towards the membrane surface and into the well culture) in relation to the original infection's MOI. The motivation for this work was the need for information on this particular inaccessible (to current harvesting methods) sub-population of virus particles which could then be in future experiments which study this system.

7.1 Background

In an infected cell culture, HSV spreads cell-to-cell or egresses into the supernatant before attachment to a new host cell [240, 78, 241]. From a manufacturing stand-point, the retention of virus particles within cells can reduce overall yields significantly. Accessing these viruses requires lysis of the cells which causes heavier contamination, and increases downstream processing costs. Furthermore, viruses that bud towards the solid substrate on which the cells are growing may be inaccessible to standard harvesting techniques. Quantifying this subset of progeny virus particles could inform changes to harvesting, which, in turn, could improve the recovery yield of virus from the process. The goal of this investigation was to establish a novel way of studying the preferential downwards budding of ACAM529 using materials designed for the co-culture of animal cells (Figure 39).
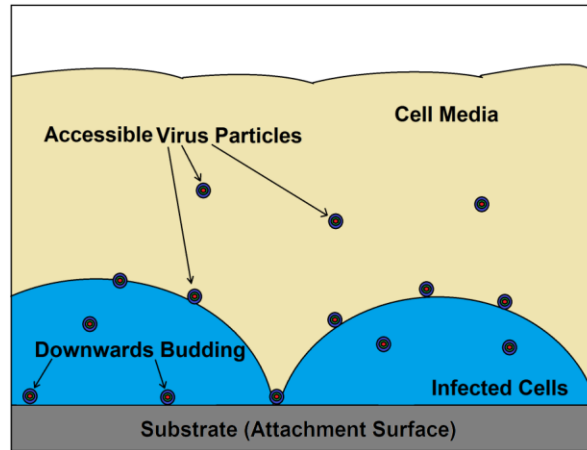
Figure 39: Downward budding and subsequent inaccessibility of progeny ACAM529 Virus Particles

Co-culturing of cells is used extensively to create more realistic *in vivo* models of cellular environments [242, 243, 244, 245]. Co-culturing refers to two or more distinct cell types cultured together, where they are allowed to interact physically and chemically [246]. While culturing a single cell line is much simpler and less expensive, some processes cannot be studied without the additional complexity of interactions between different cell types.

7.2 Validation of cell culture insert membrane as a valid Vero cell substrate

Cells displayed healthy attachment and propagation on the cell culture insert membranes. It can be seen in Figure 40 A that the AV529-19 cells adhered to the insert membrane and formed a fully confluent monolayer. The cells also retained their polyhedral shape and very few unattached cells were observed (potentially due to the translucent nature of the membrane resulting in an inability to observe cells not attached to its surface). The culture appeared as healthy as the one grown on the cell culture plate (Figure 40 B).
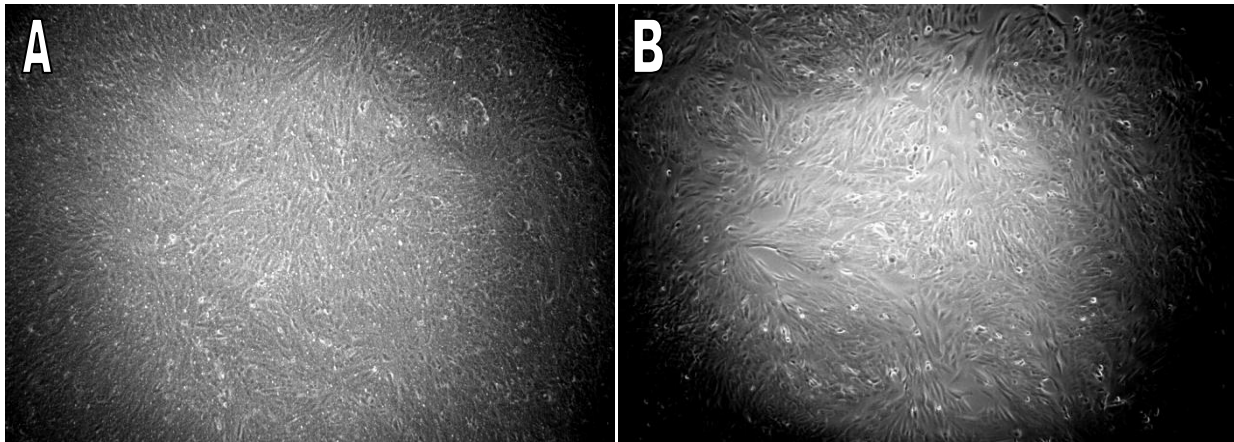
Figure 40: Uninfected AV529-19 culture (A: Insert culture, B: Well culture) (40x magnification)

7.3 Progression of Infection in "Insert Cultures"

Cells cultured in tissue culture inserts did not usually show any signs of infection until 15 hpi. Figure 41A and Figure 41B show no cell rounding or detachment, which would be expected if the cells were experiencing any cytopathic effect. Since the cell monolayers were completely confluent prior to infection (Figure 41A), no cell replication or spread was observed (Figure 41B-E). In fact, the small size of the cells and lack of elongation (like that which can be seen in Figure 40B) indicated that the density of the monolayer was higher than the minimum required for complete coverage of the substrate. Lower seeding density could be used in the future.

At 15 hpi (Figure 41C) the cytopathic effect became easily discernible with cells rounding and becoming larger throughout the insert culture. The infection was evenly distributed and its effects were well synchronized in all cells infected. The infection did not seem to compromise the monolayer at this stage of infection. Figure 41D and E show a steady increase in the prevalence of virus-induced cytopathic effect. The density of the rounded cells increased and more were adjacent to one another. No significant gaps in the monolayers were observed even at 20 hpi, likely the result of limited cell detachment and the high cell density. The Vero cell culture did not appear to be affected by the change in substrate and grew very effectively on the cell culture insert membranes. Infected cells responded in the same fashion as Vero cells growing in cell culture plates and the monolayers showed no observable gaps (plaques) by 20 hpi.
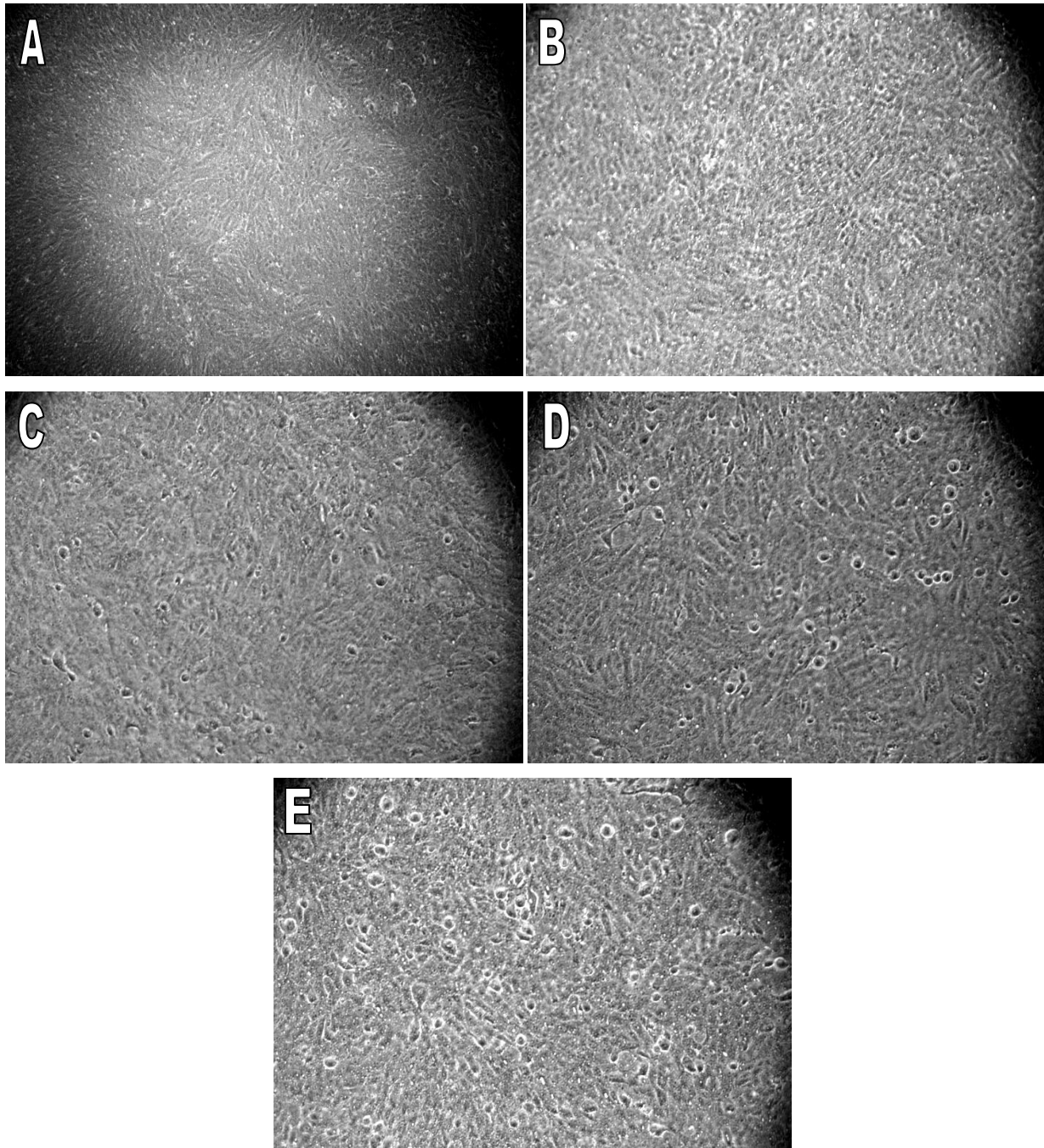
Figure 41: Infected AV529-19 insert culture (A: No infection, B: 12hpi, C: 15hpi, D: 18hpi, E: 20hpi) (40x magnification)

7.4 Infective titer reduction between primary and secondary infection for infected cell culture inserts

The quantification of viral titer in cell culture insert was conducted in much the same way as in a plaque assay (Section 4.2). Plaques formed in the monolayer by cell death were counted by visual inspection to determine titer. Just as with plaque assays, the number of plaques present in

a given monolayer had to fall within a certain range (approximately 10-150) for the result to be statistically significant while also allowing the operator to differentiate between individual plaques. A minimum allowable MOI had to be determined for initial insert culture infection which would produce a number of well culture plaques within this range. In order to calculate this value, the fraction of the progeny virus particle population which budded downwards and could therefore pass through the membrane to infect the well culture had to be determined. Ideally, these plaques represented particles which budded through the insert membrane and were previously inaccessible to harvesting methods (

Figure 42: Schematic of viral transfer and loss in the directional assay).
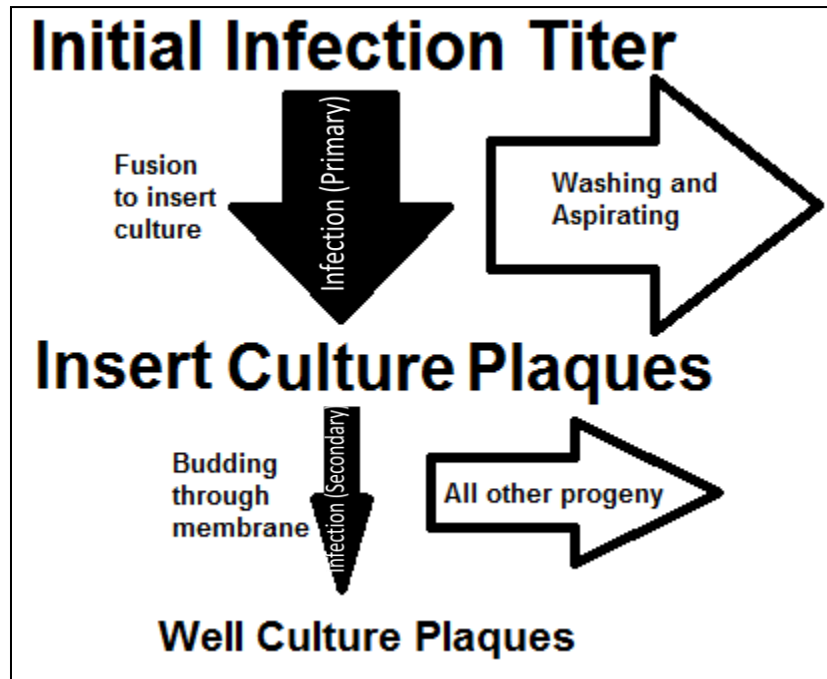
Figure 42: Schematic of viral transfer and loss in the directional assay

The entire experiment was conducted twice to assess the reproducibility of the results. These are referred to as Experiment 1 and 2 in this section. The titer of the viral stock used for initial infection was determined by plaque assay to be $2.4 \times 10^6 \pm 4.8 \times 10^5$ PFU/mL in Experiment 1 and $2.2 \times 10^6 \pm 3.5 \times 10^5$ PFU/mL in Experiment 2 (n=3).
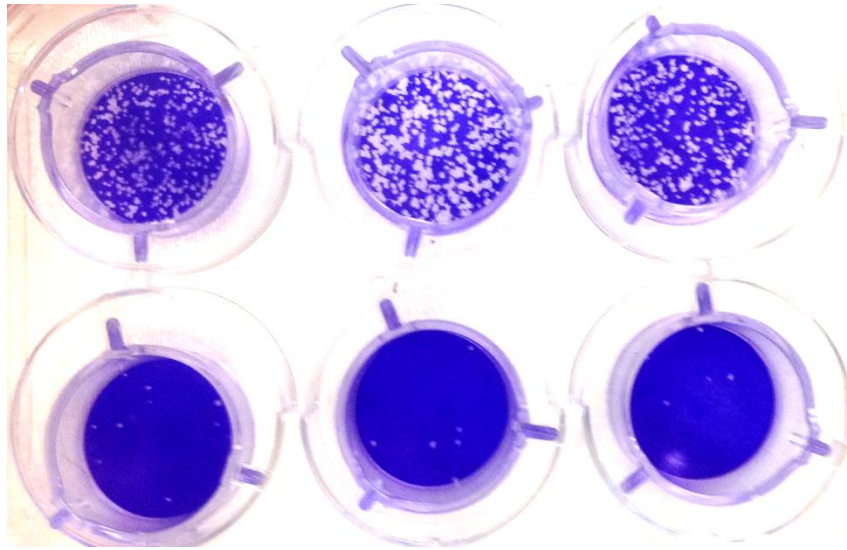
Figure 43: Insert culture plaques (top row 10^{-3}, bottom row 10^{-5})

The plaques in the insert and well cultures were counted whenever possible and these results were compared to the calculated viral titer to determine the extent to which each step of the cell culture insert experiment affected the titer. Figure 43 shows the plaques in the inserts of the 10^{-3} and 10^{-5} viral dilutions of Experiment 1. While the plaques were completely indiscernible from each other in the inserts infected at 1:10 dilution (10^{-1}), the plaques of the 1:1000 (10^{-3}) inserts were fairly close to the range of allowable counts. Approximate counts (made in spite of the plaques being outside of the 10-150 countable plaque range) placed them at between 250 to 350 PFU for both experiments.

Expected plaques counts were calculated based on the volume of diluted virus stock added to each cell culture insert, the dilution factor of the viral stock, and the titer calculated from the plaque assay. A mean of 2.38x10^5 PFU was expected for the 10^{-1} insert cultures, 2.4x10^3 for the 10^{-3} cultures, and 2.4 for the 10^{-5} cultures (2.2x10^5, 2.2x10^3, and 22 PFU respectively for Experiment 2). While there is no way to determine how close the 10^{-1} cell inserts' plaque counts were to the expected values, it was clear that the other inserts had fewer plaques than expected. The plaque counts in the 10^{-3} inserts were lower than those expected by almost an order of magnitude and the mean count in the 10^{-5} inserts was lower by a factor of 3.4 in Experiment 1 and 3.2 in Experiment 2 (a difference of 5%).

While the losses in effective titer did not invalidate the experiment, they did have to be accounted for in later calculations. The titer was calculated again using only the plaque counts in the cell inserts and found to be roughly $7.0 \times 10^5 \pm 2.0 \times 10^5$ PFU/mL for Experiment 1 and $6.7 \times 10^5 \pm 1.3 \times 10^5$ PFU/mL for Experiment 2. These titers were used in later calculations to ensure that the effects of mass transfer limitations at the initial infection stage were accounted for.

Table 4: Well culture plaque counts (Experiment 1)

2hpi at 10^{-1}	10^{-1}	10^{-3}	10^{-5}
2	16	0	0
2	3	0	0
0	6	0	0

Table 5: Well culture plaque counts (Experiment 2)

2hpi at 10^{-1}	10^{-1}	10^{-3}	10^{-5}
10	25	2	0
11	21	2	0
17	32	1	0

The well culture plaque counts (Table 4 and Table 5) were much lower than those of the inserts. This was not unexpected, but did present an issue for calculations. For the first experiment, only the well cultures corresponding to the inserts infected at 10^{-1} showed countable plaques, with the inserts infected at lower MOIs producing no plaques at all.

For Experiment 1, the 2hpi control wells contained an average of 1.3 ± 1.1 plaques (95% confidence interval), which was well below the plaque assay's range of allowable counts. The lower limit of the 2hpi control well's 95% confidence interval was 0.3, meaning that statistically speaking it could still be differentiated from an uninfected well. When compared to the titer of the initial infection in the 2hpi controls, the percentage of PFU that infected the well culture was only 5.6×10^{-4} %.

The second experiment's 2hpi control wells had far higher plaque counts at an average of 13 ± 3.5 PFU. This corresponded to 5.9×10^{-3}% of the initial infection of the insert. The significant differences between the well culture plaques of the first and second experiment could

not be attributed to initial infective titers, which were relatively close (a 9.8% difference in titers compared to a 68% difference between well plaque counts).

The plaque counts in the well cultures corresponding to the 10^{-1} cell inserts showed a high degree of variability. In Experiment 1, the average plaque count in these wells was 8.3 ± 7.7 (95% confidence interval). The lower limit was therefore well within the range covered by the false positives of the 2 hpi control (the lower limit was 0.6) and further calculations could be the result of experimental error.

Experiment 2 well culture plaques were discernible from plaques caused and attributed to experimental error by a significant margin. An average plaque count of 26 ± 6.3 meant that the lower limit of 20 did not overlap with the upper limit of the expected experimental error of 16. Further calculations for the second experiment were therefore more statistically relevant than those of the first.

The degree to which the PFU count decreased from primary infection of the insert cultures to the secondary infection of the well cultures could only be calculated using the 10^{-1} plaque data. Since the exact plaque counts of the 10^{-1} inserts was not known, the comparison was done using the expected PFU counts (based on viral titer and infection volume), which was adjusted by the observed 3.4 and 3.2 factor drops between expected and actual insert culture counts (from plaque counts of inserts infected at 10^{-5}) in the first and second experiment respectively. The result was an observed drop in plaque count by a factor of 8.4×10^3 in Experiment 1 and 2.6×10^3 in Experiment 2.

Using the calculated factor and the upper limit of the 95% confidence interval of the 2 hpi control (2.4 plaques for Experiment 1 and 16 plaques for Experiment 2), the minimum infection titer for infecting an insert culture which would be expected to produce a statistically significant number of plaques was found to be 6.9×10^4 PFU/mL for Experiment 1 and 1.3×10^5 PFU/mL for Experiment 2. Using the results for Experiment 2 (the statistically significant results), the maximum infective titer that would produce plaques in the well cultures within the 10-150 range (set forth in the plaque assay protocol) was also determined. The end result was a recommended range of infection titers of 8.3×10^4 and 1.2×10^6 PFU/mL. Using the average titer of the viral

stock determined by plaque assay in this investigation the allowable dilution factors were determined to be 1.8 – 27x (or $10^{-0.26} - 10^{-1.4}$).

The differences between Experiment 1 and 2 in terms of the well culture plaque counts could not be attributed to differences in either initial infective titer or insert culture plaque counts. A study of the method's susceptibility to differences in handling should be conducted to determine if this could account for the rather significant variations in plaque counts observed. The contribution of mass transfer limitation to this variability is also not known

.

Chapter 8 – Conclusion

Using a spectrofluorometer and induced fluorescence to perform an EPDA for the rapid quantification of ACAM529 provided mixed results in Chapter 5 of this thesis. While the positive control (titration of Baculovirus in Sf9 cells) established the viability of this approach, the assay was required 10 days to provide accurate titers. This invalidated it as a rapid quantification method. In addition, the HSV2012-121 Vero cells required the addition of NaBu in order to enhance the expression of eGFP. This increased the difference between infected and uninfected cell fluorescence by 525% and should allow for EPDA using the ACAM529/HSV2012-121 system.

Immunofluorescent staining of the ACAM529/HSV system provided unique insights into the level of expression of virus proteins and the efficacy of available tagging antibodies. a-gC, a-gE+FITC, a-ICP5, a-gB, and a-gD were all found to be effective in binding their respective viral proteins at late stages of infection. a-gB was found to be uniquely capable of being detected as early as 6hpi, allowing for a wider range of future experiments. Tracking of mature virus particles through co-localization of a capsid protein and an outer envelope protein was not successful. Evidence pointed to bleeding of the signals between the 488 and 405 nm channels, as well as to a lack of capsid staining in the presence of a tegument of envelope layer.

The results of the cell culture insert experiments provided a good starting point for the use of this pseudo co-culturing to study the budding of ACAM529. The wash steps and addition of plaque overlay media kept the level of false positive error very low (5.9×10^{-3} %) and staining and counting of plaques in both the insert and well cultures was used to establish rough guidelines for future experiments. In order to produce well culture plaques within a statistically significant and countable range (10 – 150 based on plaque assay protocol), a required initial infection titer of between 8.3×10^4 and 1.2×10^6 PFU/mL was calculated.

Overall, while the initial goals of locating inaccessible localizations of ACAM529 in infected cells and determining the prevalence of downward budding were not met, the experiments conducted provided useful information on the system studied and form a solid basis for ongoing research on this topic.

Chapter 9 – Recommendations

Based on the findings in this thesis, it is recommended that future work on the optimization of ACAM529 yield and localization of inaccessible virus particle sub-populations focus on indirect quantitative methods. While direct imaging of the viral localizations seemed like the more straightforward approach, it proved more problematic and less useful than anticipated. On the other hand, those methods which probed the system indirectly (namely the cell culture insert protocol, induced fluorescence with NaBu enhancement, and even immunofluorescent staining of individual viral proteins) provided useful and often more quantitative information.

While certain features of both the virus/cell system and the fluorescent tagging prevented mature virus particles from being located, individual virus proteins were imaged effectively. IS is therefore recommended as a method for studying variations in viral protein expression, both in terms of expression strength and the proteins' distribution within the host cell. Studying glycoproteins associated with cell-to-cell transmission was of particular interest since reducing this mode of transmission could increase budding into the supernatant. This could then improve the overall yield of virus particles in production processes. In a similar vein, the effect of Dextran Sulfate could be studied with the use of IS of individual glycoproteins and lend further aid to improving virus production.

While the cell culture insert experiments showed great promise for the study of virus budding, several properties of the system remained undefined. Before the protocol is used to draw conclusions about the cell/virus system, it is recommended that the mass transfer effects are investigated. Tracking the passage of virus particles through membranes of different pore sizes could yield information on the limitations of passage through a membrane imposes on the system. Similarly, the direction in which the infection travels can be reversed by adjusting the protocol and infecting the well cultures instead of the insert cultures. The quantification of plaques in the insert cultures could then provide an indicator of the importance of Brownian motion. Once the system is better understood, any attempts to manipulate or change virus budding could utilize the cell culture insert protocol to quantify the changes which occurred. Incorporating the quantification directly into the experiment decreases the opportunity for error and reduces the impact of virus instability on titer calculations.

References

[1]   R. M. Mingo, J. Han, W. W. Newcomb and J. C. Brown, "Replication of Herpes Simplex Virus: Egress of Progeny Virus at Specialized Cell Membrane Sites," *Journal of Virology,* vol. 86, no. 13, pp. 7084-7097, 2012.

[2]   D. M. Knipe and P. Howley, Field's Virology, 6th ed., Lippincott Williams & Wilkins, 2013.

[3]   M. Studahl, P. Cinque and T. Bergström, Herpes Simplex Viruses, Boca Raton: Taylor & Francis, 2006.

[4]   L. Corey, A. G. M. Langenberg, A. Rhoda, R. E. Sekulovich, A. E. Izu, J. M. Douglas, H. Handsfield, T. Warren, L. Marr, S. Tyring, R. DiCarlo, A. Adimora, P. Leone, C. Dekker, R. L. Burke, W. P. Leong and S. E. Straus, "Recombinant Glycoprotein Vaccine for the Prevention of Genital HSV-2 Infection," *The Journal of the Americal Medical Association,* vol. 4, no. 282, pp. 331-340, 1999.

[5]   K. J. Looker, G. P. Garnetta and G. P. Schmid, "An estimate of the global prevalence and incidence of herpes simplex virus type 2 infection," *Bull World Health Organ.,* vol. 10, no. 86, pp. 805-812, 2008.

[6]   CDC National Prevention Information Network, American Sexual Health AssociationExternal Web Site Icon, "Genital Herpes - CDC Fact Sheet," Centers for Disease Control and Prevention, 9 December 2014. [Online]. Available: http://www.cdc.gov/std/herpes/stdfact-herpes-detailed.htm. [Accessed 9 January 2015].

[7]   R. Whitley and B. Roizman, "Herpes simplex virus infections," *The Lancet,* vol. 357, no. 9267, pp. 1513-1518, 2001.

[8]   G. Mertz, S. Rosenthal and L. Stanberry, "Is herpes simplex virus type 1 (HSV-1) now more common than HSV-2 in first episodes of genital herpes?," *Sexually Transmitted Diseases,* vol. 30, no. 10, pp. 801-802, 2003.

[9]   A. Cunningham, R. Diefenbach, M. Miranda-Saksena, L. Bosnjak, M. Kim, C. Jones and M. Douglas, "The Cycle of Human Herpes Simplex Virus Infection: Virus Transport and Immune Control," *The Journal of infectious diseases,* vol. 194 Supp 1, no. Suppl 1, pp. S11-S18, 2006.

[10]   E. Tronstein, C. Johnston, M.-L. Huang, S. Selke, M. Amalia, T. Warren, C. Lawrence and A. Wald, "Genital Shedding of Herpes Simplex Virus Among Symptomatic and Asymptomatic Persons With HSV-2 Infection," *Journal of the American Medical Association,* vol. 14, no. 305, pp. 1441-1449, 2011.

[11]   A. Dolan, F. Jamieson, C. Cunningham, B. Barnett and D. McGeoch, "The genome sequence of herpes simplex virus type 2," *Journal of virology,* pp. 2010-21, 1998.

[12]   "Herpesviruses," 11 September 2007. [Online]. Available:

http://www.microbiologybytes.com/virology/Herpesviruses.html. [Accessed 23 February 2015].

[13] P. Wildy, W. Russell and R. Horne, "The Morphology of Herpes Virus," *Virology,* vol. 12, no. 2, pp. 204-222, 1960.

[14] D. Henaff, K. Radtke and R. Lippé, "Herpesviruses exploit several host compartments for envelopment," *Traffic (Copenhagen, Denmark),* pp. 1443-1449, 2012.

[15] T. Bergstrom and E. Trybala, "Antigenic differences between HSV-1 and HSV-2 glycoproteins and their importance for type-specific serology," *Intervirology,* vol. 39, no. 3, pp. 176-184, 1996.

[16] F. Xu, J. Schilliger, M. Sternberg, R. Johnson, F. Lee, A. Nahmias and L. Markowitz, "Seroprevalence and Coinfection with Herpes Simplex Virus Type 1 and Type 2 in the United States, 1988– 1994," *Journal of Infectious Diseases,* vol. 185, no. 8, pp. 1019-1024, 2002.

[17] J. Akhtar and D. Shukla, "Viral entry mechanisms: cellular and viral mediators of herpes simplex virus entry.," *The FEBS journal,* vol. 276, no. 24, pp. 7228-7236, 2009.

[18] K. Roth, V. Ferreira and C. Kaushic, "HSV-2 vaccine: current state and insights into development of a vaccine that targets genital mucosal protection.," *Microbial Pathogenesis,* vol. 58, pp. 45-54, 2013.

[19] M. Muggeridge, "Characterization of cell – cell fusion mediated by herpes simplex virus 2 glycoproteins gB , gD , gH and gL in transfected cells," *Journal of General Virology,* vol. 81, pp. 2017-2027, 2000.

[20] F. Cocchi, D. Fusco, L. Menotti, T. Gianni, R. Eisenberg, G. Cohen and G. Campadelli-Fiume, "The soluble ectodomain of herpes simplex virus gD contains a membrane-proximal pro-fusion domain and suffices to mediate virus entry," *Proceedings of the National Academy of Sciences of the United States of America,* vol. 101, pp. 7445-7450, 2004.

[21] E. Avitabile, C. Forghieri and G. Campadelli-Fiume, "Cross talk among the glycoproteins involved in herpes simplex virus entry and fusion: the interaction between gB and gH/gL does not necessarily require gD.," *Journal of Virology,* vol. 83, no. 20, pp. 10752-10760, 2009.

[22] Y. Takai, K. Irie, K. Shimizu, T. Sakisaka and W. Ikeda, "Nectins and nectin-like molecules: roles in cell adhesion, migration, and polarization," *Cancer Science,* vol. 94, no. 8, pp. 655-667, 2003.

[23] R. Morin, M. Mendez-Lago, A. Mungall, R. Goya, K. Mungall, R. Corbett, N. Johnson, T. Severson, R. Chiu, M. Field, S. Jackman, M. Krzywinski, D. Scott, D. Trinh, J. Tamura-Wells, S. Li, M. Firme, S. Rogic, M. Griffith, S. Chan, O. Yakovenko, I. Meyer, E. Zhao, D. Smailus, M. Moksa, S. Chittaranjan, L. Rimsza, A. Brooks-Wilson, J. Spinelli, S. Ben-Neriah, B. Meissner, B. Woolcock, M. Boyle, H. McDonald, A. Tam, Y. Zhao, A. Delaney, T. Zeng, K. Tse, Y. Butterfield, I. Birol, R. Holt, J. Schein, D. Horsman, R. Moore, S. Jones, J. Connors, M. Hirst, R. Gascoyne and M. Marra, "Frequent mutation of histone-modifying genes in non-Hodgkin lymphoma," *Nature,* vol. 476, pp. 298-303, 2011.

[24]   B. Gorsi and S. Stringer, "Tinkering with heparan sulfate sulfation to steer development,"
         Treands in Cell Biology, vol. 17, pp. 173-177, 2007.

[25]   S. Hadigal and D. Shukla, "Exploiting herpes simplex virus entry for novel therapeutics," *Viruses,*
         vol. 5, pp. 1447-1465, 2013.

[26]   M. J. Oh, J. Akhtar, P. Desai and D. Shukla, "A role for heparan sulfate in viral surfing,"
         Biochemical and Biophysical Research Communications, vol. 391, no. 1, pp. 176-181, 2010.

[27]   G. Campadelli-Fiume, M. Amasio, E. Avitabile, A. Cerretani, C. Forghieri, T. Gianni and L.
         Menotti, "The multipartite system that mediates entry of herpes simplex virus into the cell,"
         Reviews in Medical Virology, vol. 17, no. 5, pp. 313-326, 2007.

[28]   R. Subramanian and R. Geraghty, "Herpes simplex virus type 1 mediates fusion through a
         hemifusion intermediate by sequential activity of glycoproteins D , H , L , and B," *Proceedings of
         the National Academy of Sciences of the United States of America,* vol. 104, no. 8, pp. 2903-
         2908, 2007.

[29]   A. Nicola, A. Mcevoy and S. Straus, "Roles for Endocytosis and Low pH in Herpes Simplex Virus
         Entry into HeLa and Chinese Hamster Ovary Cells," *Journal of virology,* vol. 77, no. 9, pp. 5324-
         5332, 2003.

[30]   K. Stiles, R. Milne, G. Cohen, R. Eisenberg and C. Krummenacher, "The herpes simplex virus
         receptor nectin-1 is down-regulated after trans-interaction with glycoprotein D," *Virology,* vol.
         373, pp. 98-111, 2008.

[31]   N. Cheshenko, J. Trepanier, P. González, E. Eugenin, W. Jacobs and B. Herold, "Herpes simplex
         virus type 2 glycoprotein H interacts with integrin αvβ3 to facilitate viral entry and calcium
         signaling in human genital tract epithelial cells," *Journal of Virology,* vol. 88, no. 17, pp. 10026-
         38, 2014.

[32]   H. Filippakis, D. Spandidos and G. Sourvinos, "Herpesviruses: hijacking the Ras signaling
         pathway," *Biochimica et biophysica acta,* vol. 1803, no. 7, pp. 777-785, 2010.

[33]   J. Hunter, C. Smith, B. Debashish, M. Kulka, R. Broderick and L. Aurelian, "Intracellular
         Internalization and singaling Pathways Triggered by the Large Subunit and HSV-2 Rinonucleotide
         Reductase (ICP10)," *Virology,* vol. 210, pp. 345-360, 1995.

[34]   K. Topp, L. Meade and J. LaVail, "Microtubule polarity in the peripheral processes of trigeminal
         ganglion cells: relevance for the retrograde transport of herpes simplex virus," *The Journal of
         neuroscience : the official journal of the Society for Neuroscience,* vol. 14, pp. 318-325, 1994.

[35]   T. Wisner and D. Johnson, "Redistribution of Cellular and Herpes Simplex Virus Proteins from
         the Trans-Golgi Network to Cell Junctions without Enveloped Capsids," *Journal of Virology,* vol.
         78, no. 21, pp. 11519-11535, 2004.

[36]   E. Avitabile, S. Di Gaeta, M. Torrisi, P. Ward, B. Roizman and G. Campadelli-Fiume,
         "Redistribution of microtubules and Golgi apparatus in herpes simplex virus-infected cells and

their role in viral exocytosis," *Journal of virology,* vol. 69, no. 12, pp. 7472-7482, 1995.

[37]   K. Sugimoto, M. Uema, H. Sagara, M. Tanaka, T. Sata and Y. Hashimoto, "Simultaneous tracking of capsid, tegument, and envelope protein localization in living cells infected with triply fluorescent herpes simplex virus 1," *Journal of virology,* vol. 82, no. 11, pp. 5198-5211, 2008.

[38]   C. Morgan, H. Rose and B. Mednis, "Electron microscopy of herpes simplex virus," *Journal of Virology,* vol. 2, p. 507–516, 1968.

[39]   C. Morgan and C. Howe, "Structure and development of viruses as observed in the electron microscope. IX. Entry of parainfluenza I (Sendai) virus," *Journal of Virology,* vol. 2, no. 10, pp. 1122-1132, 1968.

[40]   K. Poffenberger and B. Roizman, "Studies on noninverting genome of a viable herpes simplex virus 1: presence of head-to-tail linkages in packaged genomes and requirements for circularization after infection," *Journal of Virology,* vol. 53, pp. 587-595, 1985.

[41]   C. Lilley, C. Carson, A. Muotri, F. Gage and M. Weitzman, "DNA repair proteins affect the lifecycle of herpes simplex virus 1," *Proceedings of the Nationall Academy of Science of the U S A 2005,* vol. 102, pp. 5844-5849, 2005.

[42]   D. Wilkinson and S. Weller, "Recruitment of cellular recombination and repair proteins to sites of herpes simplex virus type 1 DNA replication is dependent on the composition of viral proteins within prereplicative sites and correlates with the induction of the DNA damage response," *Journal of Virology,* vol. 78, no. 9, pp. 4783-4796, 2004.

[43]   Q. Tang, L. Li, A. Ishov, V. Revol, A. Epstein and G. Maul, "Determination of minimum herpes simplex virus type 1 components necessary to localize transcriptionally active DNA to ND10," *Journal of Virology,* vol. 77, no. 10, pp. 5821-5828, 2003.

[44]   G. Sourvinos and R. Everett, "Visualization of parental HSV-1 genomes and replication compartments in association with ND10 in live infected cells," *EMBO Journal,* vol. 21, no. 18, pp. 4989-4997, 2002.

[45]   R. Everett and J. Murray, "ND10 components relocate to sites associated with herpes simplex virus type 1 nucleoprotein complexes during virus infection," *Journal of Virology,* vol. 79, p. 5078–5089, 2005.

[46]   A. de Bruyn Kops and D. Knipe, "Formation of DNA replication structures in herpes virus-infected cells requires a viral DNA binding protein," *Cell,* vol. 55, pp. 857-868, 1988.

[47]   K. Monier, J. Armas, S. Etteldorf, P. Ghazal and K. Sullivan, "Annexation of the interchromosomal space during viral infection," *Nature Cell Biology,* vol. 2, pp. 661-665, 2000.

[48]   B. Meignier, R. Longnecker, P. Mavromara-Nazos, A. Sear and B. Roizman, "Virulence of and establishment of latency by genetically engineered deletion mutants of herpes simplex virus I," *Virology,* vol. 162, pp. 251-254, 1988.

[49] T. Mettenleiter, "Budding events in herpesvirus morphogenesis.," *Virus Research,* vol. 106, no. 2, pp. 167-180, 2004.

[50] S. Kohl, "Human immune response to herpes simplex virus," *The Journal of infectious diseases,* vol. 146, no. 2, p. 292, 1982.

[51] S. Meuller, C. Jones, W. Chen, Y. Kawaoka, M. Castrucci, W. Heath and F. Carbone, "The Early Expression of Glycoprotein B from Herpes Simplex Virus Can Be Detected by Antigen-Specific CD8+ T Cells," *Journal of Virology,* vol. 77, no. 4, pp. 2445-2451, 2003.

[52] W. Antonin, R. Ungericht and U. Kutay, "Traversing the NPC along the pore membrane Targeting of membrane proteins to the INM," *Nucleus-Austin,* vol. 2, no. 2, pp. 87-91, 2012.

[53] N. Zuleger, A. Kerr and E. Schirmer, "Many mechanisms, one entrance: Membrane protein translocation into the nucleus," *Cellular and Molecular Life Sciences,* vol. 69, pp. 2205-2216, 2012.

[54] N. Pante and M. Kann, "Nuclear pore complex is able to transport macromolecules with diameters of similar to 39 nm," *Molecular Biology of the Cell,* vol. 13, no. 2, pp. 425-434, 2002.

[55] T. Mettenleiter, F. Müller, H. Granzow and B. Klupp, "The way out: what we know and do not know about herpesvirus nuclear egress," *Cellular microbiology,* vol. 15, no. 2, pp. 170-178, 2013.

[56] M. Szpara, D. Gatherer, A. Ochoa, B. Greenbaum, A. Dolan, R. Bowden, L. Enquist, M. Legendre and A. Davison, "Evolution and diversity in human herpes simplex virus genomes," *Journal of Virology,* vol. 88, no. 2, pp. 1209-1227, 2014.

[57] W. Muranyi, J. Haas, M. Wagner, G. Krohne and U. Koszinowski, "Cytomegalovirus recruitment of cellular kinases to dissolve the nuclear lamina," *Science,* vol. 297, no. 5582, pp. 854-857, 2002.

[58] V. Sanchez and D. Spector, "CMV Makes Timely Exit," *Science,* vol. 297, pp. 778-779, 2002.

[59] M. Simpson-holley, J. Baines, R. Roller and D. Knipe, "Herpes Simplex Virus 1 U L 31 and U L 34 Gene Products Promote the Late Maturation of Viral Replication Compartments to the Nuclear Periphery," *Journal of Virology,* vol. 78, no. 11, pp. 5591-5600, 2004.

[60] E. Wills, F. Mou and J. Baines, "The U(L)31 and U(L)34 gene products of herpes simplex virus 1 are required for optimal localization of viral glycoproteins D and M to the inner nuclear membranes of infected cells.," *Journal of Virology,* vol. 83, no. 10, pp. 4800-4809, 2009.

[61] A. Farnsworth, T. Wisner, M. Webb, R. Roller, G. Cohen, R. Eisenberg and D. Johnson, "Herpes simplex virus glycoproteins gB and gH function in fusion between the virion envelope and the outer nuclear membrane," *Proceedings of the National Academy of Sciences of the United States of America,* vol. 104, no. 24, pp. 10187-10192, 2007.

[62] A. Forrester, H. Farrell, G. Wilkinson, J. Kaye, N. Davispoynter and T. Minson, "Construction and properties of a mutant of herpes simplex virus type 1 with glycoprotein H coding sequences

deleted," *Journal of Virology,* vol. 66, no. 1, pp. 341-348, 1992.

[63]   M. Ligas and D. Johnson, "A herpes simplex virus mutant in which glycoprotein D sequences are replaced by beta-galactosidase sequences binds to but is unable to penetrate into cells," *Journal of Virology,* vol. 62, pp. 1486-1494, 1988.

[64]   C. Roop, L. Hutchinson and D. Johnson, "A mutant herpes simplex virus type 1 unable to express glycoprotein L cannot enter cells, and its particles lack glycoprotein H," *Journal of Virology,* vol. 67, pp. 2285-2297, 1993.

[65]   P. Wild, M. Engels, C. Senn, K. Tobler, U. Ziegler, E. Schraner, E. Loepfe, M. Ackermann, M. Mueller and P. Walther, "Impairment of nuclear pores in bovine herpesvirus 1-infected MDBK cells," *Journal of Virology,* vol. 79, pp. 1071-1083, 2005.

[66]   W. Mears and S. Rice, "The herpes simplex virus immediate-early protein ICP27 shuttles between nucleus and cytoplasm," *Virology,* vol. 242, no. 1, pp. 128-137, 1998.

[67]   C. Van Sant, R. Hagglund, P. Lopez and B. Roizman, "The infected cell protein 0 of herpes simplex virus 1 dynamically interacts with proteasomes, binds and activates the cdc34 E2 ubiquitin-conjugating enzyme, and possesses in vitro E3 ubiquitin ligase activity," *Proceedins of the National Academy of Sciences of the USA,* vol. 98, no. 15, pp. 8815-8820, 2001.

[68]   T. Mettenleiter, "Herpesvirus assembly and egress," *Journal of Virology,* vol. 76, no. 4, pp. 1537-1547, 2002.

[69]   Z. Zhou, D. Chen, J. Jakana, F. Rixon and W. Chiu, "Visualization of tegument-capsid interactions and DNA in intact herpes simplex virus type 1 virions," *Journal of Virology,* vol. 73, no. 4, pp. 3210-3218, 1999.

[70]   H. Browne, S. Bell and T. Minson, "Analysis of the requirement for glycoprotein M in herpes simplex virus type 1 morphogenesis," *Journal of Virology,* vol. 78, no. 2, pp. 1039-1041, 2004.

[71]   A. Farnsworth, K. Goldsmith and D. Johnson, "Herpes simplex virus glycoproteins gD and gE/gI serve essential but redundant functions during acquisition of the virion envelope in the cytoplasm," *Journal of Virology,* vol. 77, no. 15, pp. 8481-8494, 2003.

[72]   T. McMillan and D. Johnson, "Cytoplasmic domain of herpes simplex virus gE causes accumulation in the trans-Golgi network, a site of virus envelopment and sorting of virions to cell junctions," *Journal of Virology,* vol. 75, no. 4, pp. 1928-1940, 2001.

[73]   A. Whiteley, B. Bruun, T. Minson and H. Browne, "Effects of targeting herpes simplex virus type 1 go to the endoplasmic reticulum and trans-golgi network," *Journal of Virology,* vol. 73, no. 11, pp. 9515-9520, 1999.

[74]   M. Komuro, M. Tajima and K. Kato, "Transformation of Golgi membrane into the envelope of Herpes simplex virus in rat anterior pituitary cells," *European Journal of Cell Biology,* vol. 50, no. 2, pp. 398-406, 1989.

[75]   H. Granzow, B. G. Klupp, W. Fuchs, J. Veits, N. Osterrieder and T. C. Mettenleiter, "Egress of alphaherpesviruses: comparative ultrastructural study," *Journal of Virology,* vol. 75, no. 8, pp. 3675-3684, 2001.

[76]   I. Van Genderen, R. Brandimarti, M. Torrisi, G. Campadelli and G. Van Meer, "The Phospholipid Composition of Extracellular Herpes Simplex Virions Differs from That of Host Cell Nuclei," *Virology,* vol. 200, no. 2, pp. 831-836, 1994.

[77]   J. N. Skepper, A. Whiteley, H. Browne and A. Minson, "Herpes Simplex Virus Nucleocapsids Mature to Progeny Virions by an Envelopment -> Deenvelopment -> Reenvelopment Pathway," *Journal of Virology,* vol. 75, no. 12, p. 5697–5702, 2001.

[78]   F. Abaitua, R. Zia, M. Hollinshead and P. O'Hare, "Polarized cell migration during cell-to-cell transmission of herpes simplex virus in human skin keratinocytes.," *Journal of virology,* vol. 87, no. 14, pp. 7921-7932, 2013.

[79]   D. C. Johnson and M. T. Huber, "Directed egress of animal viruses promotes cell-to-cell spread," *Journal of Virology,* vol. 76, no. 1, pp. 1-8, 2002.

[80]   T. Wisner, C. Brunetti, K. Dingwell and D. C. Johnson, "The extracellular domain of herpes simplex virus gE is sufficient for accumulation at cell junctions but not for cell-to-cell spread," *Journal of virology,* vol. 74, no. 5, pp. 2278-2287, 2000.

[81]   K. S. Dingwell and D. C. Johnson, "The herpes simplex virus gE-gI complex facilitates cell-to-cell spread and binds to components of cell junctions," *Journal of Virology,* vol. 72, no. 11, pp. 8933-8942, 1998.

[82]   D. Johnson, M. Webb and T. Wisner, "Herpes Simplex Virus gE / gI Sorts Nascent Virions to Epithelial Cell Junctions , Promoting Virus Spread Herpes Simplex Virus gE / gI Sorts Nascent Virions to Epithelial Cell Junctions , Promoting Virus Spread," *Journal of Virology,* vol. 75, no. 2, pp. 821-833, 2001.

[83]   W. Cai, S. Person, S. Warner, J. Zhou and N. Deluca, "Linker-insertion nonsense and restriction-site deletion mutations of gB-glycoprotein gene on herpes simplex virus type-1," *Journal of Virology,* vol. 61, no. 3, pp. 714-721, 1987.

[84]   R. Manservigi, R. Argnani and P. Marconi, "HSV Recombinant Vectors for Gene Therapy," *The open virology journal,* pp. 123-156, 2010.

[85]   I. Steiner and P. Kennedy, "Herpes simplex virus latent infection in the nervous system," *Journal of NeuroVirology,* vol. 1, no. 1, pp. 19-29, 1995.

[86]   J. P. Katz, E. T. Bodin and D. M. Coen, "Quantitative polymerase chain reaction analysis of herpes simplex virus DNA in ganglia of mice infected with replication-incompetent mutants," *Jounral of Virology,* vol. 64, p. 4288–4295, 1990.

[87]   F. Sedarati, T. P. Margolis and J. G. Stevens, "Latent infection can be established with drastically restricted transcription and replication of the HSV-1 genome," *Virology,* vol. 192, p. 687–691,

1993.

[88]   B. Sodeik, "Microtubule-mediated Transport of Incoming Herpes Simplex Virus 1Capsids to the Nucleus," *The Journal of Cell Biology,* vol. 136, no. 5, pp. 1007-1021, 1997.

[89]   M. Kosz-Vnenchak, D. M. Coen and D. M. Knipe, "Restricted expression of herpes simplex virus lytic genes during establishment of latent infection by thymidine kinase-negative mutant viruses," *Journal of Virology,* vol. 64, pp. 5396-5402, 1990.

[90]   M. F. Kramer, S. H. Chen, D. M. Knipe and D. M. Coen, "Accumulation of viral transcripts and DNA during establishment of latency by herpes simplex virus," *Journal of Virology,* vol. 72, p. 1177–1185, 1998.

[91]   T. Liu, Q. H. Tang and R. L. Hendricks, "Inflammatory infiltration of the trigeminal ganglion after herpes simplex virus type 1 corneal infection," *Journal of Virology,* vol. 70, no. 1, pp. 264-271, 1996.

[92]   C. Shimeld, J. L. Whiteland, S. M. Nicholls, E. Grinfeld, D. L. Easty, H. Gao and T. J. Hill, "Immune cell infiltration and persistence in the mouse trigeminal ganglion after infection of the cornea with herpes simplex virus type 1," *Journal of Neuroimmunity,* vol. 61, no. 1, pp. 7-16, 1995.

[93]   T. M. Kristie, J. L. Vogel and A. E. Sears, "Nuclear localization of the C1 factor (host cell factor) in sensory neurons correlates with reactivation of herpes simplex virus from latency," *Proceedings from the National Academy of Sciences of the United States of America,* vol. 96, no. 4, pp. 1229-1233, 1999.

[94]   T. Valyinagy, S. Deshmane, A. Dillner and N. W. Fraser, "Induction of cellular transcription factors in trigeminal ganglia of mice by corneal scarification, herpes simplex virus type 1 infection, and explantation of trigeminal ganglia," *Journal of Virology,* vol. 65, no. 8, p. 1991, 4142-4152.

[95]   D. A. Garber, P. A. Schaffer and D. M. Knipe, "A LAT-associated function reduces productive-cycle gene expression during acute infection of murine sensory neurons with herpes simplex virus type 1," *Journal of Virology,* vol. 71, no. 8, pp. 5885-5893, 1997.

[96]   D. C. Bloom, N. Giordani and D. Kwiatkowski, "Epigenetic regulation of latent HSV-1 gene expression," *Biochimica et Biophysica Acta-Gene Regulatory Mechanisms,* pp. 246-256, 2010.

[97]   M. Farrell, A. Dobson and L. Feldman, "Herpes-Simplex Virus Latency-Associated Transcript is a Stable Intron," *Proceedings of the National Academy of Sciences of the United States of America,* pp. 790-794, 1991.

[98]   N. Mador, A. Panet, D. Latchman and I. Steiner, "Expression and Splicing of the Latency-Associated Transcripts of Herpes-Simplex Virus Type-1 in Neuronal and Non-Neuronal Cell Lines," *Journal of Biochemistry,* pp. 1288-1297, 1995.

[99]   J. R. Kent, W. Kang, C. G. Miller and N. W. Fraser, "Herpes simplex virus latency-associated

transcript gene function," *Journal of NeuroVirology,* pp. 285-290, 2003.

[100]   R. L. Thompson and N. M. Sawtell, "The herpes simplex virus type 1 latency-associated transcript gene regulates the establishment of latency," *Journal of Virology,* pp. 5432-5440, 1997.

[101]   J. H. LaVail, A. N. Tauscher, E. Aghaian, O. Harrabi and S. S. Sidhu, "Axonal transport and sorting of herpes simplex virus components in a mature mouse visual system," *Journal of Virology,* vol. 77, no. 11, pp. 6117-6126, 2003.

[102]   M. Penfold, P. Armati and A. Cunningham, "Axonal transport of herpes simplex virions to epidermal cells: evidence for a specialized mode of virus transport and assembly," *Proceedings of the National Academy of Sciences of the United States of America,* vol. 91, no. 14, pp. 6529-6533, 1994.

[103]   J. Yedowitz and J. Blaho, "Herpes simplex virus 2 modulates apoptosis and stimulates NF-kappaB nuclear translocation during infection in human epithelial HEp-2 cells.," *Virology,* vol. 342, no. 2, pp. 297-310, 2005.

[104]   K. Dingwell, C. Brunetl, R. Hendricks, Q. Tang, M. Tang, A. Rainbow and D. Johnsoni, "Herpes Simplex Virus Glycoproteins E and I Facilitate Cell-to- Cell Spread In Vivo and across Junctions of Cultured Cells," *Journal of virology,* vol. 68, no. 2, pp. 834-845, 1994.

[105]   C. Johnston, J. Zhu, L. Jing, K. Laing, C. McClurkan, A. Klock, K. Diem, L. Jin, J. Stanaway, E. Tronstein, W. Kwok, M.-L. Huang, S. Selke, Y. Fong, A. Magaret, D. Koelle, A. Wald and L. Corey, "Virologic and immunologic evidence of multifocal genital herpes simplex virus 2 infection.," *Journal of virology,* vol. 88, no. 9, pp. 4921-31, 2014.

[106]   D. Nikolic and V. Piguet, "Vaccines and microbicides preventing HIV-1, HSV-2, and HPV mucosal transmission.," *The Journal of investigative dermatology,* vol. 130, no. 2, pp. 352-361, 2010.

[107]   J. Cohen, "Painful Failure of Promising Genital Herpes Vaccine," *Science,* vol. 330, p. 304, 2010.

[108]   A. Wald, D. Koelle, K. Fife, T. Warren, K. Leclair, R. Chicz, S. Monks, D. Levey, C. Musselli and P. Srivastava, "Safety and immunogenicity of long HSV-2 peptides complexed with rhHsc70 in HSV-2 seropositive persons," *Vaccine,* vol. 29, no. 47, pp. 8520-8529, 2011.

[109]   World Health Organization, "Vaccine Safety Basics: Live Attenuated Vaccine (LAV)," 2015. [Online]. Available: http://vaccine-safety-training.org/live-attenuated-vaccines.html. [Accessed 14 January 2015].

[110]   S. Mundle, H. Hernandez, J. Hamberger, J. Catalan, C. Zhou, S. Stegalkina, A. Tiffany, H. Kleanthous, S. Delagrave and S. Anderson, "High-purity preparation of HSV-2 vaccine candidate ACAM529 is immunogenic and efficacious in vivo.," *PloS One,* vol. 8, no. 2, pp. 1-10, 2013.

[111]   T. Peng, M. Ponce-de-Leon, H. Jiang, G. Dubin, J. Lubinski, R. Eisenberg and G. Cohen, "The gH-gL Complex of Herpes Simplex Virus (HSV) Stimulates Neutralizing Antibody and Protects Mice

against HSV Type 1 Challenge," *Journal of virology,* vol. 72, no. 1, pp. 65-72, 1998.

[112]   C. McLean, M. Erturk, R. Jennings, D. Nichallanain, A. Minson, I. Duncan, M. Boursnell and A. Inglis, "Protective vaccination against primary and recurrent disease caused by herpes simplex virus (HSV) type 2 using a genetically disabled HSV-1," *Jounal of Infectious Diseases,* vol. 170, no. 5, pp. 1100-1109, 1994.

[113]   G. de Bruyn, M. Vargas-Cortez, T. Warren, S. Tyring, K. Fife, J. Lalezari, R. Brady, M. Shahmanesh, G. Kinghorn, K. Beutner, R. Patel, M. Drehobl, P. Horner, T. Kurtz, S. McDermott, A. Wald and L. Corey, "A randomized controlled trial of a replication defective (gH deletion) herpes simplex virus vaccine for the treatment of recurrent genital herpes among immunocompetent subjects.," *Vaccine,* vol. 24, no. 7, pp. 914-920, 2006.

[114]   D. Shedlock and D. Weiner, "DNA vaccination: antigen presentation and the induction of immunity," *Journal of Leukocyte Biology,* vol. 68, no. 6, pp. 793-806, 2000.

[115]   H. Hernandez, J. Hamberger, C. Lai, H. Kleanthous, M. Parrington and S. Delagrave, "Analysis of the humoral immune response to HSV-2 glycoproteins in ACAM529-vaccinated mice," *Journal of Immunology,* vol. 190, 2013.

[116]   N. Fischer, G. Mbuy and R. Woodruff, "HSV-2 disrupts gap junctional intercellular communication between mammalian cells in vitro," *Journal of Virological Methods,* vol. 91, no. 2, pp. 157-166, 2001.

[117]   R. O'Keeffe, M. D. Johnston and N. Slater, "The Primary Production of an Infectious Recombinant Herpes Simplex Virus Vaccine," *Biotechnology and Bioengineering,* p. 57, 1998.

[118]   V. Tiwari, S. Shukla, B. Yue and D. Shukla, "Herpes simplex virus type 2 entry into cultured human corneal fibroblasts is mediated by herpesvirus entry mediator," *Journal of General Virology,* vol. 88, pp. 2106-2110, 2007.

[119]   M. Balish, M. Abrams, A. Pumfery and C. Brandt, "Enhanced Inhibition of Herpes-Simplex Virus Type-1 Growth in Human Corneal Fibroblasts by Combinations of Interferon-Alpha and Interferon-Gamma," *Journal of infectious Diseases,* vol. 166, no. 6, pp. 1401-1403, 1992.

[120]   W. Whitford and A. Fairbank, "Considerations in Scale-Up of Viral Vaccine Production," 1 September 2011. [Online]. Available: http://www.bioprocessintl.com/manufacturing/antibody-non-antibody/considerations-in-scale-up-of-viral-vaccine-production-320990/. [Accessed 27 April 2015].

[121]   World Health Organization, "Requirements for the use of animal cells as in vitro subsrates for the production of biologicals," *WHO Technical Report Series,* vol. 878, pp. 20-53, 1998.

[122]   Invitrogen Gibco by Life Technologies, "Cell Culture Basics," [Online]. Available: www.vanderbilt.edu/viibre/CellCultureBasicsEU.pdf. [Accessed 27 4 2015].

[123]   W. Kühnel, Color Atlas of Cytology, Histology, and Microscopic Anatomy, Stuttgart, Germany:

Georg Thieme Verlag, 1992.

[124]   X. Duan and H. Sheardown, "Incorporation of cell-adhesion peptides into collagen," *Journal of Biomaterial Science, Polymer Edition,* vol. 18, no. 6, pp. 701-711, 2007.

[125]   C. Paillet, G. Forno, R. Kratje and M. Etcheverrigaray, "Suspension-Vero cell cultures as a platform for viral vaccine production," *Vaccine,* vol. 27, pp. 6464-6467, 2009.

[126]   W. Whitford, "Single-Use Systems As Principal Components in Bioproduction," 1 December 2010. [Online]. Available: http://www.bioprocessintl.com/upstream-processing/upstream-single-use-technologies/single-use-systems-as-principal-components-in-bioproduction-307214/. [Accessed 28 April 2015].

[127]   A. K.-L. Chen, S. Reuveny and S. K. W. Oh, "Application of human mesenchymal and pluripotent stem cell microcarrier cultures in cellular therapy: Achievements and future direction," *Biotechnology Advances,* vol. 31, no. 7, pp. 1032-1046, 2013.

[128]   A. Vanwezel, "Growth of Cell-Strains and Primary Cells on Micro-Carriers in Homogeneous Culture," *Nature,* vol. 216, no. 5110, pp. 64-&, 1967.

[129]   G. Bluml, Microcarrier cell culture technology, Humana Press, 2007.

[130]   D. Giard, W. Thilly, D. Wang and D. Levine, "Virus Production with a Newly Developed Microcarrier System," *Applied and Environmental Microbiology,* vol. 34, no. 6, pp. 668-672, 1977.

[131]   T. Vicente, A. Roldao, C. Peixoto, M. Carrondo and P. Alves, "Large-scale production and purification of VLP-based vaccines," *Journal of Invertebrate Biology,* vol. 107, pp. 42-48, 2011.

[132]   A. Nahmias and S. Kibrick, "Inhibitory effect of heparin on herpes simplex virus," *Journal of Bacteriology,* vol. 87, pp. 1060-1066, 1964.

[133]   M. Baba, R. Sneock, R. Pauwels and E. de Clercq, "Sulfated polysaccharides are potent and selective inhibitors of various enveloped viruses, inceluding herpes simplex virus, cytomegalovirus, vesicular stomatits virus, and human immunodeficiency virus," *Antimicrobial Agents and Chemotherapy,* vol. 32, pp. 1742-1745, 1988.

[134]   J. Neyts, D. Reymen, D. Letourneur, J. Jozefonvicz, D. Schols, J. Este, G. Andrei, P. McKenna, M. Witvrouw, S. Ikeda, J. Clement and E. Declercq, "Differential antiviral activity of derivatized dextrans," *Biochemical Pharmacology,* vol. 50, pp. 743-751, 1995.

[135]   A. Dyer, B. Banfield, D. Martindale, D.-M. Spannier and F. Tufaro, "Dextran sulfate can act as an artificial receptor to mediate a type-specific herpes simplex virus infection via glycoprotein B," *Journal of Virology,* vol. 71, pp. 191-198, 1997.

[136]   C. Addison, F. J. Rixon, J. W. Palfreyman, M. O'Hara and V. G. Preston, "Characterization of a herpes simplex virus type 1 mutant which has a temperature-sensitive defect in penetration of

cells and assembly of capsids," *Virology,* vol. 138, pp. 246-259, 1984.

[137]   B. C. Herold, R. J. Visalli, N. Susmarski, C. R. Brandt and P. G. Spear, "Glycoprotein-C independent binding of herpes-simplex virus to cells requires cell-surface heparan-sulphate and glycoprotein-B," *Journal of General Virology,* vol. 75, pp. 1211-1222, 1994.

[138]   A. Tada, N. Sekine, M. Toba and K. Yoshino, "An Analysis of Factors Influencing the Isolation Rate of Herpes Simplex Virus," *Microbiology and Immunology,* vol. 21, no. 4, pp. 219-229, 1977.

[139]   Intenso Project Eu, "Intenso Project Newsletter," January 2014. [Online]. Available: http://www.google.ca/url?sa=t&rct=j&q=&esrc=s&source=web&cd=4&ved=0CDMQFjAD&url=h ttp%3A%2F%2Fintensoproject.eu%2Fwp-content%2Fuploads%2F2014%2F10%2F1st-Newsletter-Intenso.pdf&ei=bAbIVPySNoGoyAT65oKIBQ&usg=AFQjCNF7bVmYuf4H9nMeYaE-DDvekc75Hw&sig2=mmN91FCoP_. [Accessed 27 January 2015].

[140]   M. Wolff and U. Reichl, "Downstream processing of cell culture-derived virus particles," *Exepert Review of Vaccines,* vol. 10, pp. 1451-1475, 2011.

[141]   Y.-T. Tseng, S.-M. Wang, K.-J. Huang, A. I.-R. Lee and C.-C. Chiang, "Self-assembly of Severe Acute Respiratory Syndrome Coronavirus Membrane Protein," *Journal of Biological Chemistry,* vol. 285, no. 17, p. 2010, 285.

[142]   J. Haynes, "Influenza virus-like particle vaccines," *Expert Review of Vaccines,* vol. 8, no. 4, pp. 435-445, 2009.

[143]   L. Pedro, S. S. Soares and G. N. M. Ferreira, "Purification of Bionanoparticles," *Chem Eng Technol,* vol. 31, pp. 815-825, 2008.

[144]   W. Lai and A. Middelberg, "The production of human papillomavirus type 16 L1 vaccine product from Escherichia coli inclusion bodies," *Bioprocess and Biosystems Engineering,* pp. 121-128, 2002.

[145]   W. Zhang, J. Carmichael, J. Ferguson, S. Inglis, H. Ashrafian and M. Stanley, "Expression of human papillomavirus type 16 L1 protein in Escherichia coli: Denaturation, renaturation, and self-assembly of virus-like particles in vitro," *Virology,* pp. 423-431, 1998.

[146]   A. Roldao, M. Mellado, L. Castilho, M. Carrondo and P. Alves, "Virus-like particles in vaccine development," *Expert Reviews of Vaccines,* pp. 1149-1176, 2010.

[147]   T. Weigel, T. Solomaier, A. Peuker, T. Pathapati, M. Wolff and U. Reichl, "A flow-through chromatography process for influenza A and Bvirus purification," *Journal of Virological Methods,* pp. 45-53, 2014.

[148]   J. O. Konz, L. R. Pitts and S. L. Sagar, "Scaleable purification of adenovirus vectors," *Methods in Molecular Biology,* pp. 13-23, 2008.

[149]   H. Liu, J. Ma, C. Winter and R. Bayer, "Recovery and purification process development for

monoclonal antibody production," *mAbs,* p. 480–499, 2010.

[150]   S. Mundle, H. Hernandez, J. Hamberger, J. Catalan, C. Zhou, S. Stegalkina, A. Tiffany, H. Kleanthous, S. Delagrave and S. Anderson, "High-purity preparation of HSV-2 vaccine candidate ACAM529 is immunogenic and efficacious in vivo," *PLoS One,* 2013.

[151]   B. Kalbfuss, Y. Genzel, M. Wolff, A. Zimmermann, R. Morenweiser and U. Reichl, "Harvesting and Concentration of Human Influenza A Virus Produced in Serum-Free Mammalian Cell Culture for the Production of Vaccines," *Biotechnology Bioengineering,* pp. 73-85, 2006.

[152]   T. Gotoh, Y. Miyazaki, K. Kikuchi and W. Bentley, "Investigation of sequential behavior of carboxyl protease and cysteine protease activities in virus-infected Sf-9 insect cell culture by inhibition assay," *Appl. Microbiol. Biotechnol,* p. 742–749, 2001.

[153]   H. Vieira, C. Estevao, A. Roldao, C. Peixoto, M. Sousa, P. Cruz and e. al., "Triple layered rotavirus vlp production: Kinetics of vector replication, mRNA stability and recombinant protein production," *J Biotechnol,* pp. 72-82, 2005.

[154]   S. Tsoka, O. Ciniawskyj, O. Thomas, N. Titchener-Hooker and M. Hoare, "Selective flocculation and precipitation for the improvement of virus-like particle recovery from yeast homogenate," *Biotechnology Progress,* p. 661–667, 2000.

[155]   B. Minow, F. Egner, F. Jonas and B. Lagrange, "High–Cell-Density Clarification By Single-Use Diatomaceous Earth Filtration," *BioProcess International,* 2014.

[156]   P. E. Cruz, "Characterization and downstream processing of HIV-1 core and virus-like- particles produced in serum free medium," *Enzyme and Microbial Technology,* pp. 61-70, 2000.

[157]   M. Segura, A. Kamen and A. Garnier, Viral Vectors for Gene Therapy, O.-W. Merten & M., 2011.

[158]   D. Thomas and e. al., "Scalable recombinant adeno-associated virus production using recombinant herpes simplex virus type 1 coinfection of suspension-adapted mammalian cells," *Human gene therapy,* p. 861–870, 2009.

[159]   A. Shukla and U. Gottschalk, "Single-use disposable technologies for biopharmaceutical manufacturing," *Trends in Biotechnology,* p. 147–154, 2013.

[160]   R. Eibl and D. Eibl, "Editorial: Single-use technology in biopharmaceutical manufacturing," *Engineering in Life Sciences,* pp. 236-237, 2014.

[161]   D. Szarafinski, "Flexible, Scalable and Configurable Single-Use Systems for Biopharmaceutical Research and Manufacture," *Chemie Ingenieur Technik,* pp. 34-39, 2013.

[162]   M. Westoby and e. al., "Effects of solution environment on mammalian cell fermentation broth properties: Enhanced impurity removal and clarification performance," *Biotechnology and Bioengineering,* p. 50–58, 2011.

[163]   N. Singh, K. Pizzelli, J. Romero, J. Chrostowski, G. Evangelist, J. Hamzik and K. Cheng, "Clarification of recombinant proteins from high cell density mammalian cell culture systems using new improved depth filters," *Biotechnology and Bioengineering,* p. 1964–1972, 2013.

[164]   A. Negrete, A. Pai and J. Shiloach, "Use of hollow fiber tangential flow filtration for the recovery and concentration of HIV virus-like particles produced in insect cells," *Journal of Virological Methods,* p. 240–246, 2014.

[165]   T. Vicente, S. Burri, S. Wellnitz, K. Walsh, S. Rothe and J. Liderfelt, "Fully aseptic single-use cross flow filtration system for clarification and concentration of cytomegalovirus-like particles," *Engineering in Life Sciences,* pp. 318-326, 2014.

[166]   T. Lee and T. D'Amore, "Membrane Separation Theoretical and Applicable Considerations for Optimum Industrial Bioprocessing," *Journal Bioprocess Biotechnology,* pp. 1-88, 2011.

[167]   J. Curling, Production of Plasma Proteins for Therapeutic Use, NJ: Wiley-Blackwell: Hoboken, 2012.

[168]   "Blood Separation and Plasma Fractionation," in *Purification of Albumin from Plasma*, New Jersey, Wiley-Liss: Hoboken, 1991.

[169]   M. Stucki and e. al., "Investigations of Prion and Virus Safety of a New Liquid IVIG Product," *Biologicals,* p. 239–247, 2008.

[170]   T. Van der Meer, B. Minow, B. Lagrange, F. Krumbein and F. Rolin, "Diatomaceous Earth Filtration: Innovative Single-Use Concepts for Clarification of High-Density Mammalian Cell Cultures," *BioProcess International,* 2014.

[171]   B. Kalbfuss, M. Wolff, L. Geisler, A. Tappe, R. Wickramasinghe, V. Thom and U. Reichl, "Direct capture of influenza A virus from cell culture supernatant with Sartobind anion-exchange membrane adsorbers," *Journal of Membrane Science,* p. 251–260, 2007.

[172]   R. R. Vennapusa, S. Binner, R. Cabrera and M. Fernandez-Lahore, "Surface energetics to assess microbial adhesion onto fluidized chromatography adsorbents," *Eng Life Sci,* vol. 8, pp. 530-539, 2008.

[173]   P. Guo, Y. El-Gohary, K. Prasadan, C. Shiota, X. Xiao, J. Wiersch, J. Paredes, S. Tulachan and G. K. Gittes, "Rapid and simplified purification of recombinant adeno-associated virus.," *J Virol Methods,* vol. 183, pp. 139-46, 2012.

[174]   J. Dutra Molino, D. Viana Marques, A. Pessoa, P. Mazzola and M. Gatti, "Different Types of Aqueous Two-Phase Systems for Biomolecule and Bioparticle," *Biotechnology Progress,* pp. 1343-1353, 2013.

[175]   J. Benavides and M. Rito-Palomares, "Practical experiences from the development of aqueous two-phase processes for the recovery of high value biological products," *Journal of Chemical Technology and Biotechnology,* pp. 133-142, 2008.

[176] J. Asenjo and B. Andrews, "Aqueous two-phase systems for protein separation: A perspective," *Journal of Chromatography A,* pp. 8826-8835, 2011.

[177] C. Ladd Effio, L. Wenger, O. Ötes, S. A. Oelmeier, R. Kneusel and J. Hubbuch, "Downstream processing of virus-like particles: Single-stage and multi-stage aqueous two-phase extraction," *J Chromatogr A,* 2015.

[178] K. S. Vijayaragavan, A. Zahid, J. W. Young and C. L. Heldt, "Separation of porcine parvovirus from bovine serum albumin using PEG–salt aqueous two-phase system," *Journal of Chromatography B,* pp. 118-126, 2014.

[179] V. Klyushnichenko, A. Bernier, A. Kamen and E. Harmsen, "Improved high-performance liquid chromatographic method in the analysis of adenovirus particles," *Journal of Chromatography B,* pp. 27-36, 2001.

[180] E. Norrby and P. Albertsson, "Concentration of Poliovirus by an Aqueous Polymer 2-Phase System," *Nature,* pp. 1047-1048, 1960.

[181] G. Schloer and S. Breese, "Purification of African Malignant Catarrhal Fever Virus Using a 2-Phase Aqueous Polymer System," *Journal of General Virology,* pp. 101-110, 1982.

[182] C. Peixoto, M. F. Q. Sousa, A. C. Silva, M. J. T. Carrondo and P. M. Alves, "Downstream processing of triple layered rotavirus like particles.," *J Biotechnol,* vol. 127, pp. 452-61, 2007.

[183] M. W. O. Liew, Y. P. Chuan and A. P. J. Middelberg, "Reactive diafiltration for assembly and formulation of virus-like particles," *Biochem Eng J,* vol. 68, pp. 120-128, 2012.

[184] T. Vicente, J. Mota, C. Peixoto, P. Alves and M. Carrondo, "Rational design and optimization of downstream processes of virus particles for," *Biotechnology Advances,* vol. 29, pp. 869-878, 2011.

[185] C. Peixoto, T. B. Ferreira, M. F. Q. Sousa, M. J. T. Carrondo and P. M. Alves, "Towards purification of adenoviral vectors based on membrane technology.," *Biotechnol Prog,* vol. 24, pp. 1290-6, 2008.

[186] M. M. Segura, A. A. Kamen and A. Garnier, "Overview of current scalable methods for purification of viral vectors," *Methods Mol Biol,* vol. 737, pp. 89-116, 2011.

[187] Y. Li, X. Liu, X. Dong, L. Zhang and Y. Sun, "Biomimetic Design of Affinity Peptide Ligand for Capsomere of Virus-Like Particle," *Langmuir,* pp. 8500-8508, 2014.

[188] G. Fassina and D. Palomba, "Combinatorial technologies in biotechnology: Design of affinity ligands," *Chimica Oggi - Chemistry Today,* pp. 38-41, 2003.

[189] A. R. Kattur Venkatachalam, M. Szyporta, T. K. Kiener, P. Balraj and J. Kwang, "Concentration and purification of enterovirus 71 using a weak anion-exchange monolithic column," *Virol J,* vol. 11, p. 99, 2014.

[190]   D. Forcic, M. Brgles, J. Ivancic-Jelecki, M. Santak, B. Halassy, M. Barut, R. Jug, M. Markušić and A. Strancar, "Concentration and purification of rubella virus using monolithic chromatographic support.," *J Chromatogr B Analyt Technol Biomed Life Sci,* vol. 879, pp. 981-6, 2011.

[191]   T. A. Grein, Z. Kovacs, M. Ebrahimi, R. Michalsky and P. Czermak, "Membrane supported virus separation from biological solutions," *Chem Ing Tech,* vol. 85, pp. 1183-1192, 2013.

[192]   U. Gottschalk, "Bioseparation in antibody manufacturing: The good, the bad and the ugly," *Biotechnology Progress,* vol. 24, no. 3, pp. 496-503, 2008.

[193]   P. Kramberger, M. Peterka, J. Boben, M. Ravnikar and A. Strancar, "Short monolithic columns--a breakthrough in purification and fast quantification of tomato mosaic virus," *J Chromatogr A,* vol. 1144, pp. 143-9, 2007.

[194]   J. Marlind, M. Kaspar, E. Trachsel, R. Sommavilla, S. Hindle, C. Bacci, L. Giovannoni and D. Neri, "Antibody-Mediated Delivery of Interleukin-2 to the Stroma of Breast Cancer Strongly Enhances the Potency of Chemotherapy," *Clinical Cancer Research,* vol. 14, no. 10, pp. 6515-6524, 2008.

[195]   A. M. Davidoff, C. Y. C. Ng, S. Sleep, J. Gray, S. Azam, Y. Zhao, J. H. McIntosh, M. Karimipoor and A. C. Nathwani, "Purification of recombinant adeno-associated virus type 8 vectors by ion exchange chromatography generates clinical grade vector stock.," *J Virol Methods,* vol. 121, pp. 209-15, 2004.

[196]   T. Vicente, C. Peixoto, M. J. T. Carrondo and P. M. Alves, "Purification of recombinant baculoviruses for gene therapy using membrane processes.," *Gene Ther,* vol. 16, pp. 766-75, 2009.

[197]   C. Wu, K. Soh and S. Wang, "Ion-exchange membrane chromatography method for rapid and efficient purification of recombinant baculovirus and baculovirus gp64 protein," *Human Gene Therapy,* pp. 665-672, 2007.

[198]   V. Slepushkin, N. Chang, R. Cohen, Y. Gan, B. Jiang, E. Deausen, D. Berlinger, G. Binder, K. Andre, L. Humeau and B. Dropulic, "Large-scale purification of a lentiviral vector by size exclusion chromatography or mustang Q ion exchange capsule," *Bioprocessing Journal 2,* p. 89–95, 2003.

[199]   R. H. Kutner, S. Puthli, M. P. Marino and J. Reiser, "Simplified production and concentration of HIV-1-based lentiviral vectors using HYPERFlask vessels and anion exchange membrane chromatography.," *BMC Biotechnol,* vol. 9, p. 10, 2009.

[200]   K. Zimmermann, O. Scheibe, A. Kocourek, J. Muelich, E. Jurkiewicz and A. Pfeifer, "Highly efficient concentration of lenti- and retroviral vector preparations by membrane adsorbers and ultrafiltration," *BMC Biotechnology,* vol. 11, 2011.

[201]   B. Kalbfuss, M. Wolff, L. Geisler, A. Tappe, R. Wickramasinghe, V. Thom and U. Reichl, "Direct capture of influenza A virus from cell culture supernatant with Sartobind anion-exchange membrane adsorbers," *J Membrane Sci,* vol. 299, pp. 251-260, 2007.

[202]   M. W. Wolff, C. Siewert, S. P. Hansen, R. Faber and U. Reichl, "Purification of cell culture-derived modified vaccinia ankara virus by pseudo-affinity membrane adsorbers and hydrophobic interaction chromatography," *Biotechnol Bioeng,* vol. 107, pp. 312-20, 2010.

[203]   M. W. Wolff, C. Siewert, S. Lehmann, S. P. Hansen, R. Djurup, R. Faber and U. Reichl, "Capturing of cell culture-derived modified Vaccinia Ankara virus by ion exchange and pseudo-affinity membrane adsorbers," *Biotechnol Bioeng,* vol. 105, pp. 761-9, 2010.

[204]   L. Opitz, S. Lehmann, U. Reichl and M. W. Wolff, "Sulfated membrane adsorbers for economic pseudo-affinity capture of influenza virus particles," *Biotechnol Bioeng,* vol. 103, pp. 1144-54, 2009.

[205]   L. Opitz, J. Hohlweg, U. Reichl and M. W. Wolff, "Purification of cell culture-derived influenza virus A/Puerto Rico/8/34 by membrane-based immobilized metal affinity chromatography.," *J Virol Methods,* vol. 161, pp. 312-6, 2009.

[206]   D.-S. Lee, B.-M. Kim and D.-W. Seol, "Improved purification of recombinant adenoviral vector by metal affinity membrane chromatography.," *Biochem Biophys Res Commun,* vol. 378, pp. 640-4, 2009.

[207]   C. Burden, J. Jin, A. Podgornik and D. Bracewell, "A monolith purification process for virus-like particles from yeast homogenate," *JOURNAL OF CHROMATOGRAPHY B-ANALYTICAL TECHNOLOGIES IN THE BIOMEDICAL AND LIFE SCIENCES,* pp. 82-89, 2012.

[208]   H. M. Oksanen, A. Domanska and D. H. Bamford, "Monolithic ion exchange chromatographic methods for virus purification.," *Virology,* vol. 434, pp. 271-7, 2012.

[209]   P. Gerster, E.-M. Kopecky, N. Hammerschmidt, M. Klausberger, F. Krammer, R. Grabherr, C. Mersich, L. Urbas, P. Kramberger, T. Paril, M. Schreiner, K. Nöbauer, E. Razzazi-Fazeli and A. Jungbauer, "Purification of infective baculoviruses by monoliths.," *J Chromatogr A,* vol. 1290, pp. 36-45, 2013.

[210]   M. Banjac, E. Roethl, F. Gelhart, P. Kramberger, B. L. Jarc, M. Jarc, A. Strancar, T. Muster and M. Peterka, "Purification of Vero cell derived live replication deficient influenza A and B virus by ion exchange monolith chromatography.," *Vaccine,* vol. 32, pp. 2487-92, 2014.

[211]   L. Urbas, B. L. Jarc, M. Barut, M. Zochowska, J. Chroboczek, B. Pihlar and E. Szolajska, "Purification of recombinant adenovirus type 3 dodecahedric virus-like particles for biomedical applications using short monolithic columns.," *J Chromatogr A,* vol. 1218, pp. 2451-9, 2011.

[212]   M. C. Cheeks, N. Kamal, A. Sorrell, D. Darling, F. Farzaneh and N. K. H. Slater, "Immobilized metal affinity chromatography of histidine-tagged lentiviral vectors using monolithic adsorbents," *J Chromatogr A,* vol. 1216, pp. 2705-11, 2009.

[213]   S. L. Williams, M. E. Eccleston and N. K. H. Slater, "Affinity capture of a biotinylated retrovirus on macroporous monolithic adsorbents: towards a rapid single-step purification process," *Biotechnol Bioeng,* vol. 89, pp. 783-7, 2005.

[214]   M. Kuiper, R. M. Sanches, J. A. Walford and N. K. H. Slater, "Purification of a functional gene therapy vector derived from Moloney murine leukaemia virus using membrane filtration and ceramic hydroxyapatite chromatography," *Biotechnol Bioeng,* vol. 80, pp. 445-453, 2002.

[215]   T. Vicente, A. Roldão, C. Peixoto, M. J. T. Carrondo and P. M. Alves, "Large-scale production and purification of VLP-based vaccines.," *J Invertebr Pathol,* vol. 107 Suppl, pp. S42--8, 2011.

[216]   T. Rodrigues, M. J. T. Carrondo, P. M. Alves and P. E. Cruz, "Purification of retroviral vectors for clinical application: biological implications and technological challenges.," *J Biotechnol,* vol. 127, pp. 520-41, 2007.

[217]   J. Curling and U. Gottschalk, "Process chromatography: Five decades of innovation," *BioPharm International,* 2007.

[218]   A. Podgornik, S. Yamamoto, M. Peterka and N. L. Krajnc, "Fast separation of large biomolecules using short monolithic columns.," *J Chromatogr B Analyt Technol Biomed Life Sci,* vol. 927, pp. 80-9, 2013.

[219]   M. Puig, J. Piedra, S. Miravet and M. Segura, "Canine adenovirus downstream processing protocol.," *Methods in Molecular Biology,* pp. 197-210, 2014.

[220]   P. Nestola, R. J. S. Silva, C. Peixoto, P. M. Alves, M. J. T. Carrondo and J. P. B. Mota, "Adenovirus purification by two-column, size-exclusion, simulated countercurrent chromatography.," *J Chromatogr A,* vol. 1347, pp. 111-21, 2014.

[221]   L. Maranga, P. Rueda, A. F. G. Antonis, C. Vela, J. P. M. Langeveld, J. I. Casal and M. J. T. Carrondo, "Large scale production and downstream processing of a recombinant porcine parvovirus vaccine.," *Appl Microbiol Biotechnol,* vol. 59, pp. 45-50, 2002.

[222]   H. Lilie, S. Richter, S. Bergelt, S. Frost and F. Gehle, "Polyionic and cysteine-containing fusion peptides as versatile protein tags.," *Biol Chem,* vol. 394, pp. 995-1004, 2013.

[223]   K. Stubenrauch, S. Gleiter, U. Brinkmann, R. Rudolph and H. Lilie, "Conjugation of an antibody Fv fragment to a virus coat protein: cell-specific targeting of recombinant polyoma-virus-like particles," *Biochemical Journal,* pp. 867-873, 2001.

[224]   J. Guerrero-Rodríguez, C. A. Manuel-Cabrera, Y. A. Palomino-Hermosillo, P. G. Delgado-Guzmán, M. Escoto-Delgadillo, L. Silva-Rosales, S. E. Herrera-Rodríguez, C. Sánchez-Hernández and A. Gutiérrez-Ortega, "Virus-like particles from escherichia coli-derived untagged papaya ringspot virus capsid protein purified by immobilized metal affinity chromatography enhance the antibody response against a soluble antigen.," *Mol Biotechnol,* vol. 56, pp. 1110-20, 2014.

[225]   T. Rodrigues, M. Carrondo, P. Alves and P. Cruz, "Purification of retroviral vectors for clinical application:," *Journal of Biotechnology,* vol. 127, pp. 520-541, 2007.

[226]   S. Ansorge, O. Henry and A. Kamen, "Recent progress in lentiviral vector mass production," in *Viral Vectors for Gene Therapy*, New York, Humana Press, 2011.

[227] F. Bost, M. Diarra-Mehrpour and J.-P. Martin, "Inter-B-trypsin inhibitor proteoglycan family: A group of proteins binding and stabilizing the extracellular matrix," *European Journal of Biochemistry,* vol. 252, pp. 339-346, 1998.

[228] S. George, A. Jauhar, J. Mackenzie, S. Kieβlich and M. Aucoin, "Temporal characterization of protein production levels from baculovirus vectors coding for GFP and RFP genes under non-conventional promoter control," *Biotechnology and Bioengineering,* vol. 112, no. 9, pp. 1822-1831, 2015.

[229] Cornell University - Biotechnology Resource Center, "Zeiss 710 Confocal Microscope User Guide," 8 June 2014. [Online]. Available: https://www.google.ca/url?sa=t&rct=j&q=&esrc=s&source=web&cd=1&ved=0CB4QFjAAahUKE wjno5nQ0oDHAhVEDZIKHVs0Dlo&url=http%3A%2F%2Fwww.biotech.cornell.edu%2Fsites%2Fde fault%2Ffiles%2Fuploads%2FImagingDocs%2FZeiss%2520710%2520User%2520Guide%25208-6-14.pdf&ei=3e-. [Accessed 29 July 2015].

[230] Pro-Lab Diagnostics, "Data Safety Sheet - Crystal Violet (Ammonium Oxalate)," November 2012. [Online]. Available: http://www.google.ca/url?sa=t&rct=j&q=&esrc=s&source=web&cd=3&ved=0CCsQFjAC&url=htt p%3A%2F%2Fwww.pro-lab.com%2Fmsds%2Fstains_pl7073_7074_7075_crystal_violet_ao_msds_eu.pdf&ei=RTxvVYesL ZadygSrhoGwCQ&usg=AFQjCNH7CQV7j8ImOsLUbLT9NYSOLGL6kQ&sig2=ktREPGzw8Htlx. [Accessed 3 June 2015].

[231] C. M. Thompson, Development of a Production Process for a Virus Like Particle Based Vaccine in Cell Culture, Montreal: Ecole Polytechnique de Montreal, 2013.

[232] J. Kruth, "Effects of sodium butyrate, a new pharmocological agent, on cells in culture," *Molecular and Cellular Biochemistry,* pp. 65-82, 1982.

[233] H. Ma, Y. Ma, W. Ma, D. Williams, T. Galvin and A. Khan, "Chemical Induction of Endogenous Retrovirus Particles from the Vero Cell Line of," *Journal of Virology,* pp. 6579-6588, 2011.

[234] D. Park, J. Lalli, L. Sedlackova-Slavikova and S. Rice, "Functional Comparison of Herpes Simplex Virus 1 (HSV-1) and HSV-2 ICP27 Homologs Reveals a Role for ICP27 in Virion Release," *The Journal of Virology,* vol. 89, no. 5, pp. 2892 - 2905 , 2015.

[235] A. Krawczyk, J. Krauss, A. Eis-Huebinger, M. Daeumer, R. Schwarzenbacher, U. Dittmer, K. Schneweis, D. Jaeger, M. Roggendorf and M. Arndt, "Impact of Valency of a Glycoprotein B-Specific Monoclonal Antibody on Neutralization of Herpes Simplex Virus," *The Journal of Virology,* vol. 85, no. 4, pp. 1793-1803, 2011.

[236] W. Newcomb and J. Brown, "Structure of the herpes simplex virus capsid: effects of extraction with guanidine hydrochloride and partial reconstitution of extracted capsids," *Journal of Virology,* vol. 65, no. 2, pp. 613-620, 1991.

[237] G. Zhou, H. Kamiyama and B. Roizman, "The restructuring of glycoprotein D of herpes simplex virus 1 (HSV-1) for cytoreductive therapy of malignant gliomas in humans," *Proceedings of the*

World Engineers' Convention 2004, Biological Engineering and Health Care, vol. B, pp. 243-246, 2004.

[238]   A. Rux, H. Lou, J. Lambris, H. Friedman, R. Eisenberg and G. Cohen, "Kinetic analysis of glycoprotein C of herpes simplex virus types 1 and 2 binding to heparin, heparan sulfate, and complement component C3b," *Virology,* vol. 294, no. 2, pp. 324-332, 2002.

[239]   M. Gorbet, Interviewee, *Glycoprotein E and ICP5 costaining for confocal microscopy.* [Interview]. 11 6 2015.

[240]   F. Cocchi, L. Menotti, P. Dubreil, M. Lopez and G. Campadelli-Fiume, "Cell-to-Cell Spread of Wild-Type Herpes Simplex Virus Type 1, but Not of Syncytial Strains, Is Mediated by the Immunoglobulin-Like Receptors That Mediate Virion Entry, Nectin1 (PRR1/HveC/HIgR) and Nectin2 (PRR2/HveB)," *Journal of Virology,* vol. 74, no. 8, pp. 3909-3917, 2000.

[241]   D. Even, A. Henley and R. Geraghty, "The requirements for herpes simplex virus type 1 cell-cell spread via nectin-1 parallel those for virus entry," *Virus Research,* vol. 119, no. 2, pp. 195-207, 2006.

[242]   C. Sayes, K. Reed, S. Subramoney, L. Abrams and D. Warheit, "Can in vitro assays substitute for in vivo studies in assessing the pulmonary hazards of fine and nanoscale materials?," *Journal of Nanoparticle Research,* vol. 11, no. 2, pp. 421-431, 2009.

[243]   S. Lundquist, M. Renftel, J. Brillault, L. Fenart, R. Cecchelli and M. Dehouck, "Prediction of drug transport through the blood-brain barrier in vivo: A comparison between two in vitro cell models," *Pharmaceutical Research,* vol. 19, no. 7, pp. 976-981, 2002.

[244]   권. and 어. , "Viable alternatives to in vivo tests to evaluate the toxicity of engineered carbon nanotubes," *Journal of Environmental Health Science,* vol. 38, no. 1, pp. 1-7, 2012.

[245]   C. Staton, M. Reed and N. Brown, "A critical analysis of current in vitro and in vivo angiogenesis assays," *International Journal of Experimental Pathology,* vol. 90, no. 3, pp. 195-221, 2009.

[246]   reinnervate - Reprocell Group, "Science Portal: Co-Culture," 2015. [Online]. Available: http://reinnervate.com/science-portal-co-culture/. [Accessed 6 8 2015].

[247]   C. Elias, "A Hybrid Single-Use Bioreactor for Scale-Up of Virus Vaccine Production Using Duck Cell Lines," in *IBC's Second Annual International Forum Vaccine Production Summit*, Westborough, 2011.

[248]   R. Eibl and D. Eibl, Single-Use Equipment in Biopharmaceutical Manufacture: A Brief Introduction, in Single-Use Technology in Biopharmaceutical Manufacture, Hoboken, NJ, USA: John Wiley & Sons, Inc., 2010.

[249]   D.-H. Lee, J.-K. Park and C.-S. Song, "Progress and hurdles in the development of influenza virus-like particle vaccines for veterinary use," *Clin Exp Vaccine Res,* vol. 3, no. 2, pp. 133-139, 2014.

[250] S. Kang, M. Kim and R. Compans, "Virus-like particles as universal influenza vaccines.," *Expert Rv Vaccines,* vol. 11, pp. 995-1007, 2012.

[251] S. Kang, P. Pushko, R. Bright, G. Smith and R. Compans, "Influenza virus-like particles as pandemic vaccines.," *Curr Top Microbiol Immunol.,* vol. 333, pp. 269-289, 2009.

[252] H. Song, V. Wittman, A. Byers, T. Tapia, B. Zhou, W. Warren, P. Heaton and K. Connolly, "In vitro stimulation of human influenza-specific CD8(+) T cells by dendritic cells pulsed with an influenza virus-like particle (VLP) vaccine," *Vaccine,* vol. 28, no. 34, pp. 5524-5532, 2010.

[253] E. Hemann, S. Kang and K. Legge, "Protective CD8 T cell-mediated immunity against influenza A virus infection following influenza virus-like particle vaccination," *Journal of Immunology,* vol. 191, pp. 2486-2494, 2013.

[254] B. Wang, F. Quan, S. Kang, J. Bozja, I. Skountzou and R. Compans, "Incorporation of membrane-anchored flagellin into influenza virus-like particles enhances the breadth of immune responses," *Jounal of Virology,* vol. 82, pp. 11813-11823, 2008.

[255] Q. Chen and H. Lai, "Plant-derived virus-like particles as vaccines," *Human Vaccines and Immunotherapeutics,* pp. 26-49, 2013.

[256] N. Kushnir, S. Streatfield and V. Yusibov, "Virus-like particles as a highly efficient vaccine platform: Diversity of targets and," *Vaccine,* vol. 31, pp. 58-83, 2012.

[257] T. Sasagawa, P. Pushko, G. Steers, S. Gschmeisssner, M. Hajibagheri, J. Finch, L. Crawford and M. Tommasino, "Synthesis and Assembly of Virus-Like Particles of Human Papillomaviruses Type-6 and Type-16 in Fission Yeast Schizosaccharomyces-Pombe," *Virology,* vol. 206, no. 1, pp. 126-135, 1995.

[258] M. Labbe, A. Charpilienne, S. Crawford, M. Estes and J. Cohen, "Expression of rotavirus VP2 produces empty corelike particles," *Journal of Virology,* vol. 65, no. 6, pp. 2946-2952, 1991.

[259] T. Latham and J. Galarza, "Formation of wild-type and chimeric influenza virus-like particles following simultaneous expression of only four structural proteins," *Journal of Virology,* vol. 75, no. 13, pp. 6154-6165, 2001.

[260] D. Gheysen, E. Jacobs, F. Deforesta, C. Thiriart, M. Francotte, D. Thines and M. Dewilde, "Assembly and release of HIV-1 precursor Pr55gag virus-like particles from recombinant baculovirus-infected insect cells," *Cell,* vol. 59, no. 1, pp. 103-112, 1989.

[261] T. Baumert, S. Ito, D. Wong and T. Liang, "Hepatitis C virus structural proteins assemble into viruslike particles in insect cells," *Journal of Virology,* vol. 72, no. 5, pp. 3827-3836, 1998.

[262] Y. Ding, Y. P. Chuan, L. He and A. Middelberg, "Modeling the Competition Between Aggregation and Self-Assembly During Virus-Like Particle Processing," *Biotechnology and Bioengineering,* vol. 107, no. 3, pp. 550-560, 2010.

[263]   R. C. Benson, R. A. Meyer, M. E. Zaruba and G. M. McKhann, "Cellular Autofluorescence - Is It Due to Flavins?," *The Journal of Histochemistry and Cytochemistry,* pp. 44-48, 1978.

[264]   E. Fontaine-Rodriguez and D. Knipe, "Herpes Simplex Virus ICP27 Increases Translation of a Subset of Viral Late mRNAs," *Journal of Virology,* vol. 82, no. 7, p. 3538–3545, 2008.

[265]   D. Huh, G. Hamilton and D. Ingber, "From 3D cell culture to organs-on-chips," *Trends in Cell Biology,* vol. 21, no. 12, pp. 745-754, 2011.

[266]   Nature Medicine, "New on the Market," 2003. [Online]. Available: http://www.nature.com/nm/journal/v9/n6/full/nm0603-801.html. [Accessed 6 8 2015].